Modification of Thermal and Mechanical Properties of Polyhydroxybutyrate (PHB) through Addition of Bio-based Plasticizing Materials and Additive Manufacturing Processing

by

Joseph Vincent Caputo

A thesis submitted in partial fulfillment of the requirements for the degree of

Master of Science

in

Materials Engineering

Department of Chemical and Materials Engineering
University of Alberta

ABSTRACT

The non-degradable polymers currently used for commercial production and application may be inexpensive; however, their excessive use is leading to unprecedented amounts of plastic waste and extensive environmental damage. The demand for biologically-derived, biodegradable polymers is therefore increasing, as these materials are an environmentally attractive alternative to polymers of petrochemical origin. The biopolymer polyhydroxybutyrate (PHB) is bio-based, biodegradable, and biocompatible, giving it a significant advantage over fossil fuel-based polymers in regards to environmental impact. It has great potential for applications in areas such as food packaging, pharmaceuticals, and biomedical engineering; however, PHB has a narrow thermal processing window and current processing methods are very expensive and lead to poor mechanical properties, such as low flexibility and high brittleness.

In this work, PHB materials and methods for thermal processing were investigated, so as to determine whether or not the material can be processed efficiently. The effects of processing PHB through extrusion, hot-pressing, and fused deposition modelling (FDM) – a relatively cheap and efficient additive manufacturing process commonly known as 3D printing – on its morphology, thermal, and mechanical properties were studied. Additionally, the introduction of epoxidized canola oil (eCO) as a green plasticizer, polylactic acid (PLA) as a polymeric plasticizer, and zinc acetate as a possible reaction catalyst to help the blending between PHB and PLA, into the PHB polymer matrix was studied to determine if the processability and flexibility drawbacks could be improved.

Pure PHB pellets were melted and extruded into blended samples (containing different amounts of PHB, PLA, eCO, and catalyst) using a twin-screw micro-extruder system. This material was then hot-pressed into 0.5 mm thick polymer sheets and tested. In addition to these samples, another set of experiments was performed where the same PHB pellets were melted

and extruded into neat filaments of 1.75 mm diameter. These filaments were fed into a desktop FDM/3D printer equipped with a hotend extruder and print bed at controlled, elevated temperatures to directly deposit (*i.e.* print) filaments into tensile specimens.

Scanning electron microscopy (SEM), stereomicroscopy, confocal microscopy, and Fourier-transform infrared spectroscopy were used to study the morphology and structure of the resulting samples. Differential scanning calorimetry (DSC) and thermal gravimetric analysis (TGA) measurements were used to study the thermal properties, stability, extent of degradation, and crystallinity of the final products. Tensile testing was also used to assess the mechanical properties of the products.

Negligible changes in thermal properties and stability were observed following the extrusion, hot-pressing and FDM processes, and neat PHB samples from the two final processes (*i.e.* hot-pressing and FDM) have comparable properties to solvent cast thin film samples of PHB (created in another work using acetic acid) while also being in the range of observed mechanical properties for bulk PHB. These results indicate that PHB can be effectively extruded, hot-pressed, and patterned using FDM printing, with little loss in properties. For FDM processing specifically, which is easy to use, cost-efficient, and commercially scalable, significant mechanical property improvements can result with optimization of the printing process.

Similarly, the addition of bio-based plasticizing agents eCO and PLA (together or separately) gave no significant changes in thermal properties or stability (as compared to neat PHB samples) at the processing and analysis temperatures chosen. The addition of 10 wt% eCO into neat PHB produced the most promising results, as the oil introduced positive plasticizing effects on the PHB matrix (*i.e.* increased flexibility with an expected decrease in strength). With the addition of PLA (25 wt%) and the blending catalyst (0.3 wt%), an improvement in flexibility and a decrease in strength parameters were also observed as

compared to pure PHB. Finally, eCO may also give promising plasticizing results when added to a PHB/PLA blend (in a 3:1 ratio of PHB:PLA), as the addition of 5 wt% eCO produced equivalent results as compared to the sample without oil. However, the addition of 10 wt% eCO gave a statistically significant decrease in both strength and flexibility, as compared to the PHB/PLA blended sample, providing evidence that an optimum point of plasticizing material had been surpassed. By fine-tuning the amount of eCO and PLA in the PHB matrix, it is possible to create a bio-based polymer product more suitable for commercial use and more beneficial for the environment.

There are a number of people without whom this thesis might not have been written, to whom I am greatly indebted and to which I dedicate this work to.

To my father John, mother Caroline Catherine, sister Loriana Frances and more recently my girlfriend Anissa Maria Armet. You have been alongside me every step of the way and I must express my very profound gratitude. Thank you for providing me with unfailing support and continuous encouragement throughout my years of study (and many reports) and through the process of researching and writing this thesis. This accomplishment would not have been possible without each and every one of you.

To the memories of Zia Rosa Caputo (1959-2003), Nonno Vincenzo Tripodi (1919-2017) and Nonno Giuseppe Caputo (1929-2018) who always showed interest in my work and continuously told me *"remember how important reading is in life."*

Love you all as big as the sky, forever and always

-Joseph Vincent Caputo

"This I believe. And I believe it passionately. Man's love of innovation will never die."
-Karl Benz

ACKNOWLEDGMENTS

I would first like to start by thanking my thesis and research advisors Dr. Anastasia Elias and Dr. Dominic Sauvageau of the Department of Chemical and Materials Engineering (CME) at the University of Alberta. The door to both advisors was always open whenever I ran into a trouble spot or had a question about my research or writing. They consistently allowed this project to be my own work but steered me in the right the direction whenever they thought I needed it. I have enjoyed all of our discussions and hope to be able to continue them in the future.

I would like to thank my defence chair, Dr. Phillip Choi, and defence committee of Dr. Elias, Dr. Sauvageau and Dr. Cagri Ayranci for their time and consideration as well as CME department faculties that took the time to speak to me throughout my degree, no matter what about, as it reminded me how important it is to stay close to those that advise you continuously. I would also like to greatly thank Neil Anderson of the Department of Chemical and Materials Engineering at the University of Alberta as a reader and reviewer of this thesis, and I am gratefully indebted to him for his valuable comments on this thesis. I am glad I had the opportunity to go through not one, but two degrees with you.

To all of my colleagues and friends from the Elias and Sauvageau research groups and Dr. Sandra Luz from the Department of Automotive Engineering at the University of Brasília Faculdade do Gama, thank you for your insights, questions and discussions throughout my degree. In particular, I want to express many thanks and appreciations to Adrian Lopera (University of Alberta) as your continued advice, leadership, technical skills and experience helped me to complete this thesis. I look forward to having a chance to work with you again in the future.

Financial support for this work came from the Natural Sciences and Engineering Research Council of Canada (NSERC), the Agriculture and Forestry division of the Government of Alberta and scholarships from the University of Alberta. In addition, thank you to Dr. Aman Ullah and his lab members from the University of Alberta, Canada for kindly preparing and providing epoxidized canola oil (eCO) for my work.

Table of Contents

LIST OF TABLES

LIST OF FIGURES

NOMENCLATURE AND ABBREVIATIONS

Symbols

α	significance level
ε_b	strain at break (%)
ρ	density (g/cm^3)
σ_{UTS}	ultimate tensile stress (MPa)
E	Young's modulus (MPa)
ΔH_m	enthalpy of melting
$\Delta H^0 m$	standard enthalpy of melting
M_n	number average molecular weight
M_w	weight average molecular weight
p	probability value
T_g	glass transition temperature (°C)
T_m	melting temperature (°C)
X_{cDSC}	degree of crystallinity (%)

Abbreviations

3D	3-dimensional
ABS	Acrylonitrile butadiene styrene
ATBC	Acetyl tributyl citrate
bio-PE	Biopolyethylene
eCO	Epoxidized canola oil
DEHP	Bis(2-ethylhexyl) phthalate
DOP	Dioctyl phthalate
DSC	Differential scanning calorimetry
FDM	Fused deposition modelling
FE-SEM	Field emission scanning electron microscopy
FTIR	Fourier transform infrared spectroscopy
GPC	Gel-permeation chromatography
mPCL	Modified poly(ε-caprolactone)
nHA	Nanoparticles of Hydroxyapatite
PBAT	Polybutyrate adipate terephthalate or polybutyrate

PC	Polycarbonate
PCL	Poly(ε-caprolactone)
PDI	Polydispersity Index
PDMS	Polydimethylsiloxane
PE	Polyethylene
PEA	Poly[di(ethyleneglycol) adipate]
PEG	Polyethylene glycol
PET	Polyethylene terephthalate
PHA	Polyhydroxyalkanoate
PHB	Polyhydroxybutyrate
PHBV	Polyhydroxybutyrate-co-valerate
PLA	Polylactic acid
PP	Polypropylene
PS	Polystyrene
PVA	Polyvinyl acetate
PVC	Poly (vinyl chloride)
SE	Secondary electrons
SEM	Scanning electron microscopy
SLS	Selective laser sintering
TB	Glyceryl tributyrate
TCA	Tricarboxylic cycle
TGA	Thermogravimetric analysis
USD	US dollars
UV	Ultraviolet
WA-XRD	Wide-angle X-ray diffraction
XPS	X-ray photoelectron spectroscopy

1. INTRODUCTION

This study investigates the processing of polyhydroxybutyrate (PHB), a thermoplastic biopolymer, using commercially scalable processes and bio-based plasticizers; a relatively unexplored topic in literature. This chapter summarizes the motivation for the research and introduces the overall study. Furthermore, the objectives of the work will be discussed followed by the outline of the thesis and the chapters within it.

1.1 Background and Motivation

Synthetic and natural polymers both play an incredibly important role in our everyday life. Usually, when people think of polymers, what comes to mind is the synthetic plastic bottle they use to stay hydrated or the bag that they put their snacks in for the day. We tend to forget that wool used for clothing is a natural polymer material along with DNA and proteins which make up the backbone of life [1]. As the world continues to evolve and the human population continues to grow, the global demand for polymers continues to rise. Commercially-used polymers of petrochemical origin are most commonly used because of their low prices and good performance [2]. However, they are usually non-degradable and, in some cases require more than 500 years to decompose in the environment [2], [3]. These same fossil fuel-based polymers, making up 80% of commercial polymers, are often disposed of inappropriately and represent 90% of the trash floating on the ocean's surface [3], [4]. This causes harm to all forms of wildlife, with more than 180 species of animals known to have ingested plastic trash [2]. In addition, many ecosystems are damaged (see Figure 1.1), hence the importance of investigating alternatives.

Figure 1.1: Plastic waste continues to build up, damaging many ecosystems (left) and harming all forms of wildlife (right). © 2009 Samuel Mann and U.S. Fish and Wildlife Services, CC by 2.0 [5], [6]

Natural polymers are generally known as those that are produced and degraded by living organisms (*i.e.* biodegradable) and are often defined by an umbrella term: biopolymers. There are multiple classes of biopolymers, as the term can define polymers that are solely degraded by microorganisms but not actually produced by them and polymers that are naturally produced but are not biodegradable [3], [7], [8]. In some cases, materials considered biodegradable break down but do not actually decompose (these types of polymers typically contain chemical additives that allow them to break down) [9]. These materials can be even worse for the environment than petroleum-based polymers because as the material disintegrates, it forms tiny pieces of microplastic that pose a threat to all life forms.

PHB, a highly crystalline thermoplastic, is both a bio-based and biodegradable polymer. Its use in commercial applications is being investigated as it has lower environmental impacts than fossil fuel-based polymers [8], [10]. The material itself, as well as its degradation products, are food safe, edible and completely biocompatible; as such, PHB could be used in applications ranging from food packaging to pharmaceutical uses (Figure 1.2) [11]–[16]. This biopolymer is also quite special as it is produced by numerous microorganisms, including through the process of bacterial fermentation of sugar [17]. One large issue with using PHB (and many other biopolymers) lies in their processing. As the material has very poor processability and thermal stability, the cost of processing is quite high, with PHB being more than 2x more expensive to process than many common petrochemical-based polymers such as polystyrene (PS) [7]. The high thermosensitivity of PHB means that avoiding its thermal degradation is key when processing at elevated temperatures [7], [18]. In addition to these processing issues, final PHB products commonly have poor mechanical properties, such as strain at break (ε_b), which is much lower than commonly used petroleum-based polymers like polyethylene (PE) or polypropylene (PP) [19], [20]. In order to make PHB a more viable solution for commercial applications, the processing and final mechanical properties of the material need to be improved. PHB processing using solvent casting has previously been investigated [13], but thermal processing methods are needed for industry to achieve lower cost and larger scale production.

One method of processing PHB that has not been examined in any detail in the literature is 3D printing. One common 3D printing technique utilized for thermoplastic polymers is fused deposition modelling (FDM). Recently, the FDM process has become more versatile, offering endless possibilities in customization [21]. It is a rapid and efficient process that can be used to print various 3D designs and be easily adapted without drastic changes to equipment.

Because the process itself is extremely efficient and cost-effective, FDM could help alleviate large costs associated with processing PHB in industry. However, FDM of PHB has not yet been demonstrated. PHB samples have been created using other forms of 3D printing; for example, Pereira *et al.* investigated the processing of PHB using selective laser sintering (SLS) for tissue engineering and tissue scaffold fabrication with success [22], [23].

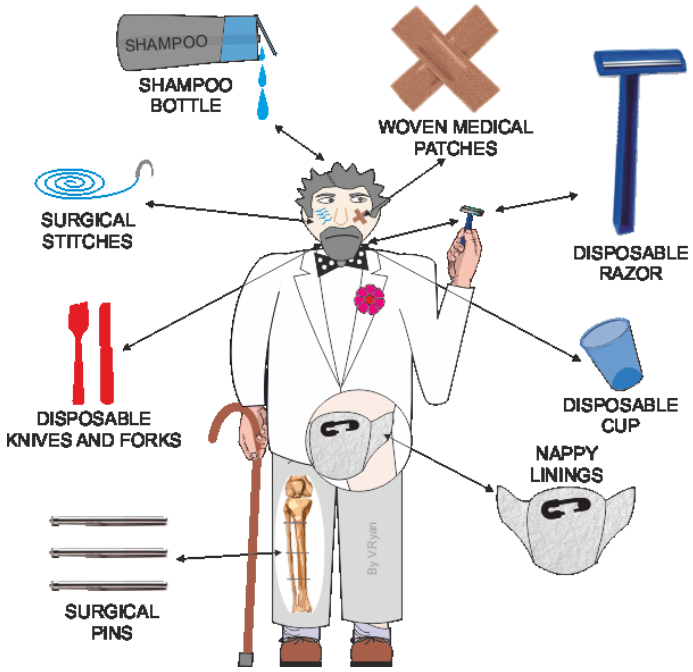

Figure 1.2: Some every day and biomedical applications for biopolymers (left). © 2014 Vincent Ryan, with permission [11]

To overcome some of the processability and flexibility drawbacks of polymers like PHB, a number of approaches can be applied. These include creating blends with other polymers or incorporating additives such as plasticizers. In either case, the overall strategy of PHB modification is to overcome the poor mechanical properties (particularly the high brittle nature of the material) while improving its ability to be thermally processed with reduced concerns of thermal degradation. For polymer blends, other versatile polymers made from renewable resources, such as polylactic acid (PLA), can be mixed with PHB in order to improve on the mechanical properties [24]. Additionally, epoxidized oils are used extensively as plasticizers, additives, and stabilizers for many polymers, as they are added to the polymer matrix to increase the flexibility and improve the processability in thermal processing methods [25]–[28]. For example, Hosney *et al.* reviewed the use of epoxidized vegetable oils as plasticizers for poly (vinyl chloride) (PVC) as compared to harmful phthalate plasticizers, while Jia *et al.* specifically looked at the use of epoxidized soybean oil with PVC [29], [30].

This same epoxidized soybean oil, along with many other bio-based plasticizers, have been studied with PHB [26]–[28]. More recently, epoxidized canola oil (eCO), another bio-based oil similar to epoxidized soybean oil, has shown great potential as a plasticizing agent for various polymers [31], [32]; however, the introduction of eCO into PHB or PHB blends has not yet been demonstrated.

In this work, PHB materials and methods for thermal processing are investigated to determine if the material can be processed efficiently, leading to potentially larger usage of the material in future commercial applications. The processes studied were extrusion, hot-pressing, and fused deposition modelling (FDM), a common form of three-dimensional (3D) printing. The extrusion step, commonly used with thermoplastic materials, was used to melt down PHB pellets and create filaments for the FDM printing work of this study. This material was printed into tensile specimens, which were thermally and mechanically tested to determine if the process gave a PHB sample comparable other processing methods of the material. Separately, the extrusion step was used to mix PHB pellets with additives in hopes of creating a product with improved thermal and mechanical properties. This mixed material was then hot-pressed into polymer sheets, which were thermally and mechanically tested to determine if the process and additives were adequate for the manufacture of PHB products. This hot-pressing technique was a tool used for the analysis of the blended PHB material, but the process itself was also examined as a viable option for commercial processing of PHB.

1.2 Objectives of Study

The overall objectives of this study were to:

1. Investigate the processing of PHB through the commercially scalable processes of extrusion, hot-pressing and the additive manufacturing technique of FDM;
2. Demonstrate that these processing techniques are viable options for PHB through the study of the experimental data, exploring the impact on tunability of material properties as well as possible thermal and mechanical degradation mechanisms of the polymer;
3. Study the use of bio-based plasticizers with PHB to create a product more suitable for commercial applications.

1.3 Organization of the Report

This thesis is divided into six chapters. Following this introductory chapter, Chapter 2 provides a literature review, while Chapter 3 describes the experimental methods used in the preparation of hot-pressed PHB plasticized and FDM printed PHB samples. Chapters 4 and 5 describe the results of the tests and associated discussions for the plasticized samples and the FDM samples, respectively. Finally, Chapter 6 presents the conclusions from these experiments and future work that could extend from the present research.

2. LITERATURE REVIEW

In this chapter, biopolymers, specifically polyhydroxybutyrate (PHB), are introduced as an alternative to petroleum-based polymers. The modes of degradation and their connection to PHB are explained, while the possible applications and processing methods to create a usable PHB product are noted.

2.1 Introduction to Polyhydroxybutyrate (PHB)

2.1.1 Biopolymers

A biopolymer is generally defined in two different ways: (1) a polymer that is produced by living microorganisms or made from renewable resources such as cornstarch (*i.e.* bio-based), or (2) a polymer that is degraded by them (*i.e.* biodegradable) [3], [7], [8]. While the global market for biopolymers has grown significantly in recent years and continues to grow (approximate market value of 2.7B USD in 2015 and is projected to see a value of 5.1B USD in 2021), 80% of all commercially used polymeric materials are being produced by the petrochemical industry [3], [4]. The goal is to increase the use of biopolymers in commercial applications to reduce the dependence on non-renewable resources and reduce the environmental impact of recalcitrant polymers. Biopolymers can be generally separated into three types [8]:

- Type A: both biodegradable and bio-based
- Type B: not biodegradable but bio-based
- Type C: biodegradable but made from fossil fuels

Figure 2.1 displays the plastics coordinate system, which puts various materials into categories based on the type of resource it is made from and whether or not it is biodegradable [3]. Type A, B, and C biopolymers are highlighted in the top right, top left, and bottom right quadrants, respectively. In the last quadrant (*i.e.* bottom left) are the fossil fuel-based and non-biodegradable materials mainly used in commercial applications. As can be seen in this figure, biopolyethylene (bio-PE) is a Type B biopolymer which is bio-based in nature; however, it is not biodegradable, with its use likely leading to long-term environmental impact [3], [8]. Poly(ε-caprolactone) (PCL), on the other hand, is a Type C biopolymer and although it is produced using fossil fuels, it is biodegradable. Arguably, this makes PCL a preferable option

as compared to bio-PE because it will not remain in the environment for as long once it is disposed of [3], [8]. The ideal material to consider is a Type A biopolymer and polyhydorxybutyrate is an excellent material to consider.

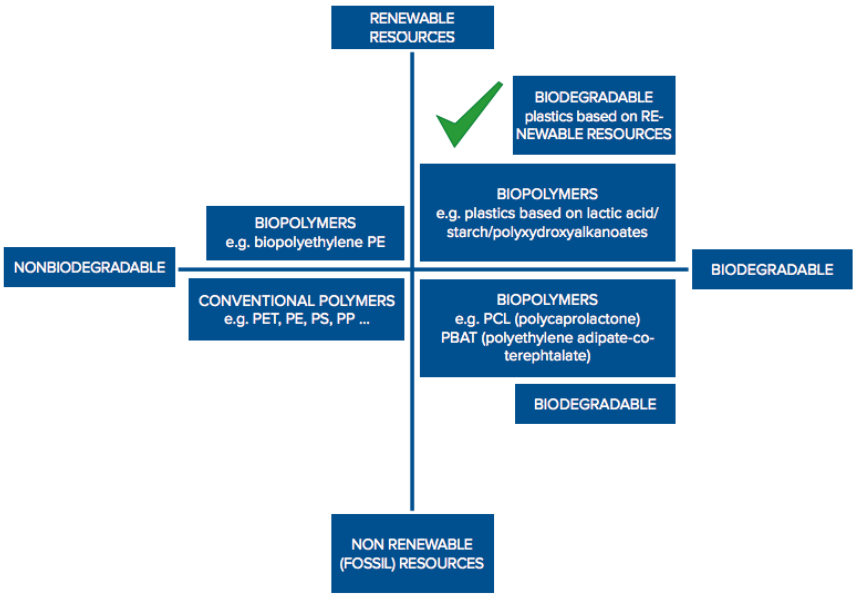

Figure 2.1: Plastics coordinate system [3]. In the conventional polymers section, PET, PE, PS and PP are short for polyethylene terephthalate, polyethylene, polystyrene and polypropylene, respectively

2.1.2 Polyhydroxybutyrate (PHB)

PHB, a highly crystalline, hydrophobic thermoplastic in the polyhydroxyalkanoate (PHA) aliphatic polyester class, was first isolated and characterized by Lemoigne *et al.* in 1927 [7], [12], [33]–[36]. This Type A bio-polyester is produced by many bacteria, with its most common form being poly(3-hydroxybutyrate); its monomer, R-3-hydroxybutyric acid, is non-toxic and can be completely catabolized [8], [10]. Figure 2.2 shows the general structure of PHA, in which the difference in properties between the various polyesters in this family is based on the R-substituent that branches off the β carbon; in the case of PHB (specifically poly(3-hydroxybutyrate)), the R-substituent is a methyl group (*i.e.* CH_3) [34], [37].

Generally, there are three distinguishable classes of properties that are taken into account when assessing the potential of a polymer for a given application: (1) intrinsic properties related to the polymer structure, further split into molecular and bulk (*e.g.* density and glass transition temperatures), (2) processing properties related to the polymer during formation (*e.g.* viscosity and melt flow index), and (3) final product properties [18]. Although these are considered as separate classes of properties, they are interrelated; for example, the mechanical properties of PHB (intrinsic) are dependent on composition, crystallinity, and

processing method used to form the product (*e.g.* hot-pressing, solvent casting or melt extrusion) [12], [18]. Some properties of PHB can be seen below in Table 2.1.

Table 2.1: General properties for PHB [18], [34], [38], [39]

Melting Temperature, T_m (°C)	175
Glass Transition Temperature, T_g (°C)	5-10
Density, ρ (g/cm^3)	1.18-1.26
Crystallinity (X_c, %)*	65-80
Polydispersity Index (PDI)	2.2-3.0
Young's Modulus, E (GPa)	1.4-3.5
Ultimate Tensile Strength, σ_{UTS} (MPa)	15-40
Elongation at Break, ε_b (%)	4-10

*PHB becomes a fully amorphous melt above T_m, where crystallization and formation of helical chains occurs upon cooling [12]

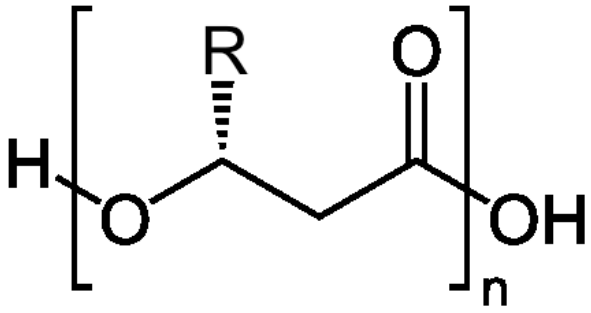

Figure 2.2: Structure of PHA [38]. For PHB, R is a methyl group

In 1927 when Lemoigne's group "found" PHB, they discovered that bacteria could produce this polyester through a process of nutrient starvation (*e.g.* phosphate or nitrogen); when the bacterial cells are starved of these critical nutrients, excess carbon is converted to PHB rather than amino acids or proteins and PHB accumulates in the cells [8], [18], [34], [39]. It was also determined that the PHB produced acts as a storage molecule for carbon and excess energy within the microorganisms, similar to how fat storage occurs in humans [8], [36], [39].

Very little literature exists between the time of Lemoigne and when PHAs were later "rediscovered" in the 1950s by chemists and biochemists, at which time a series of events took place that shaped the future of PHB and other PHAs. First, an article was published in the 1963 *Chemistry and Engineering News* describing the research being completed by W.R. Grace & Co. on a special biopolymer thermoplastic that could "be produced by fermentation" [34], [36]. The authors had discovered how to extract PHB from bacterial cells in the form of micron-sized particles; this process could be used to benefit the research that Lemoigne *et al.* completed

almost 40 years prior, and PHB could be easily collected, making industrial processing a possibility [34], [36]. This rediscovery and work by W.R. Grace & Co. was followed by this anticipated commercial use of PHAs in the mid 1980s, and then the application of genetic engineering (*i.e.* the deliberate modification of the characteristics of an organism by changing its genetic code) to produce PHAs in various optimal bacteria strains, such as *Escherichia coli* [34]. This field of genetic engineering also led to the synthesis of PHA, where gene codes were inserted into various plant tissues to produce the polyester (*i.e.* transgenic plant production) [34], [39].

Approximately 300 different microorganisms have been shown to be able to synthesize PHAs, with only a few species, such as *Alcaligenes eutrophus* and some methylotrophs, producing significant amounts [33], [39]. Formation of *in vitro* synthesized PHAs from such microorganisms became prevalent in the 1990s, at which time the Marchessault group determined the biosynthetic pathway that could be used to create *in vitro* particles of PHB. The pathway includes three key enzymes (β-ketothilase, acetoacetyl-CoA synthase, and PHB synthase) that catalyze carbon-carbon bond formation, reduction of the chiral nature and head to tail polymerization that leads to the final PHB product [34], [39]. As an example, raw (and renewable) materials like sugarcane can be used as feedstock in bacterial fermentation (following the above pathway) to synthesize PHB at large scale [40].

2.1.3 Degradation Mechanisms of PHB

In nature, PHB is generally degraded by microorganisms through enzymatic hydrolysis mechanisms; however, thermal, mechanical, photo, and chemical degradation mechanisms can also occur. Studies have been performed to understand each of these mechanisms, which are expanded upon in the following subsections, and the factors seen in Table 2.2 are generally found to affect the degradation rate of PHB.

One key factor is the processing method utilized and its associated properties (*e.g.* temperature). The main degradation mechanisms associated with processing a thermoplastic such as PHB are thermal and mechanical degradation and, typically, limiting this unwanted degradation is studied when adjusting the processing method to acquire a desired product. However, the processing adjustment can also affect how the other mechanisms are capable of degrading PHB. These other mechanisms, mentioned above, will not affect PHB during the processing stage of the material but rather during the application stage and/or future disposal. Conversely, the most important degradation mechanism when looking at some

applications and disposal of the polymer is the microbial and enzymatic mechanism, but that is not to say that the other mechanisms are not important.

Since PHB is very crystalline in nature, it is important to study the degradation associated with both amorphous and crystalline regions of the material. Generally, degradation occurs more rapidly in the amorphous PHB regions, as compared to the crystalline regions [39], [41]. For example, hydrolysis (associated with enzymatic degradation) takes place more easily in the amorphous regions of the material [35], [39].

Table 2.2: Parameters and factors that can affect the degradation rate of PHB [7], [33], [39]

Parameter	Factor
Environmental	Temperature
	pH
	Oxygen level
	Moisture level
	Nutrient supply
Microbiological	Population density
	Microbial diversity
	Microbial activity
Material Properties	Polymer composition
	Molecular weight
	Crystallinity
	Bond type between monomers
	Surface area

Note: These parameters can be associated with the (1) processing stage, (2) application stage and/or (3) disposal stage of PHB's lifespan

2.1.3.1 Microbial and Enzymatic Degradation

PHB is quite unique as it can both be synthesized and degraded by bacteria [18], [35], [39]. Bacteria of the *Bacillus, Pseudomonas and Streptomyces* families were found as the first PHA-degrading microorganisms back in 1963 [33]. In 1927, Lemoigne *et al.* discovered that PHB can be synthesized when there are limited nutrient conditions inside certain microorganisms (recall Section 2.1.2); however, it was later determined that these same organisms could degrade the PHB if the limiting conditions are later removed (note that not all of the microorganisms that can produce PHB can also degrade it) [18], [39].

Microbial degradation is the mechanism that degrades PHB through the process of random hydrolysis of the material's ester bonds in the polymer chain, leading to the complete degradation of the material and formation of CO_2 and water [42]. The clear-zone method has been incorporated to study microbial degradation in order to isolate and determine the microorganisms that will degrade PHB through this mechanism; approximately 300 strains

have been found [33], [42], [43]. This method was first introduced to test how sensitive specific bacteria are to antibiotics, but the concept is very much the same for studying microbial degradation [33]. The polymer under study (PHB) is well dispersed in a jelly-like medium as fine particles, causing it to appear opaque, and then inoculated with the desired microorganisms (usually bacteria) [33], [43]. If the organisms are capable of depolymerizing the polymer (*i.e.* breaking it down into its monomers, the first stage of biodegradation), the formation of a "clear zone" of halo like area around the colony will appear [33], [43]. This characterization method is used as it is quite fast, simple, and can study multiple microorganisms at one time [33].

Enzymatic degradation is an extension of microbial degradation, as the enzymatic degradation mechanism incorporates PHB-degrading bacteria that produce enzymes called PHA depolymerases, which catalyze PHB hydrolysis [13], [18], [42]–[44]. First, the enzyme attaches itself to the polymer and initiates a hydrolytic cleavage, either inside or outside of the bacteria's cells [33], [35], [43]. These enzymes degrade PHB at a given rate, depending on multiple factors (including temperature, pH, and environmental conditions) [13], [18]. Through the biodegradation of PHB, no harmful by-products are produced, which is one reason that it is being extensively studied for biodegradable products. The main by-product of the hydrolysis of PHB is its water-soluble monomer R-3-hydroxybutyric acid [39]. This monomer is found in large quantities in human blood plasma, which means PHB can be a viable option for biomedical applications such as blood vessel replacements [39]. As this monomer is quite small, it passes through the bacterial cell wall without any resistance and metabolized through oxidation and the tricarboxylic cycle (TCA) to form CO_2 and water under aerobic conditions (*i.e.* free oxygen present) [3], [39]. In an environment lacking in free oxygen (*i.e.* anaerobic), CH_4 is also produced [3], [39]. Therefore, the rate at which the biodegradation occurs can be determined by the amount of CH_4 or CO_2 produced [39]. This mechanism of degradation is commonly introduced on purpose and would be most associated with the application or disposal stage of the PHB product's lifespan. Refer to Figure 2.3 and Figure 2.4 below for a schematic of the degradation pathway and the PHA cycle of carbon, respectively.

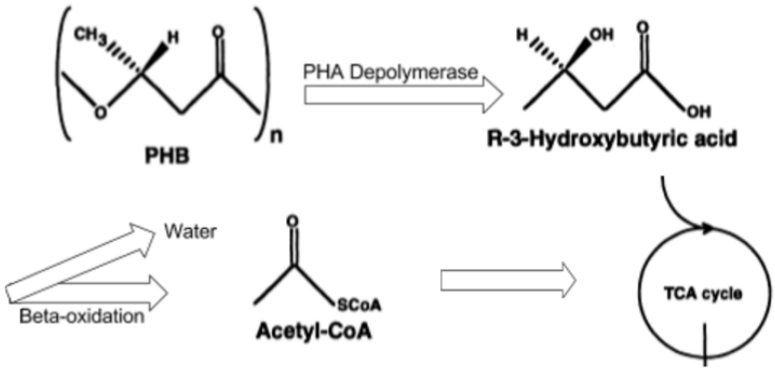

Figure 2.3: Degradation pathway of PHAs. The TCA cycle leads to energy generation and biosynthetic precursors like CO_2 and water [39]

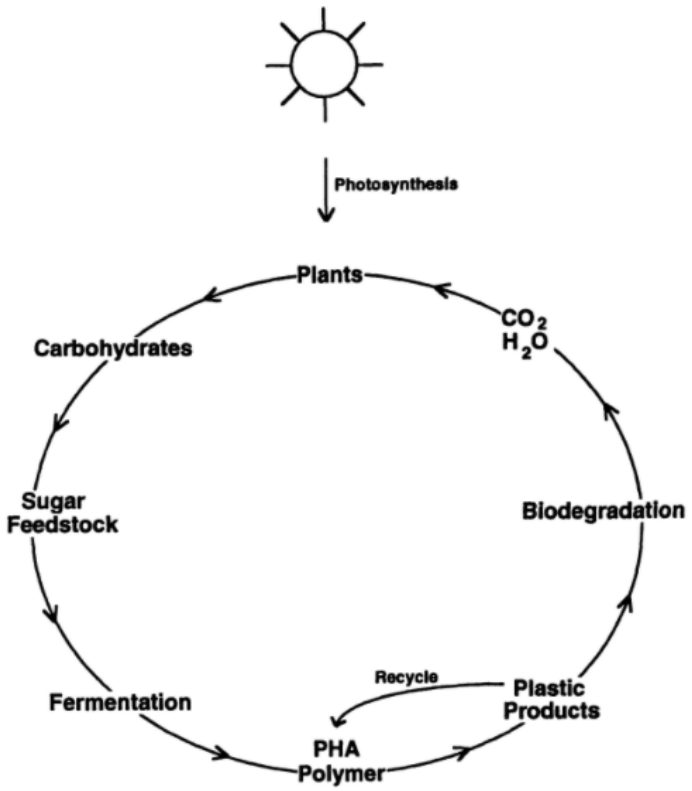

Figure 2.4: PHA carbon cycle. The left side of the cycle relates to the synthesis and production of PHAs (like PHB) where the right side covers the degradation process, as described above [39]

2.1.3.2 Thermal Degradation

Remarkably, thermal degradation is one of the better-studied degradation mechanisms for PHB due to its thermosensitivity; it is easily the most detrimental mechanism that affects the properties of PHB and avoiding this degradation is key during thermal processing [7], [18]. This degradation mechanism, involving the random scission of PHB's ester bond is commonly initiated at temperatures slightly above 175 °C, which is the approximate melting temperature of PHB [18], [34]–[36], [40]. Between 190 and 220 °C, the degradation rate is low and the

amount of degradation is highly dependent on the exposure time at these elevated temperatures [13], [34]. Above 220 °C, the degradation rate increases (*i.e.* even if the PHB is at 220 °C for an extremely short period of time, degradation is noticeable) [13], [18]. This degradation rate continues to increase as temperature increases and around 285 °C, the maximum degradation rate is commonly observed [12], [45]. This can make it quite difficult to process PHB with thermal methods that use elevated temperatures.

2.1.3.3 Mechanical Degradation

Mechanical degradation is based on mechanical forces (*e.g.* shear force, compression or tension) exceeding a critical value, promoting the scission of the polymer chains [18], [46]. This scission, more likely to occur at the center of the polymer chain than at the ends, leads to a decrease in the polymer molecular weight [18], [46]. This specific mechanism is often studied alongside thermal degradation and can be seen during mixing, agitation, grinding or extrusion processes [18]. For example, increasing rotational speeds (and thus the associated torque) of an extrusion system can lead to faster degradation – both initiation and progression – especially at the elevated temperatures generally associated PHB processing [46], [47].

2.1.3.4 Additional Degradation Mechanisms

Photodegradation occurs when ultraviolet (UV) light or a source of high-energy radiation degrades polymers such as PHB. In this environmentally friendly method (that is when UV light is used), degradation will progress fairly rapidly following a slow initiation [18], [43]. Generally speaking, PHB has a higher resistance to UV light in comparison to other polymers such as polypropylene (PP) [3][39].

Finally, chemical degradation is very much related to mechanical, thermal, photo and the biotic mechanisms in that they change the polymer properties through chemical reactions, resulting in the formation of new functional groups, general chemical transformation or random chain scission [43]. Generally, there are many different subsets of chemical degradation but the most common for polyesters such as PHB is hydrolysis (a chemical process that occurs during microbial/enzymatic degradation as well), creating a lower molecular weight product [33], [43], [48].

2.1.3.5 Measuring the Changes in Degradability

As stated above, an important property of many biopolymers is their biodegradability. In some cases, the onset of degradation can be easily observed through changes in polymer colour, surface roughness or formation of cracks in the polymer [43]. However, more sophisticated methods are required to fully understand the degradation mechanism taking place, especially since the degradability properties of bulk PHB are not the same as those seen in polymer sheets, thin films and filaments [49]. Unfortunately, characterization methods commonly used to assess bulk polymer degradation, such as thermogravimetric analysis (TGA) and spectroscopy techniques, are not amenable to characterize materials of small size and mass such as films and filaments.

The degradability of a polyester such as PHB is heavily dependent on its chemical and physical structure, with the weight average and number average molecular weight (Mw and Mn, respectively) often being important factors in determining the how well it degrades [41], [43], [49]. At increased temperatures (especially for longer processing times) the molecular weight of the polymer will decrease (along with its mechanical properties), which leads to decreased degradation time since smaller chains are easier to degrade [41], [43], [50]. Note that the polydispersity index (PDI, used as a measure of the broadness of a molecular weight distribution of a polymer) can increase or decrease, depending on the thermal history of the polymer. The Mw, Mn and the PDI (*i.e.* Mw/Mn) of thin film products can be measured using GPC [49], [51], [52]. Simplified weight loss measurements or studying the materials melt flow index (*i.e.* a measure of the mass of polymer that flows through a standardized die in 10 minutes) can also be used for studying the degradation [40], [49], [51].

One other way to study the degradation of PHB is to expose it to natural environments and burying plastic samples under soil; however, in such a case, conditions such as pH, temperature and humidity are not controllable and it can be difficult to monitor them in real time, making it difficult to obtain accurate results [41], [43], [53]–[55]. Therefore, environment simulation tests and/or other laboratory tests are more commonly used to assess degradation. Refer to Figure 2.5 for a schematic of such degradation tests. For example, aerobic or anaerobic conditions can be set to see how the polymer degrades in the presence or absence of air, respectively, with the consumption of O_2 and formation of CO_2 directly correlating to degradation of the tested polymer (i.e. Sturm test) [41], [43], [53]–[55]. Additionally, experiments can also be completed with purified enzymes known to degrade PHB or with

microorganism cultures and the incorporation of the clear-zone method mentioned previously in Section 2.1.3.1 and shown in Figure 2.5.

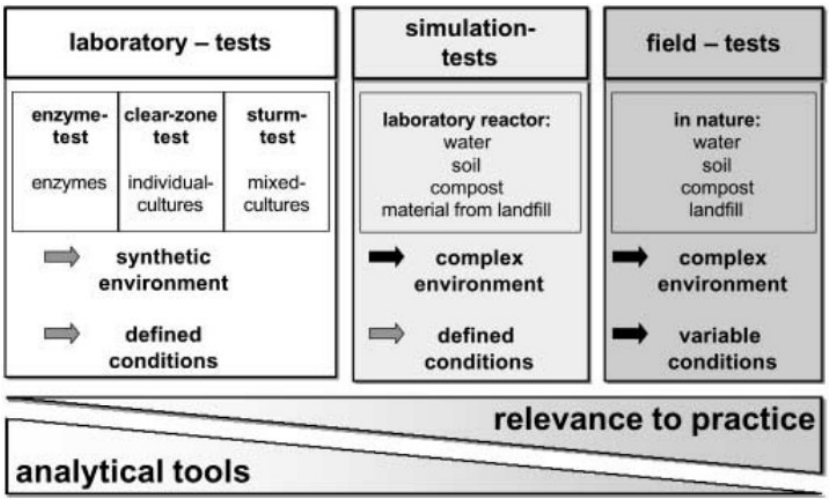

Figure 2.5: Schematic overview of tests for biodegradable plastics: (1) laboratory tests, (2) simulation tests and (3) field tests [55]

2.1.4 Applications of PHB

PHB is one of few commercially available polymers out of the large PHA class of polymers and it has been used in a broad range of applications, with many more under consideration for the future (see Table 2.3 for commercial sources of PHB and applications) [43], [56]. These many applications (both current and proposed) fall into various fields of study, but the two main areas are in packaging and for pharmaceutical/medical purposes [12]–[14], [33], [37], [43], [56]–[59].

Table 2.3: Commercial PHBs available for various applications [7], [8], [26]

Commercial Name	Manufacturer*	Applications
Biogreen®	Mitsubishi Gas Chemical Co., Inc. (Japan)	Component material for biodegradable polymers (cast films, latex gloves)
Mirel™ (3000 or 400 series)	Metabolix (USA)	Used in injection moulding, extrusion, cast film and thermoforming
Biocycle™ (various)	PHB Industrial S/A (Britain)	Films and medical applications
Biomer® (various)	Biomer Inc. (Germany)	Used in extrusion and products that involve food contact

*The manufacturers generally scale up PHB production through fermentation of sugars with bacteria bioreactors [26]

2.1.4.1 Packaging Applications

The polymer materials generally used for packaging have a wide range of application types, from short time storage followed by disposal (*e.g.* food packaging) to items meant for more long-term storage (*e.g.* electronics and cosmetic containers) [7], [14]. Most commonly, materials like PP, polyethylene (PE), poly (vinyl chloride) (PVC) and polyethylene terephthalate (PET) are used due to their low production costs, their favourable sealing/barrier properties and their acceptable mechanical properties [14]. More recently, polylactic acid (PLA) has been used as it has the same upsides as above while also being a bio-based polymer [14]. The largest drawback of these materials is their associated biodegradability (or lack thereof), and as such, an alternative to these materials is PHB, which is typically used for film packaging and rigid containers (see an example of such packaging in Figure 2.6) [14]. In either case, due to its excellent oxygen barrier properties, biocompatibility and efficient biodegradability, PHB is considered as a good potential candidate for food-related packaging, as most of these items are thrown out in a short period of time and will need to undergo complete degradation [12]–[15].

Although PHB can be used for such applications (and considered for many more), its biggest limitations for use as a packaging material is its poor mechanical properties and its high production cost [7], [14], [33], [39], [60]. For example, Bucci *et al.* purchased Biocycle® PHB in powder form, shaped the material into a jar and accompanying cap through injection moulding and the tested properties were compared to a similar product made of polypropylene (PP) [15]. They found that the overall performance of the pure PHB was worse than the products made of PP (in various environmental conditions) [15]. Injection moulding is a relatively inexpensive process so that was not a limitation in this case; however, excessive amounts of degradation and defects were observed following the processing of PHB (related to thermal degradation during processing) [15]. Therefore, introducing appropriate additives or blending other polymers with PHB is required [15], [26], [37], [41], [51], [61]. Refer to Section 2.2.3 for more on this.

PHB-based polymer films used for agriculture are also of interest, mostly due to the biodegradability of PHB. In fact, PHB has been used for packaging that degrades over a desired time, for controlled release of fertilizer and agrochemicals and as biodegradable plant pots that can be planted straight into the ground [14], [43].

Figure 2.6: Example of rigid polymer packaging. Note that this image is not of packages made from PHB [62]

2.1.4.2 Pharmaceutical and Medical Applications

Since packaging is often disposed of after a short period of utilization, the high cost associated with processing PHB (or similar Type A biopolymers) can be a concern; whereas in pharmaceutical and medical applications, there is often more importance placed on the material functions, structural and surface properties, and biocompatibility as opposed to solely the cost [14], [16]. PHB (as well as its degradation products) has excellent biocompatibility, and because of this, can potentially be used in tissue engineering scaffolds, targeted and controlled drug delivery carriers, surgical pins, sutures, artificial blood vessels and bone healing [8], [12], [64], [65], [13]–[16], [39], [43], [57], [63]. For example, porous PHB has more easily controllable biodegradation, useful for some of these biomedical applications [13]. Therefore, various processing methods and forms of PHB (*e.g.* porous, spray coated or thin films) need to be developed for targeted applications. At the same time, the purity of the materials used is quite important, as the presence of impurities in the material can reduce biocompatibility between the material and the body, and thus the material should not be used for certain applications as to avoid unwanted damage [33].

One more specific biomedical area in which PHB could be applied is osteogenics, an area of study concerned with tissues used for bone growth or repair [12], [16], [63], [65]. Gredes *et al*. have done research in this field, specifically looking at biopolymers like PHB as beneficial materials for bone grafting, based on similar piezoelectric properties to natural bone [66]. They found that finely tuned pure PHB patching (thermocompression molding of Biocycle® 1000) has excellent biocompatibility with human bone and has the potential to be a good osteoconductor (*i.e.* a guide for reparative growth of natural bone), stimulating bone growth and healing [12], [16], [63], [65], [66].

Similarly, tissue scaffolds for bone tissue repair were designed and fabricated by Ramier *et al.* [63]. The authors created 3 different types of scaffold mats using the processes of electrospinning and electrospraying, one made from pure PHB and two made from PHB and bioceramic nanoparticles of hydroxyapatite (nHA). Overall, they concluded, based on characterization and *in vitro* testing, that these biocompatible and biodegradable scaffolds have an extremely high potential for tissue regeneration, showing excellent compatibility, adhesion to tissue cells and cell proliferation [63]. The added benefit to both examples above is that these PHB products are degradable in the body. Therefore, after serving their purpose, they would degrade, saving the patient from having to have a second surgery for removal of a device. For these and other applications, processing techniques are required that can impart the desired properties to the material.

For both packaging and medical applications, proper processing techniques need to be used as to ensure the final characteristics and properties of the PHB product meet standards for the targeted application. Some of the current techniques could work but additional methods are being explored as to find the best options available.

2.2 Processing of PHB

2.2.1 Current Industry Processing Techniques

Like many other thermoplastics used in industry, PHB is generally processed by either extrusion or injection molding, with the former most commonly used for fibers, thin films and cast sheets, while the latter is used to create more complex shapes like bottles and packages for the food industry [7], [18], [67]. As previously stated, for PHB, it is important to keep the processing temperature below 190 °C as temperatures higher than this can lead to depolymerization and degradation [13], [18], [34], [40], [67].

Thin films of PHB with tuneable crystallinity, mechanical properties, and surface morphology have also been created by solvent casting in acetic acid at temperatures between 80 and 160 °C [13]. Typically, chloroform is used as the solvent because it of its excellent compatibility with PHB but other suitable solvents have been explored such as ethyl lactate, acetic anhydride and pyridine [13], [18], [26]. High-quality polymer films are obtained by dissolving PHB in a solvent and controlling the evaporation of the latter. The use of acetic acid was explored because (1) it is considered safer to use due to reduced health risks and environmental impact as compared to chloroform, which can remain in the thin film for long periods of time, (2) it is more cost efficient with less expensive solvent and less processing

time required, and (3) the process can be adjusted to provide a broader range of properties for the resulting polymeric material [13]. However, this solvent casting process is not ideal for large-scale processing or for creating blended thin film samples, and, thus, thermal processing methods such as injection moulding are still the best options. Generally, these thermal methods are more cost-effective, especially when additives or blending is performed. However, the addition of certain additives or other blending constituents can negatively affect the biodegradation rates and can increase health hazards through the release of toxic degradation products (*e.g.* leaching of plasticizers) [13]. This idea of blending polymers or introducing additives is studied further in Section 2.2.3.

In addition to extrusion and injection moulding, which require optimization for use with PHB, electrospinning and thermo-compression moulding are two techniques that have been used to process PHB; the former to create nanofiber mats and the latter to create thin films and polymer sheets (refer to Section 2.2.4 for more details) [12], [63]. Also, some forms of additive manufacturing or 3-Dimensional (3D) printing have been used to create thin films and fibres of PHB with promising results. However, processing PHB with the method known as fused deposition modelling (FDM), a specific form of additive manufacturing, has not been studied in literature. However, this technique has been studied in great detail with many thermoplastics, giving rise to promising results for use with PHB.

2.2.2 Extrusion and Additive Manufacturing Processing

2.2.2.1 Extrusion

Extrusion is a relatively simple process and is widely used for thermoplastics like PHB. In this process, a material is inserted into an extruder chamber that is at an elevated temperature. This elevated temperature is required for thermoplastics to flow; however, some materials can be extruded while cold. Inside the machine is a single screw or twin-screw setup (the latter being more common and often found to perform better) that rotates at a specified speed, and when all the material has been inserted into the machine and allowed to melt, the material is flushed through a die of desired shape and cross-section, forming a product. This process' biggest advantage is its ability to create complex cross-sections, based on the shape and size of the die used, as well as items like fibres, thin films and cast sheets. However, this process can be detrimental to PHB when operating above or near its degradation temperature – mainly due to the fact that the residence time of the polymer is set proportionally to the polymer molecular weight and that the polymer must spend time at an elevated temperature in the machine before

flushing [40]. Generally, the longer the PHB is exposed to the elevated temperature and shearing force of the rotating screw(s), the lower the molecular weight of the resulting product, due to thermal and mechanical degradation [13], [18], [34], [40], [67].

2.2.2.2 Fused Deposition Modelling (FDM) or 3D Printing

The process of FDM, often referred to as 3D printing, lies in the field of additive manufacturing. In these processes, structures are made by depositing material onto a heated bed layer-by-layer using an extruder nozzle element commonly known as a hotend and x-y-z-axes controls to allow complex and precise movements of the hotend (see Figure 2.7) [21], [68]–[71]. Four distinct zones can be associated with a 3D printed sample [69]:

1. Zone 1: solid layers deposited forming the base of the sample
2. Zone 2 and 3: perimeter filaments are deposited forming the main structure, with the interior built based on the chosen infill density and pattern
3. Zone 4: solid layers deposited forming the top of the sample

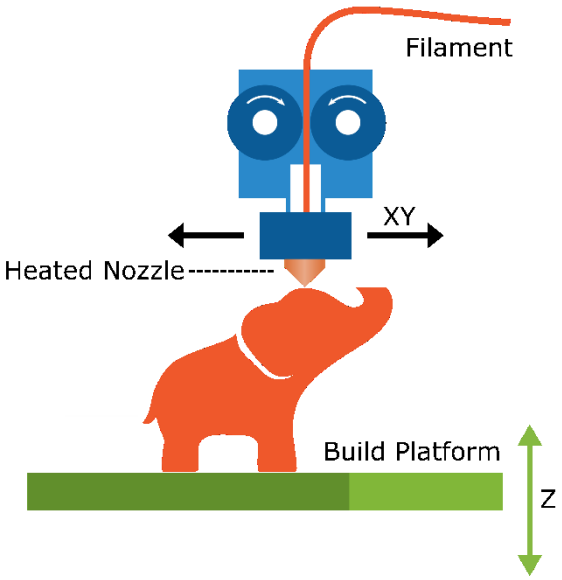

Figure 2.7: Schematic of Fused Deposition Modelling (FDM, commonly known as 3D printing). © 2017 Kholoudabdolqader. Modified with permission, CC by-SA 4.0 [21]

Typically, when working with thermoplastic polymer filaments, the filament is pushed through the hotend at temperatures above the T_g, as the material shows flexibility and flow characteristics [68]–[70]. This processing and laying of deposited filaments leads to "air gap, "void space" or the space between these deposited filaments. Adjusting the printing process to reduce this air gap through ideal filament adhesion in one layer and the fusion between layers

is necessary as this will lead to improved properties and an optimally printed sample [69], [70], [72]. The air gap percentage itself cannot be programmed into the printing process, which is why controlling temperature, environmental conditions (*e.g.* humidity and temperature), printing speeds, pattern, and density are key parameters (Figure 2.8) [69], [70], [72]. These parameters can also ensure that there is no warping, inner-layer delamination, or cracking caused by residual stresses during the printing process [69].

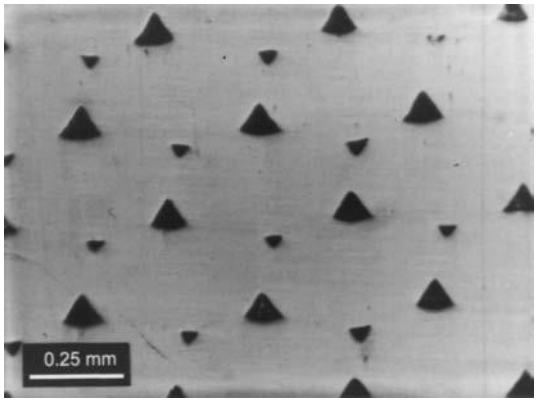

Figure 2.8: Mesostructure of an FDM acrylonitrile butadiene styrene (ABS) sample. This sample was built with optimum gap settings for ABS, producing minimum void density and structural defects while also maximizing bond density [70]

FDM printed structures made from well-studied 3D printing materials such as acrylonitrile butadiene styrene (ABS), PLA, nylon and polycarbonate (PC) commonly show decrease in mechanical properties as compared to bulk counterparts of the same material; approximately 45% decrease in E is observed while 30-60% decrease is often seen for σ_{UTS} [73]. An anisotropic effect is introduced by the layering and direction of the deposited filaments that greatly influence the overall strength of the 3D printed part [69], [72], [73]. Therefore, adapting the printing process to improve the strength of the material is necessary, and controlling air gaps is the most influential way of doing so [69]. In literature, recommended layer thickness (which should be kept small), deposition speed and flow rate have been noted for different types of materials [69]. In addition, the study of printing patterns and infill on the density and mechanical properties of printed ABS parts has been investigated by Fernandez-Vicente *et al.* [69]. In this work, a printing pattern known as rectilinear (see Figure 2.9) with 100% printing infill was the best option for improving E, $\sigma_{UTS,}$ and ε_b of ABS parts, as the higher level of structure density led to a minimal amount of air gap [69]. The authors also observed a decrease of over 54% in E as compared to raw injection moulded ABS [69], [73].

It should be noted that in this study, hotend and bed temperatures, layer thickness, and printing speeds were kept constant for all experiments based on recommended values for ABS [69].

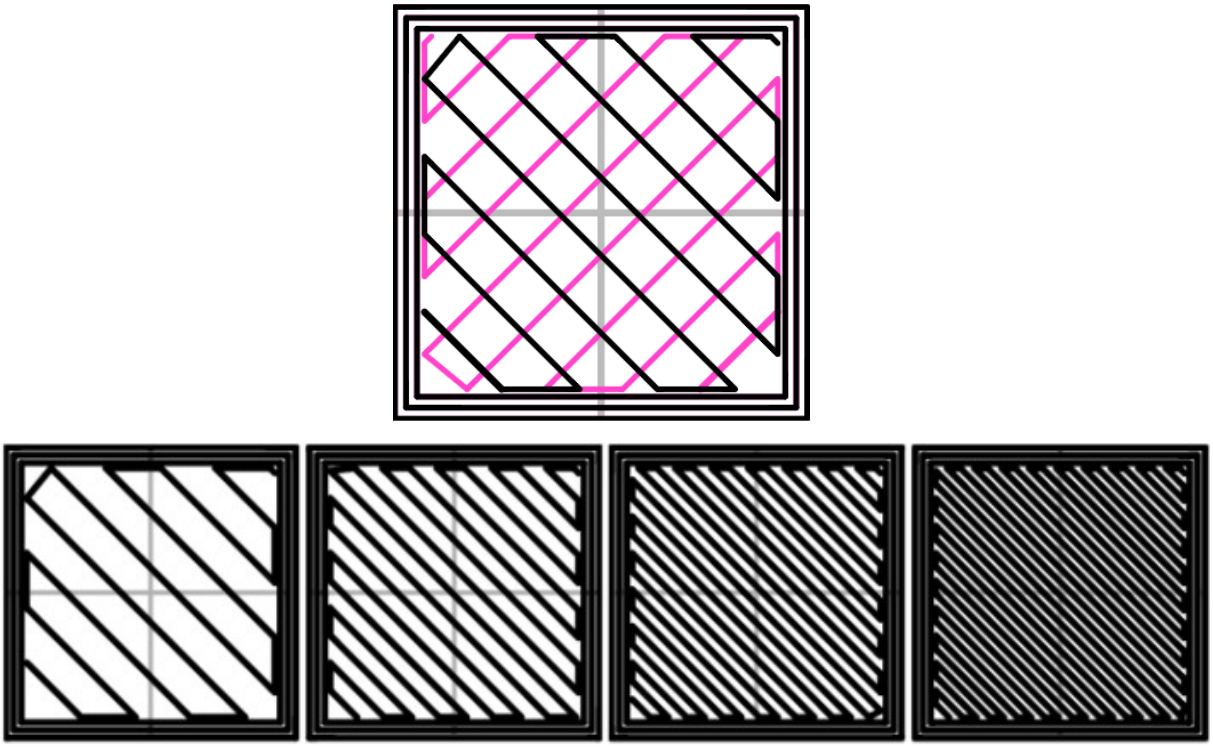

Figure 2.9: Rectilinear printing pattern (top); infill pattern at varying densities. Left to right: 20, 40, 60 and 80% (bottom). © Aleph Objects, Inc., CC by-SA 3.0 [74]

Therefore, with the proper printing process and associated parameters, complex, lightweight structures can be created for food packaging and medical applications such as artificial tissues, organs and arteries [71], [75]. No matter which polymer is investigated, the biocompatibility, biodegradability and mechanical properties are very important for medical applications, which is where the use of PHB will be extremely beneficial [57].

PHB processing with additive manufacturing is becoming more popular especially for certain biomedical applications since it can be completed without any additives or plasticizers [57], [64], [71]. These processes can be customized and scaled up for mass production all while having the capability of forming complex structures with minimal waste [71]. Selective laser sintering (SLS), a form of 3D printing technology, has been used for pure powdered PHB where each layer of the desired product is prepared by a CO_2 laser beam that sinters the powder particles together into a thin film or fibre; this technique was found suitable for PHB based porous tissue scaffolds (which can be used for bone tissue regeneration) [21]–[23], [64], [65], [71], [76], [77]. Pereira *et al.* used this manufacturing method to create scaffolds (as seen below

in Figure 2.10) with the physical product having dimensional properties nearly identical to those of the computer model [22], [23], [64]. For the scaffold seen in Figure 2.10, nearly 32.5 hours of SLS processing was required, but it was found that the thermal properties of the product and unprocessed powder were only slightly different, even after the extensive processing time [22], [23], [64]. This is quite different than what is seen with extruded samples of complex nature and this suggests 3D printing could be a more reproducible process than more traditional PHB processing approaches [22], [23], [64].

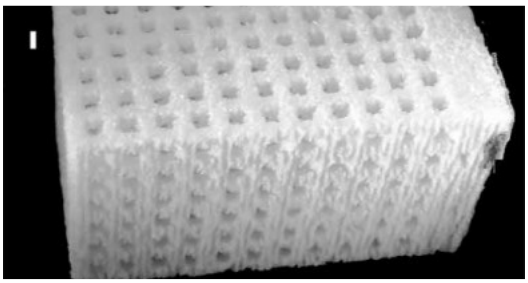

Figure 2.10: Printed PHB scaffold using SLS. The scan spacing was set at 0.15 mm, with a powder layer thickness of 0.18 mm [22]

Although printing with pure PHB has been completed using SLS, many challenges remain for processing PHB through FDM, especially when incorporating additives to improve the final properties of the printed product. A patent was filed back in 2016 that looks at creating more "ideal" 3D printable degradable PHB [78]. The author looked at combining pure PHB with modified starch and auxiliaries consisting of a plasticizer (ex. Di(2-ethylhexyl) phthalate or DEHP), antioxygen agent (ex. antioxygen 1010) and a lubricant (ex. fatty acid amide) in various ratios [78]. In the author's research, they found that the printing material had improved mechanical properties as well as thermal stability when the PHB composed more than 50 wt% of the material, and the auxiliaries were between 2-4% [78]. Such improvements in properties may be required if 3D printing is to be considered as a large-scale manufacturing process for food packaging (or related) applications, rather than for small-scale products for biomedical applications.

2.2.3 Plasticizers and Polymer Blending with PHB

Although some studies using PHB as functional components have been performed (*e.g.* packaging and biomedical applications), primarily this material is used for the creation of prototypes; the main reason being the poor mechanical properties and functionality of the pure polymer [75]. This leads to a restriction on commercial applications of pure PHB. Therefore,

there is a rationale for the relatively inexpensive modification of PHB's thermal and mechanical properties through the creation of plasticized PHB, blended polymers, or composites [7], [45], [79]. This is done by introducing particles, fibres, nanomaterials or other polymers to the PHB matrix.

2.2.3.1 Plasticizers

Since the early 2000s, worldwide production of plasticizers is approximately 4.5 million tonnes per year [80]. They are used in over 60 different types of polymers ranging from polymers of petrochemical origin to those of biological origin. Plasticizers will continue to play a large role in our economy, with a market size expected to reach 26.3B USD by 2025 globally, and our ecosystems [80], [81]. Plasticizers are low molecular weight substances added to polymers to promote processability, toughness and flexibility, which is especially key for PHB as one of the main challenges is to reduce its brittleness [7], [80], [82]–[88]. These substances change the behaviour of the polymer by interacting with its amorphous phase, reducing secondary bonds between polymer chains. This, in turn, reduces the overall interactions between polymer molecules and increases the mobility and chain flexibility without reducing the degree of crystallinity within the polymer [84], [87]. That being said, plasticizers may actually lead to a slight increase in crystallinity as a result of the enhanced mobility of the amorphous phase [87]. This increased chain mobility also helps to decrease the T_g and T_m of the polymer, and provides an improved processing window for the materials, helping to limit and/or completely prevent thermal degradation [80], [82]–[88]. Overall, the incorporation of plasticizing materials into polymers is a relatively simple step that helps reduce costs and improve processability [85]. However, the inclusion of additives such as plasticizers often leads to decreases in tensile properties and the modification of the polymer's degradability. These factors must be understood and controlled according to the desired application of the final polymeric product [80], [82]–[87].

PHB is quite different than common commercial polymers like PVC, as the average degree of crystallinity is in excess of 65% (as compared to 10% or less in PVC) [87]. This means that only a small portion of the PHB polymer matrix is amenable to the inclusion of plasticizers. Since these additives lodge themselves in the amorphous region, the maximum (useful) plasticizer loading is less than 30 wt% of the PHB (compared to more than 50 wt% for PVC) [87]. Depending on the plasticizer used, weight percentages up to 30 wt% can still lead

to substantial decreases in T_m and melt processing temperature, as well as an increase in ε_b, all desirable property changes for plasticized polymers [80], [82]–[87].

It should be noted that some plasticizers, known as prodegradants, are capable of introducing a negative effect on the thermal degradation properties of PHB, effectively accelerating its degradation [82]. Impurities present in the PHB itself can often be prodegradants, while inorganic materials such as aluminum and silica have been shown to have similar effects [82]. For example, from their solvent evaporation and compression moulding experiments, Janigova *et al.* found that glycerol, in amounts up to 10 wt% of PHB, has this prodegradant effect on PHB, likely due to an alcoholysis reaction [82]. However, further increases in the amount of glycerol resulted in the opposite effect – noticeable especially at 20 wt% – which could be due to recombination of fragmented PHB [82].

2.2.3.2 Bio-plasticizers and their use with PHB

As mentioned, the role of plasticizers is growing year after year and currently, there is a large assortment of plasticizers used in industry and just as many being studied in literature. DEHP, a xenobiotic compound that has been used with PHB, was first introduced as a potential plasticizing agent in 1930, and since then has been the most widely used plasticizing compound, due to its desirable properties and low cost [80], [81], [89]. However, DEHP, like many other diester phthalates and the metabolites resulting from their degradation, carries health hazards, such as disruption of the endocrinal system, carcinogenic properties, and high acute toxicity [89]. For these reasons, significant efforts are put forth to identify bio-based plasticizers which would be innocuous, biodegradable, more sustainable and safer to use. It was reported that the global market for bio-plasticizers is expected to grow at a compounded annual growth rate of 10.7% per year, reaching 2.7B USD by 2025, because of the widespread interest of replacing phthalate-based plasticizers [27].

One of the issues with PHB is its brittleness and thus, many recent studies have been performed with the inclusion of bio-plasticizers in PHB matrices in hopes of overcoming this drawback [80], [82]–[88]. Examples of bio-plasticizers tested with PHB include oxypropylated glycerin (or laprol) [26], [28], [88], glycerol [26], [28], [41], [82], [83], [88], polyethylene glycol (PEG) [26], [83], [88], [90], acetyl tributyl citrate (ATBC) [26], [28], [83], [88], glyceryl tributyrate (TB) [88], poly[di(ethylene glycol) adipate] (PEA) [88], soybean oil [26]–[28] and epoxidized soybean oil [26]–[28]. These compounds were selected based on their relatively low cost, high availability and natural origin.

As an example of their use, Seydibeyoğlu *et al*. studied the improvements of the mechanical and thermal properties when 10 wt% of epoxidized soybean oil was added to a PHB copolymer known as polyhydroxybutyrate-co-valerate (PHBV) [28]. This concentration of plasticizing oil was determined to be optimal to achieve improvements in impact strength compared to the neat polymer material [28]. In addition, the plasticized polymer had a lower E and σ_{UTS}, higher percent elongation, and approximately 4 °C lower melting temperature as compared to neat PHBV, as found from tensile testing and DSC analysis, respectively [28]. Similar changes in mechanical and thermal properties are expected with the addition of any of the above bio-plasticizers to the matrix of neat PHB.

Epoxidized canola oil (eCO) (Figure 2.11) is a similar material to epoxidized soybean oil, made from the conversion of canola oil, an important resource in Alberta [31]. This bio-based material shows potential as a plasticizing agent in various polymers, especially green polymers such as PHB as the eCO molecules could easily penetrate the macromolecules of the PHB chain (Figure 2.12) [28]. Additionally, eCO is non-toxic, is biodegradable and has a low environmental impact [31], [32]. The cost of this eCO material is not fully defined; however, the starting canola oil product sells for approximately 45% less than common petrochemical plasticizers [91], [92]. eCO is expected to have better plasticizing effects on PHB than neat canola oil because of its epoxy groups, which can interact with the carboxylic acid groups of PHB [28], [32]. If effective as a plasticizer for PHB, eCO could provide new markets and new sources of revenue for the canola sector, while providing a green, sustainable option to the polymer industry.

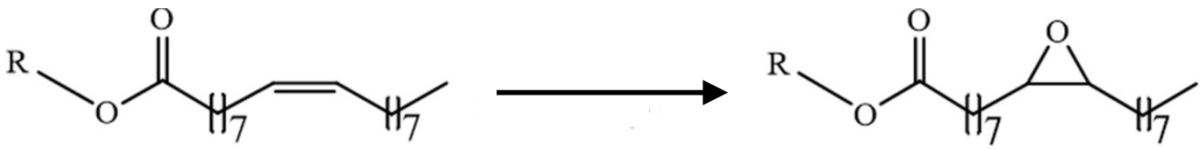

Figure 2.11: Structure of canola oil (left) and the conversion to eCO and its structure (right)

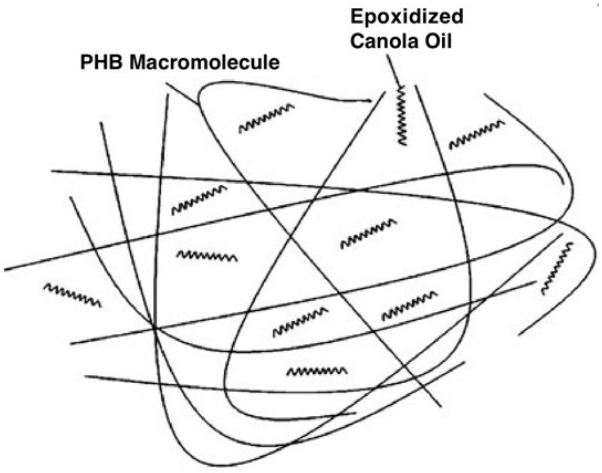

Figure 2.12: Schematic of the interaction between PHB and eCO. Modified (with permission) from [28]

2.2.3.3 PHB and Other Polymers

The blending of polymers is very similar to the concept of metal alloying, where two or more materials, in this case, polymers, are blended together to create a new material, which may have very different properties than the constituents it is made from [18], [93]. The goal for PHB specifically is to improve processability (by reducing the T_m) and the mechanical properties. These blends can be divided into three different categories: (1) immiscible/heterogeneous (2) miscible/homogeneous and (3) compatible [93]. Knowing the category that a specific polymer blend falls into is quite important for understanding what kind of properties should be expected and which kind of processing methods could be used [26].

PLA is one of the most widely studied Type A biopolymers, commonly synthesized through ring-opening polymerization of lactic acid [7], [8], [94]. PLA has generally better mechanical properties than PHB but has poor biodegradability. Although it is classified as an amorphous biodegradable polymer, it is not a "home degradable" biopolymer: it degrades biologically but not very easily, even under ideal conditions (temperature, humidity etc.) [94], [95]. Therefore, as pure materials, PHB and PLA both have drawbacks, leading to studies that incorporate a blend of the two polymers (at different ratios). This blending could lead to a polymer product that has improved characteristics and properties useful for applications such as food packaging and biosensors (*e.g.* improved stiffness and strength over pure PHB with improved biodegradability over pure PLA). Studies incorporating Fourier transform infrared spectroscopy (FTIR) and wide-angle x-ray diffraction (WAXD) characterization have shown that PHB/PLA blends are immiscible in nature but still have interactions at the molecular level, with the level of interaction depending on the molecular weight of the respective polymers

[24]. Additionally, the thermal, mechanical and degradation properties were found to be affected by both the molecular weights and the ratio of the polymers [24].

Additional work has been completed to improve the miscibility, interaction and mechanical properties of PHB/PLA blends. For example, Xiuyu *et al.* showed that interactions between PHB and PLA can be improved by adding a solubilizing agent such as polybutyrate adipate terephthalate (PBAT, otherwise known as polybutyrate) [96]. After characterizing the resulting mechanical properties, it was found that the addition of PBAT to the system led to a reduction in E and σ_{UTS}, but an increase in elongation at break [96]. In addition, it was determined that degradation (as measured by % weight loss after a specified amount of time in a controlled environment) of PHB/PLA blends with PBAT was greater than that of just PHB and PLA, and that the degradation rate was greater with increasing amounts of PBAT in the system [96]. A similar analysis was performed with the addition of zinc acetate, a high-efficiency transesterification reaction catalyst, during the melt blending process of PHBV and PLA [97]. The addition of this catalyst was expected to improve the miscibility and subsequently the mechanical properties of a PHBV/PLA blend through the exchange of an ester group of PLA with an alcohol group in PHBV [97]. Figure 2.13 shows how the transesterification mechanism takes place, specifically for PHB and PLA [97].

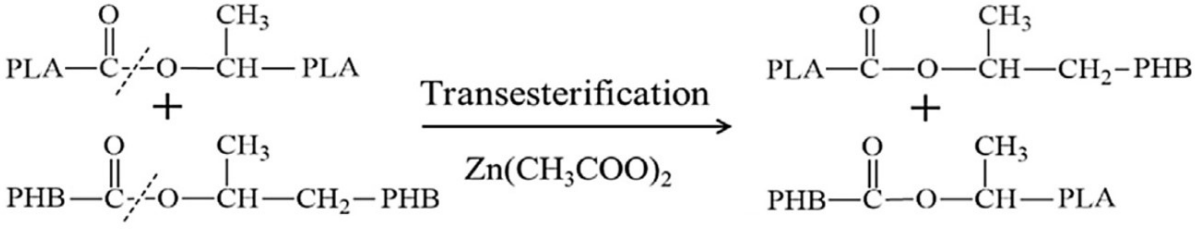

Figure 2.13: Transesterification mechanism of PHB and PLA [97]

Although PHB has been used with additive manufacturing processes such as SLS (refer to Section 2.2.2.2), PLA is currently one of the main material choices for FDM style 3D printing work, especially when prototyping products, due to its ease of use and relatively low cost. Therefore, there is plenty of literature that can help with understanding how to work with this material, which can lead to beneficial information on how to create blends of PHB and PLA.

PEG is another polymer that has recently been used in blends with PHB [90]. For example, Bugnicourt *et al.* produced a blended solution of PEG and PHB mixed at different

compositions [26]. Using different characterization methods, they found that the T_m of the blend was slightly lower than that of pure PHB. This was attributed to the plasticizing effect that PEG has on the PHB polymer chains [26]. At the same time, the elongation at break increased approximately four-folds compared to pure PHB [26]. Such blends can be used as water-soluble brushes for medical field applications [37].

Melt extrusion has also been used to mix together PHB and another polymer to create a blended product. One example where this concept was used was when PHB and polyethylene (PE) were blended together using single screw melt extrusion with many of the constituent's properties (*e.g.* mechanical and thermal) being enhanced for packaging applications [60]. Similarly, the company Wacker makes a polyvinyl acetate (PVA)-based resin product called Vinnex® that can be added to various biopolymers by extrusion to improve their processability [61]. This product has been used with PHB to improve physical properties and processability, depending on the grade and quantity of Vinnex® used [37], [61]. For example, it was determined that the crystallinity of the PHB could be controlled and the T_m of the polymer could be lowered, all while increasing the elongation at break and σ_{UTS} [37], [61].

PCL is another biocompatible and biodegradable polyester that has been blended with PHB to improve its end-use properties, increase the biodegradability and reduce cost [37], [51]. Like PLA, it has been found (using differential scanning calorimetry (DSC), scanning electron microscopy (SEM) and polarized optical microscopy) that the two materials are immiscible in the entire composition range [51]. However, there is a possibility that these two materials can be blended together and used with 3D printing technology [51]. Lovera *et al.* produced high molecular weight PHB/PCL blends as well as PHB/low molecular weight chemically modified PCL blends (*i.e.* PHB/mPCL) and investigated their morphology, crystallinity and enzymatic degradation [51]. Films were created by mixing various compositions of the materials, dissolving them in chloroform and solvent casting them at room temperature for 7 days [51]. Blended products were also created by solution blending followed by extrusion; however, extreme degradation was observed from this method and, thus, the solvent casting method was prioritized [51]. The authors concluded, that PHB and PCL are completely immiscible over the range of mixing ratios (in the case of the high molecular weight products) [51]. However, the PHB/mPCL blends were determined to be partially miscible, with clear phase formation and signs of the PCL plasticizing the PHB chains [51]. In addition, both the T_m and T_g were lower than that of pure PHB, with the difference increasing with more mPCL in the system [51]. This improved interaction between PHB and mPCL also lead to a reduction in degradation rate when

exposed to *Aspergillus flavus*, a fungus known to degrade both polymers [51]. Note that although PCL might be a viable option for improving PHB for commercial use, one downside of using it as a blend material is that it is not a bio-based polyester but rather a synthetic biodegradable polymer based on fossil fuels (*i.e.* Type C) [3], [8].

2.2.4 General Changes in PHB during Processing

In addition to blending or incorporating plasticizers, using processes such as melt extrusion, hot-pressing and/or 3D printing can lead to altered characteristics of the resulting polymer material. These processes are chosen as they are relatively easy and efficient, and can be used for blending polymers quickly, unlike solvent casting. However, each method does incorporate elevated temperatures and could lead to different final properties, such as crystallinity, molecular weight, mechanical properties and degradability [40], [41], [75]. Therefore, these characteristics must be studied and compared for each technique and polymer ratios.

Generally, the extrusion process can drastically change the mechanical properties as well as degradability of PHB [40]. Studies have shown that the σ_{UTS} and ε_b decrease as the temperature and screw speed are increased, while the elastic modulus remains unaffected [40], [41]. At the same time, the average molecular weight decreases with increasing extrusion temperature and screw speed, leading to an increased biodegradation rate of PHB [40], [41]. This occurs due to thermal degradation of the PHB when temperatures are above its melting temperature, decreasing crystallinity, and the shearing stress brought on by the rotating screws (*i.e.* introduction of mechanical degradation). When the shear stress is high enough, the polymeric chains of PHB can be cleaved, leading to a reduction in molar mass and viscosity of the polymer (*i.e.* chains have higher mobility), and thus, increased degradation [40], [41]. This highlights how processing temperature and screw speed are important parameters defining the desired final mechanical properties of PHB products and the degradation of PHB even before the product is formed. In addition, the rate of cooling of the material influences crystallization (*i.e.* faster cooling means fewer crystals formed) [50].

Thellen *et al.* prepared three different PHB cast films using single screw extrusion with the machine's temperature zones ranging between 165 and 173 °C, and the chilling rollers sitting at 60 °C (which correlates to the cooling rate of the final product) [98]. Using gel-permeation chromatography (GPC), the final polymer molecular weight (film form) was found to be 8-19% smaller than the original value (pellet form) [98]. This can be compared to a 43-78% difference when twin-screw setups are used, likely due to the aggressive shear stress in

this system [98]. Therefore, extrusion can introduce significant degradation, from both thermal and mechanical processes, if the processing parameters are not well controlled. On the other hand, the mechanical analysis showed that the fabricated PHB films had comparable σ_{UTS} and E to other thermoplastics such as PE, which is commonly used in food packaging [14], [98]. Finally, it was found that the biodegradation of the resulting PHB films was unchanged from pellets; 88-99% biodegradation under static optimum laboratory conditions (note that it was specifically tested for marine use) [98].

Mottin *et al.* found that the final properties of PHB are affected by the degree of the crystallization in the material, which in turn is dependent on processing conditions [12]. In their experiments, they produced PHB nanofiber mats, through electrospinning, and thermo-compressed films [12]. Using FTIR and WAXD, the authors determined that the film produced by thermo-compression had a higher crystallinity than the electrospun mat [12]. One interesting observation was that as processing temperatures were increased for the electrospun process, the degree of crystallinity increased, as metastable amorphous phases within the material transformed to crystalline phases (as confirmed by DSC characterization) [12].

3. EXPERIMENTAL PROCEDURES

In this chapter, the materials used in this study and the preparation methods for the hot-pressed polymer sheets and FDM printed tensile specimens are introduced. These materials include polyhydroxybutyrate (PHB), which is the main material of this work, polylactic acid (PLA) epoxidized canola oil (eCO), and zinc acetate crystalline powder. Additionally, the different characterization techniques for the analysis of the products are described. These include microscopy, spectroscopy, calorimetry, thermal gravimetric analysis, and tensile testing.

3.1 Materials

The PHB material used in this work was obtained as thermally processed pellets (BRS Bulk Bio-Pellets, Bulk Reef Supply, Golden Valley, USA). X-ray photoelectron spectroscopy (XPS) surface analysis was used to measure the chemical composition of the as-received pellets and it was found that the surface contained ~ 5 wt% Ca and Si, which likely remained as impurities after the pelletization of PHB. This gives a PHB purity of 95%. In addition, gel-permeation chromatography (GPC) was performed on the PHB pellets and the weight average molecular weight (Mw) was determined to be 247,700 ± 1,473 Da, with a polydispersity index (PDI) of 3.10 ± 0.07. Thermally processed pellets of PLA (4043D PLA Pellets, Mw: 390,000 Da, NatureWorks LCC, Minnetonka, MN, USA) were also used. PLA is an amorphous polymer that can act as a polymeric plasticizer when blended with PHB [88]. The PHB and PLA pellets were either used as-received or washed with isopropyl alcohol (to remove surface impurities) and dried at 70°C for at least 8 hours prior to use to prevent microbial contamination and remove absorbed water from the environment.

eCO was kindly prepared and provided by Dr. Aman Ullah's lab from the University of Alberta, Canada (see chemical structure in Section 2.2.3.2 and provided FTIR data in Appendix A). Zinc acetate crystalline powder (No. 383317, Sigma-Aldrich, St. Louis, MO, USA) was used as a catalyst to enhance the miscibility and improve the mechanical properties of PHB/PLA blends [97].

3.2 Preparation of Samples

3.2.1 Hot-Pressed Plasticized Samples

PHB and plasticized PHB samples were processed to obtain hot-pressed samples to be tested for mechanical properties. Plasticized PHB samples contained the polymer combined with one

or a combination of PLA, eCO, and zinc acetate. The compositions of the different plasticized PHB materials tested are summarized in Table 3.1.

The secondary and ternary material blends were initially mechanically-mixed before being placed in a HAAKE Minilab II micro compounder (Thermo Scientific, USA). This extruder system (Figure 3.1) has a conical twin-screw setup with counter-rotating screws, which provides remarkable mixing capabilities and better control over process parameters, in comparison to single screw setups [99]. Extrusion temperature and screw speed were set at 175 °C and 35 rpm, respectively, with a residence mixing time of approximately 5 min. These parameters were chosen to obtain void-free pellet-like materials while preventing thermomechanical degradation that could be brought on by the extrusion process [70].

To form sheets, the extruded material was then transferred to a Carver #4386 hydraulic hot-press (Carver, Inc., USA) in which it was pressed into polymer sheets with a length, width, and thickness of 70 mm, 80 mm, and 0.5 mm, respectively, using an AISI 1008 low carbon steel mould with these dimensions. In order to acquire these samples, the blended material was placed on the bottom plate of the press (heated to 175 °C) and allowed to soften for approximately 1.5 min. Light pressure was then introduced between the top plate (also at 175 °C) for 30 s to allow the material to spread throughout the mould. Finally, 2.13 MPa of pressure was applied for 1 min. The pressure was then released, and the sample and mould were removed from the press and allowed to cool at ambient temperature to obtain the final samples. Following pressing, the resulting sheets were cut into the required dimensions for tensile testing (refer to Section 3.3.1).

Table 3.1: Sample codes and compositions of blends used in this work

Sample	PHB:PLA (wt:wt)	eCO (wt%)*	Zinc Acetate Catalyst (wt%)*
NeatPHB	1:0	0	0
PHB/5eCO	1:0	5	0
PHB/10eCO	1:0	10	0
PHB/20eCO	1:0	20	0
PHB/30eCO	1:0	30	0
PHB/PLA	3:1	0	0
PHB/PLA/Cat	3:1	0	0.3
PHB/PLA/5eCO/Cat	3:1	5	0.3
PHB/PLA/10eCO/Cat	3:1	10	0.3

*wt% or weight percent, in this case, is defined as the weight of the component divided by the weight of the entire polymer blend, multiplied by 100%

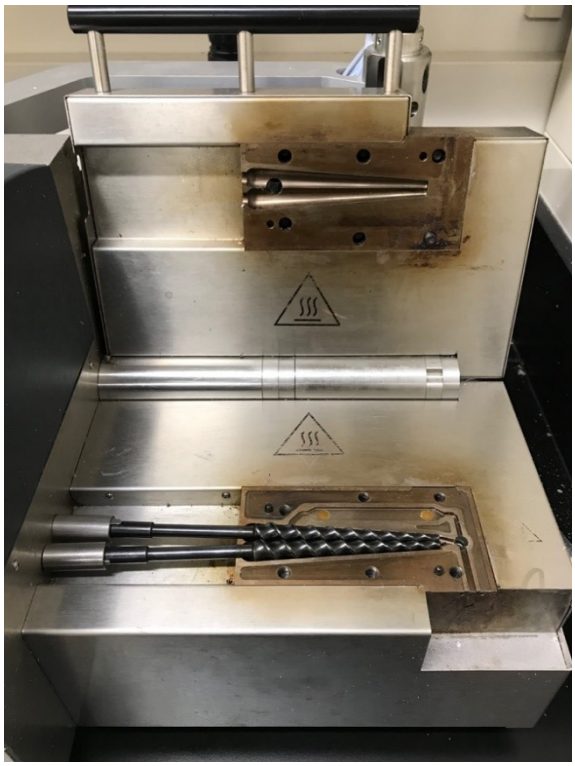

Figure 3.1: HAAKE Minilab II micro compounder with a conical twin-screw setup

3.2.2 FDM Samples

The as-received PHB pellets (Figure 3.2(a)) were placed in the same HAAKE Minilab II micro compounder (Thermo Scientific, USA), which has a twin, counter-rotating screw setup (Figure 3.1). Extrusion temperature, screw speed and nozzle diameter were set at 175 °C, 35 rpm, and

1.75 mm, respectively, with a residence mixing time of approximately 5 min. Similarly to the hot-pressing sample preparation, these parameters were chosen to achieve a material viscous enough to create void-free material and to prevent thermomechanical degradation that could be brought on by the extrusion process [70], [100]. The difference in sample preparation from the hot-pressed plasticized samples was the incorporation of a 1.75 mm nozzle die that was placed on the outlet of the extruder. This die allowed the extrusion of void-free filaments that could be used directly in FDM printing (Figure 3.2(b)). The extrudate (*i.e.* material that was extruded through the die) was flushed out manually with the 35 rpm screw speed dictating the rate at which the material extruded, with the collected filaments having a diameter of 1.75 ± 0.15 mm (n = 5) and approximate lengths of 600 mm. The filaments with diameters of 1.75 mm or less were chosen for the printing process as anything larger could not be fed into the printer itself, due to the restrictions of the printer's extruder setup.

The FDM 3D printer used to create the samples was a GEEE Tech Prusa i3 with an MK8 extruder setup (GEEE Tech, Shenzhen, China) along with Repetier-Host as the 3D printing application (Hot-World GmbH & Co. KG., Germany). The nozzle diameter of the FDM extruder unit was 0.30 mm, giving a center-to-center spacing between printed lines (*i.e.* printing wavelength) of 8.4 μm. Printing parameters for the prepared samples were set in the printer software and can be seen below in Table 3.2. To assist in the printing process, two different methods were used: (1) a 3D printing brim and (2) additional bracing in the design of the tensile dog bone specimens. A 3D printing brim (a commonly used printing technique that is selected in the software) is an outline of printed material that attaches to the edge of the printed sample, creating a large ring around the main part [101]. This brim, with a thickness of 0.1 mm (*i.e.* 1 deposited layer) and width of 5 mm, peeled off from the sample easily after the printing process was complete. It was used at it helped prime the hotend (*i.e.* prepared the extruder nozzle for continuous deposition) as well as prevent sample warping and delamination from the print bed. On its own, this approach was not sufficiently strong to prevent warping. Therefore, in addition to this technique, bracing was built into the design of the tensile specimen. Each layer for the bracing material was printed after the perimeter and infill of the specimen itself was printed, following the same printing parameters as seen in Table 3.2. The bracing was cut from the specimen before characterization. This approach also helped prevent sample delamination from the print bed, which in turn improved the part quality and was expected to reduce stress from warping. See Figure 3.2 for a schematic of the overall process and for an example of a printed tensile sample with the aforementioned bracing (brim not

included). The total length, gauge length, and gauge width of the tensile specimens were 76 mm, 20, mm and 4 mm, respectively, with approximate thicknesses of 1 mm for both the tensile specimen and the bracing.

Table 3.2: Printing Parameters for FDM processing

	Tested Range	Chosen
Nozzle Temperature (°C)	175-185	180
Print Bed Temperature (°C)	90-110	110
Layer Thickness (mm)	n/a	0.1
Total Number of Layers	n/a	10
Print Speed (mm/s)	n/a	15
Infill Pattern (degrees, °)	n/a	Rectilinear, 45
Infill Density (%)	n/a	100

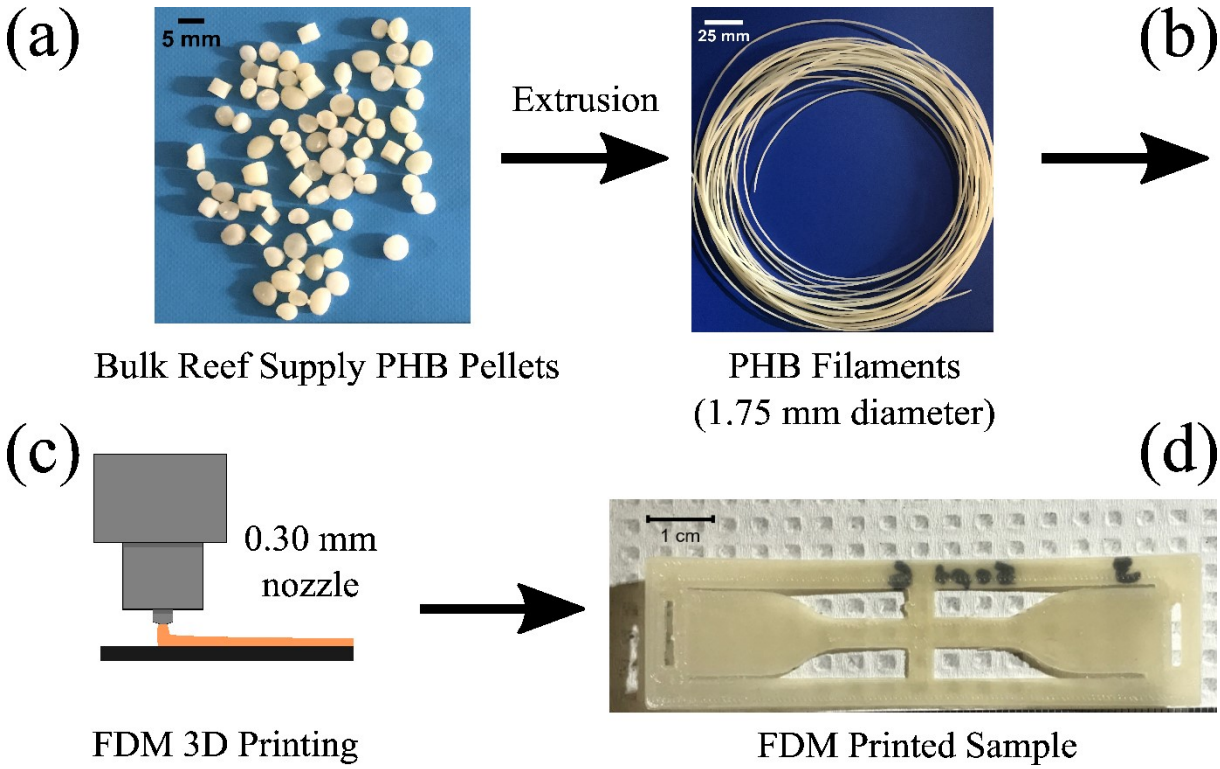

Figure 3.2: FDM processing schematic. As received Bulk Reef Supply PHB Pellets (a) are extruded into PHB filaments with 1.75 mm diameters, (b) and are used in the FDM 3D printer, (c) to create mechanical testing samples with bracing, (d) for characterization

3.3 Characterization of Material Properties

3.3.1 Mechanical Properties

An Instron 5943 tensile tester (Instron, Norwood, MA, USA) equipped with a 1kN load cell was used to carry out all of the mechanical testing. Testing was performed according to ISO

Standard 527 (Part 1 and 2): a strain rate of 2 mm/min (due to the brittle nature of the material) was applied to flat, bone-shaped specimens (Type 5A, n = 5) [102], [103]. The Young's modulus (E) was calculated as the slope over the linear region of the stress-strain curve. Ultimate tensile strength (σ_{uts}) and strain at break (ε_b) were also determined. Statistical t-test analyses were performed between different sets of results; unequal variances and a significance level of $\alpha = 0.05$ were used in the evaluations, corresponding to a 95% confidence interval.

3.3.2 Microscopy

A Zeiss Sigma 300 VP field emission scanning electron microscope (FE-SEM) (Zeiss, Cambridge, UK) was used to investigate the morphology of the plasticized samples. A thin film of carbon (approximately 10-20 nm) was deposited onto the samples by using an EM SCD 005 carbon evaporation system (Leica Baltec Instruments, Balzers, Liechtenstein) to avoid surface charging during SEM. The images were captured using the secondary electron (SE) mode with a voltage of 5.00 kV. For top surface images, unaltered samples were used, while cross-sectional images were collected of the fracture surface of mechanically tested samples.

A Leica M205 C stereomicroscope (Leica Microsystems Inc., Canada) equipped with FusionOptics was used to collect high-resolution surface images of the FDM printed samples. This microscope has an optical resolution of 0.952 microns and uses a surface reflected light setting. In addition, an Olympus Laser OLS 3000 Confocal Microscope (Olympus America Inc., Center Valley, USA) was used to collect optical images of the same FDM printed samples. This microscope provides imaging of higher resolution and contrast using a spatial pinhole and laser light. Multiple images were collected by the camera and then pieced together by the software to form a 3D image, showing not only the top layer of the samples but also subsequent layers. These intensity map images enabled a comparison of the regions of PHB material versus volume of air gaps, as opposed to the surface images collected from the stereomicroscope.

3.3.3 Fourier-Transform Infrared Spectroscopy

Fourier-transform infrared spectroscopy (FTIR) was performed on the plasticized samples with an Agilent Cary 600 Series FTIR Spectrometer (Agilent Technologies Inc., Santa Clara, CA, USA) equipped with a universal attenuated total reflectance (UATR) accessory. The spectra were recorded at frequencies between 400 and 4000 cm^{-1} and the data was analyzed using the program *FTIR Spectrum Software*. This software helps to examine the infrared absorption

bands associated with the samples to identify molecular components, structure, and dispersibility.

3.3.4 Differential Scanning Calorimetry

Differential scanning calorimetry (DSC) was used to obtain the melting temperature and the shape of the melting endotherm of the PHB pellets, extruded materials, hot-pressed blends, and FDM printed samples. This thermal analysis was performed for each sample within 24 hours of its production in order to limit the effects of polymer ageing at room temperature [84], [104]. A Mettler-Toledo Flash DSC Model 1 (Mettler-Toledo, Canada) was used under a nitrogen flow of 50 mL/min for the experiments after being calibrated using indium and zinc standards. Samples of approximately 5 mg were placed in closed aluminum pans for each run and thermal analysis was carried out from -20 to 195 °C, followed by a steady temperature of 195 °C for 5 min (to remove any prior thermal history), and concluding with a cooling run from 195 to -20 °C, all at a heating/cooling rate of 20 °C/min. This heating/cooling rate was selected to limit the extent of recrystallization and thermal effects during the heating cycle [13]. The measures of T_m and enthalpy of melting (ΔH_m) obtained from this technique are parameters used to assess the PHB thermal degradation [82]. The degree of crystallinity of PHB (X_{cDSC}) was determined using Equation 3.1 as a function of melting peak area:

$$X_{cDSC}\ (\%) = \frac{\Delta H_m}{\Delta H_m^0 \cdot w} \times 100 \tag{3.1}$$

where, ΔH_m is melting enthalpy, ΔH_m^0 is the melting heat associated with pure crystalline material (146 J/g for PHB), and w is the weight fraction of the PHB in the blend [40], [88], [105], [106]. The ΔH_m was measured from the DSC using an integral tangential baseline setting in the Mettler Toledo STAR^e thermal analysis software in order to most closely reflect the true area under the melting peaks (see Figure 3.3).

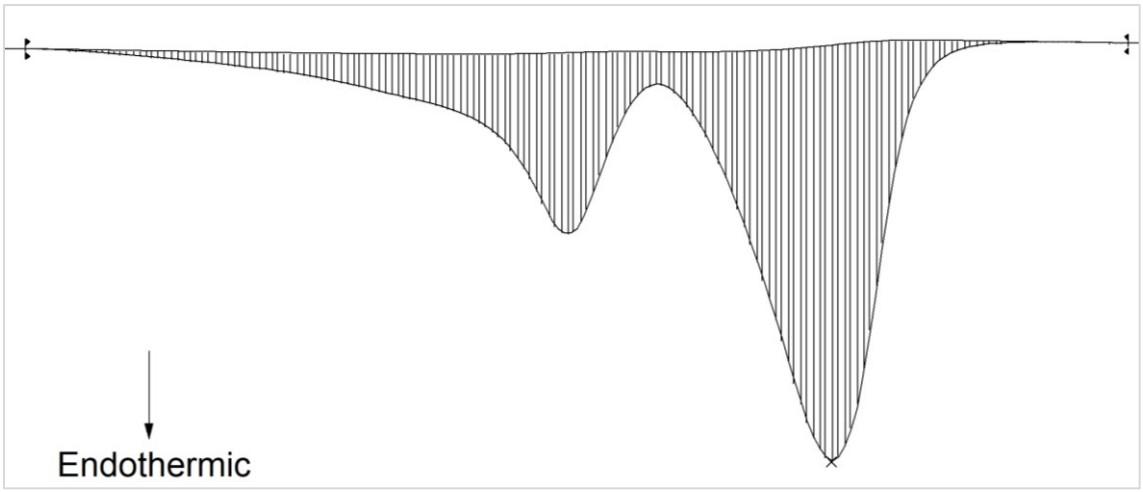

Figure 3.3: Example of how the integral tangential baseline method was used to acquire ΔH_m from the DSC curve.

3.3.5 Thermal Gravimetric Analysis

Thermal gravimetric analysis (TGA) was used to study the thermal stability (related to thermal decomposition) and extent of thermal degradation of the material caused by the processing methods (*i.e.* extrusion, hot-pressing, and FDM) as well as the addition of eCO and/or PLA. A Mettler Toledo TGA/DSC 1 (Mettler-Toledo, Canada) system equipped with an ultra-microbalance cell and differential thermal analysis (DTA) sensors was used for this analysis, with scans being carried out from 25°C to 380 °C at a heating rate of 10 °C/min under a purge of 20 mL/min nitrogen in unsealed alumina crucibles. The sample mass in all tests was approximately 10 mg.

4. RESULTS AND DISCUSSION – PLASTICIZED SAMPLES

In this chapter, the results obtained from the characterization techniques noted in Chapter 3 are highlighted for the hot-pressed plasticized PHB samples (Table 3.1) followed by a discussion of the findings. The first set of tested samples contained different amounts of eCO (5, 10, 20 and 30 wt%) in order to study the effects of the bio-based plasticizing oil on the PHB matrix and to determine if it can reduce the brittleness of the material while maintaining thermal stability. The second set of samples introduced PLA into the PHB matrix (ratio of 3:1 for PHB:PLA), along with a blending catalyst for the polymers (zinc acetate, 0.3 wt%) and the eCO plasticizer (5 and 10 wt%). These samples were characterized to determine if a bio-based oil (*i.e.* eCO) and polymeric plasticizer (*i.e.* PLA) can improve the overall properties of PHB to create a product more suitable for commercial applications.

4.1 Mechanical Properties

eCO was added to the polymer matrix to provide plasticizing effects on the system. It was expected that the eCO would plasticize the material, causing the E and σ_{UTS} to decrease, and the ε_b to increase, which, overall, decrease the brittleness of the polymer. Stress-strain curves of hot-pressed NeatPHB and four eCO plasticized samples are shown in Figure 4.1(a). The experimental results of the performed tensile tests for these samples (*i.e.* Young's modulus, E, ultimate tensile strength, σ_{UTS}, and strain at break, ε_b) are reported in Figure 4.1(b-d). As expected, the NeatPHB samples showed characteristics of a brittle thermoplastic material (*i.e.* a low ε_b value of 4.5 ± 0.4%) with relatively high modulus (E = 1194 ± 102 MPa). This parallels other values from the literature [18], [34], [38], [39]. With the addition of 5 wt% eCO (*i.e.* PHB/5eCO), an increase in ε_b from 4.5 ± 0.4% to 5.4 ± 1.4% was observed (as compared to hot-pressed NeatPHB), although this value was not found to be statistically significant (p = 0.13). This same amount of eCO also gave decreases in E and σ_{UTS} (from 1194 ± 102 MPa to 989 ± 72 MPa and 26 ± 1 MPa to 25 ± 1 MPa, respectively) where a significant difference between the E of the NeatPHB samples and the PHB/5eCO samples (p = 0.01) was observed. However, there was no statistically significant difference between the two samples in regards to the σ_{UTS} (p = 0.09). The PHB/10eCO samples showed even more of an improvement in ε_b (from 4.5 ± 0.4% to 8.0 ± 1.5%), with decreases in E and σ_{UTS} (from 1194 ± 102 MPa to 855 ± 32 MPa, and 26 ± 1 MPa to 22 ± 3 MPa, respectively). There were significant differences in all three parameters tested between the NeatPHB samples and the PHB/10eCO samples (p = 0.001, 0.01 and 0.002 for E, σ_{UTS}, and ε_b, respectively). This analysis suggests that eCO at

10 wt% works well as a plasticizer with PHB, whereas 5 wt% of eCO is not a high enough content to significantly change the properties of the material. With an eCO-content greater than 10 wt%, the material's E and σ_{UTS} continued to decrease; however, the ε_b decreased below that of hot-pressed NeatPHB instead of increasing, as would be typically expected with an increasing plasticizer content. This trend change is likely due to the release and/or segregation of the eCO from the polymer matrix, as a saturation point may have been reached [86]. Similar results were observed by Balitieri *et al.* when the weight percent of the petrochemical-based plasticizer dioctyl phthalate (DOP) was increased past 10 wt% in a PHB matrix [86].

Stress-strain curves of hot-pressed NeatPHB, hot-pressed NeatPLA (as a reference) and four plasticized samples containing eCO, PLA and/or catalyst are shown in Figure 4.2(a). The experimental results of the performed tensile tests for these samples (*i.e.* E, σ_{UTS}, and ε_b) are reported in Figure 4.2(b-d). Hot-pressed NeatPLA was tested as a reference sample to compare to both hot-pressed NeatPHB and the samples that blend PHB and PLA together. From Figure 4.2(b-d), the mechanical properties were determined to be better than the NeatPHB samples, as expected; however, the main reason for studying PHB is its superiority in biodegradability and biocompatibility as compared to PLA (see Section 2.2.3.3). Since each of the polymer materials have weaknesses, with the main focus of this work being improvement of the mechanical properties of PHB, the addition of PLA into the PHB matrix was explored. The addition of 25 wt% PLA showed drastic improvements in both the E (1194 ± 102 MPa to 1531 ± 70 MPa) and σ_{UTS} (26 ± 1 MPa to 31 ± 2 MPa) as compared to hot-pressed NeatPHB (Figure 4.2(b and c), respectively), which were found to be statistically significant (*i.e.* $p < 0.05$). As expected, this increase in material strength also resulted in a statistically significant decrease in ε_b compared to hot-pressed NeatPHB (from 4.5 ± 0.4% to 3.2 ± 0.5%), meaning that the material became more brittle. These improvements in strength are associated with strong polymer-polymer blending through the extrusion and hot-pressing processes.

To further improve the blending between the two polymers, zinc acetate was added [97], [107]. Zinc acetate is known to help catalyze the transesterification reaction between different sets of thermoplastic polymers which is why it was investigated in this work [97], [107]. For example, Ardal *et al.* used 0.5 wt% zinc acetate for a blend of polycarbonate (PC) and a polycaprolactone (PCL)-polydimethylsiloxane (PDMS)-PCL copolymer [107] while Yang *et al.* investigated amounts between 0.05 and 0.4 wt% for a blend of PLA and polyhydroxybutyrate-co-valerate (PHBV) (in a 2.33:1 ratio of PLA:PHBV) [97]. As both of these polymer blends, and the base matrix, were different than what is studied in this work, a

value of 0.3 wt% was chosen, aiming to explore the effect of zinc acetate in the blending and plasticizing of the polymers studied here.

With the addition of this catalyst (*i.e.* PHB/PLA/Cat), a reduction in E and σ_{UTS} was seen as compared to the PHB/PLA samples (from 1531 ± 70 MPa to 1056 ± 62 MPa, and 31 ± 2 MPa to 26 ± 1 MPa, respectively); however, the observed values were similar to those of the NeatPHB samples (E = 1194 ± 102 MPa and σ_{UTS} = 26 ± 1 MPa) with decreases still seen with respect to this sample. Furthermore, an increase in ε_b (*i.e.* reduction of material brittleness) was observed as compared to both the NeatPHB and PHB/PLA samples (from 4.5 ± 0.4% and 3.2 ± 0.5%, respectively, to 6.2 ± 1.0%). The difference in mechanical property values between the NeatPHB and PHB/PLA/Cat samples as well as the PHB/PLA and PHB/PLA/Cat samples was examined and determined to be statistically significant (*i.e.* $p < 0.05$), while the difference in mechanical property values between the PHB/PLA/Cat and the NeatPLA reference samples were only statistically significant for the E and σ_{UTS} (*i.e.* $p = 0.17$ for the ε_b). Although the mechanical properties were deemed significantly different (as compared to the hot-pressed NeatPHB and PHB/PLA blend), the catalyst did not give the expected results (*i.e.* increase in strength) and from these mechanical results alone, it cannot be concluded that the blending between PHB and PLA was improved with the addition of 0.3 wt% of the zinc acetate.

The results obtained with the zinc acetate are different than those shown previously in the literature. For example, Yang *et al.* added zinc acetate as a transesterification catalyst in amounts up to 0.4 wt%, to a PLA/polyhydroxybutyrate-co-valerate (PHBV) polymer blend (2.33:1 blend of PLA:PHBV) [97]. For this polymer blend, the catalyst was found (using SEM and dynamic mechanical analysis, DMA) to improve the miscibility between the PLA and PHBV. This study showed that the surface tension between the PLA matrix and PHBV was reduced because of the transesterification reaction [97]. This reaction mechanism joins the PLA and PHBV chains together by the exchange of an ester group of PLA with an alcohol group of PHBV, giving an improved interfacial or surface blending (see Section 2.2.3.3 for a schematic of the mechanism) [97]. This improvement in miscibility led to an increase in the strain-at-break value (as compared to the neat PLA:PHBV blend) for catalyst amounts up to 0.2 wt%, while the E did not change for each of the tested samples [97]. In this work, the zinc acetate catalyst was used with a different polymer blend (*i.e.* PHB:PLA in 3:1 ratio) and thus, the results cannot be directly compared to the work done by Yang *et al.* However, the introduction of the catalyst into the polymer blend from this work also led to an increase in the ε_b, as compared to the neat polymer blend samples (*i.e.* PHB/PLA), but also a decrease in the E. This

decrease in modulus is different than what was observed by Yang *et al.* (for catalyst amounts up to 0.4 wt%). A possible reason for this reduction in *E* could have been caused by the catalyst crystals themselves not completely dissolving in this specific polymer blend. In this case, they could act as stress concentrators, reducing the strength parameters of the material. The mechanical testing results highlighted above do not show this directly and do not give evidence of the transesterification reaction observed by Yang *et al.* and thus, SEM, FTIR and thermal analysis were completed (see Sections 4.2, 4.3 and 4.4, respectively).

To further study the effects of eCO in a polymer matrix, two samples were tested with 5 and 10 wt% of eCO along with PLA and the catalyst (*i.e.* PHB/PLA/5eCO/Cat and PHB/PLA/10eCO/Cat, see Figure 4.2). The ratio of PHB:PLA in these samples was kept constant at 3:1. With the addition of 5 wt% eCO to the polymer blend (*i.e.* PHB/PLA/5eCO/Cat), no significant difference in mechanical properties was observed when compared to the PHB/PLA/Cat blended samples (p = 0.99, 0.08 and 0.10 for E, σ_{UTS}, and ε_b, respectively). However, when 10 wt% of eCO was added, the average E and σ_{UTS} saw significant decreases (from 1056 ± 62 MPa to 900 ± 51 MPa, and 26 ± 1 to 19 ± 2 MPa, respectively), while the average ε_b decreased, but within standard deviation (from 6.2 ± 1.0% to 5.0 ± 1.2%), as compared to the PHB/PLA/Cat samples. For all three tested parameters, there was a significant difference observed between the PHB/PLA/Cat samples and the PHB/PLA/10eCO/Cat samples (*i.e.* $p < 0.05$ for E, σ_{UTS}, and ε_b). The reverse in the effect of ε_b for the PHB/PLA/10eCO/Cat samples as compared to the PHB/PLA/5eCO/Cat samples might have occurred due to an optimum point of eCO loading being surpassed for the PHB/PLA blended product, similar to what was found when more than 10 wt% of eCO was added to pure PHB (*i.e.* without PLA in the matrix). This same phenomenon was observed by Chieng *et al.* where epoxidized palm oil and a mixture of this oil and epoxidized soybean oil was melt blended with PLA [25]. With more than approximately 7 and 5 wt% of epoxidized palm oil and of the mixture of oils in the matrix, respectively, the elongation at break decreased, causing the biocomposite sample to be more brittle [25]. Additionally, in this work, the strength parameters (*i.e.* E and σ_{UTS}) also decreased, a trend that was observed with the addition of 10 wt% of eCO in the PHB/PLA blended matrix.

Recall that one of the largest limitations for pure PHB is its poor strain at break. From the results of mechanical properties obtained, the addition of eCO shows improvements over hot-pressed NeatPHB, specifically when looking at the ε_b, with 10 wt% eCO. The inclusion of PLA itself, which has a ε_b of approximately 5%, does not improve this parameter; but adding

the catalyst to enhance the polymer blending led to a much larger ε_b (even greater than that of hot-pressed NeatPHB) as expected [97], [108]–[110]. In turn, the catalyst reduced the *E* of the samples as compared to both the NeatPHB and PHB/PLA blend samples; as this was not expected, a conclusion that the blending of the PHB and PLA was improved with the addition of the catalyst cannot be made (from the mechanical data alone). Lastly, with both eCO and PLA present in the PHB matrix, constant ε_b is observed up to 10 wt% eCO (*i.e.* no statistically significant change with 5 wt% but significant decrease with 10 wt%), although the strength of the material was found to decrease. Overall, the PHB/10eCO samples gave the greatest improvement in ε_b (8.0 ± 1.5%) over the NeatPHB samples (4.5 ± 0.4%), while having a statistically significant decrease in *E* as compared to the NeatPHB samples (from 1194 ± 102 MPa to 855 ± 32 MPa).

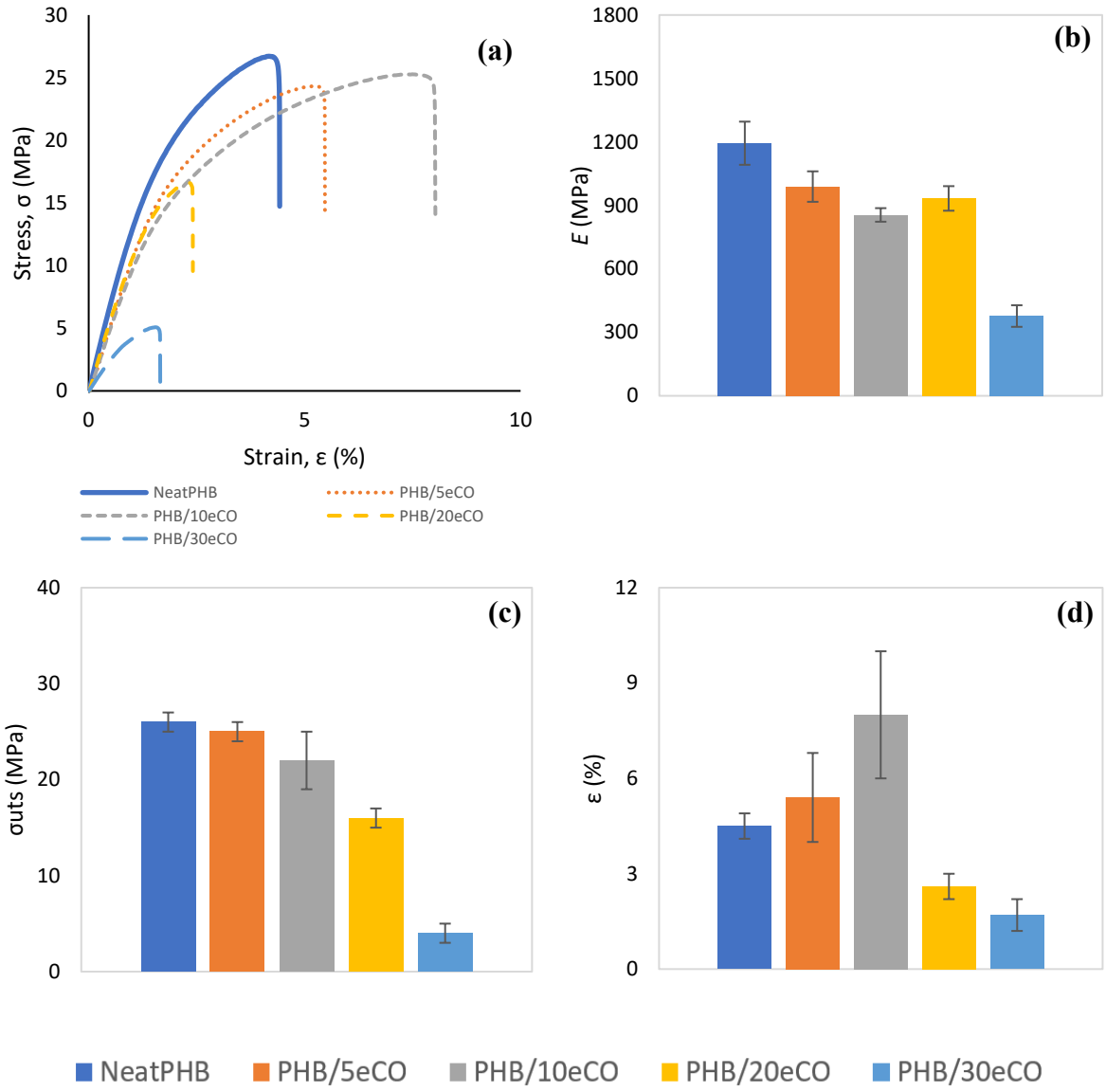

Figure 4.1: Stress-strain curves (a) as well as E (b), σ_{UTS} (c), and ε_b (d) values for NeatPHB and four eCO plasticized PHB samples: PHB/5eCO, PHB/10eCO, PHB/20eCO and PHB/30eCO

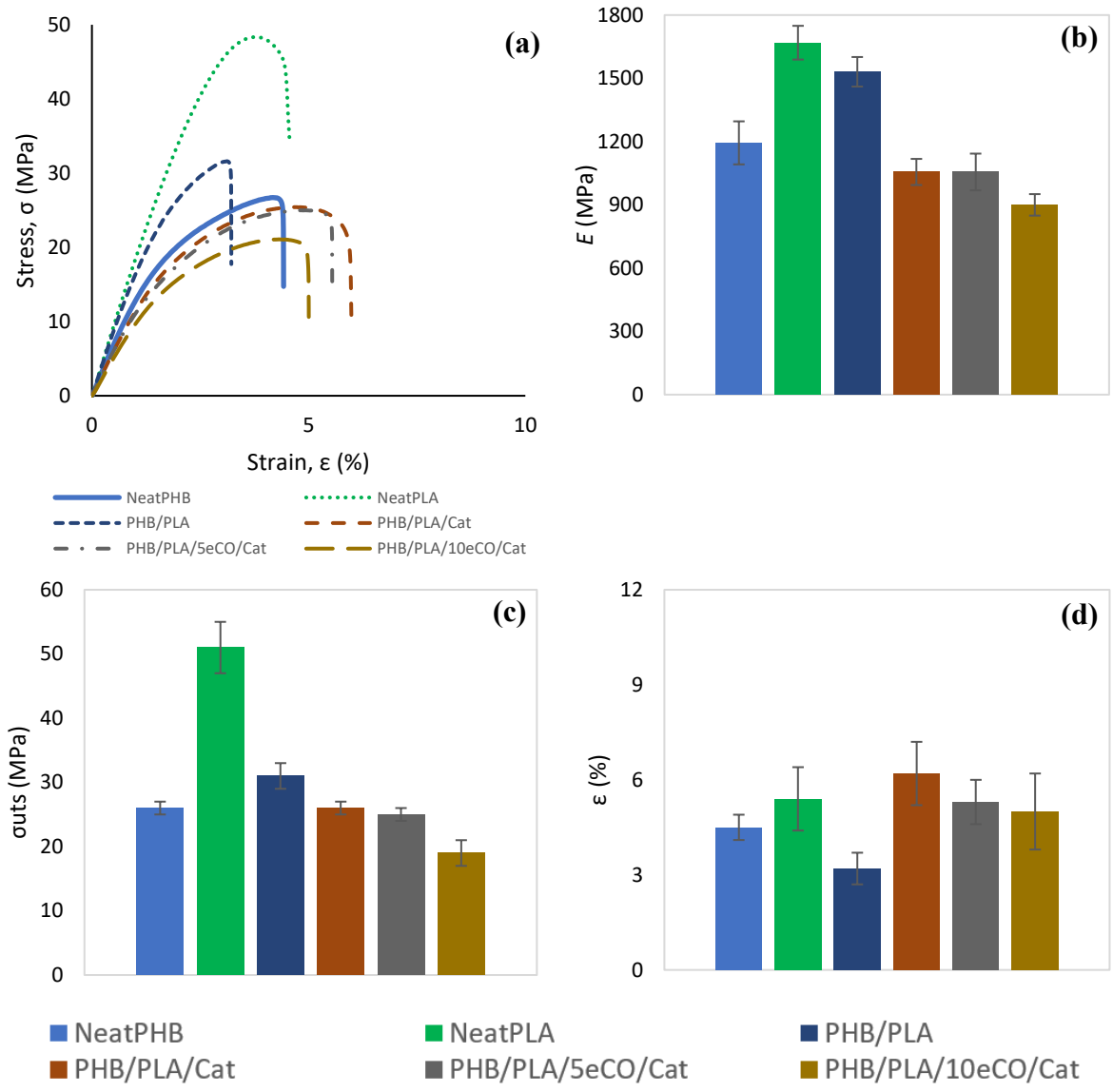

Figure 4.2: Stress-strain curves (a) as well as *E* (b), σ_{UTS} (c), and ε_b (d) values for NeatPHB, NeatPLA and four plasticized PHB samples: PHB/PLA, PHB/PLA/Cat, PHB/PLA/5eCO/Cat and PHB/PLA/10eCO/Cat

4.2 Microscopy

To determine the presence of eCO in the polymer matrix and how it affected the mechanical properties of the sample as well as the blending characteristics between PHB and PLA (with and without zinc acetate), scanning electron microscopy (SEM) was performed. SEM micrographs were collected to analyze the surface morphology of the plasticized PHB samples. Figure 4.3 shows four different samples: hot-pressed NeatPHB, PHB/PLA, PHB/10eCO, and PHB/30eCO. These specific samples and their micrographs are shown as they were representative of all the created samples. For example, under SEM, there were no visible differences between the NeatPHB sample (Figure 4.3(a)), PHB/PLA sample (Figure 4.3(b)),

and the sample containing the catalyst (*i.e.* PHB/PLA/Cat). These samples appeared to have a homogenous surface with no change in structure from the addition of PLA into the PHB matrix, meaning that PHB and PLA blended well. No noted differences in morphology between the samples with and without catalyst (*i.e.* PHB/PLA and PHB/PLA/Cat) could be inferred from these images; however, as was described above, the addition of the zinc acetate catalyst improved the ε_b of the polymer blend. These results suggest that the catalyst might be facilitating a reaction between the two materials, blending the two polymer chains together (see Section 4.1) [97].

Voids were observed in all of the samples containing eCO, which was not the case in NeatPHB samples. Figure 4.3(c and d) shows some of these voids. eCO plasticizer deteriorated the structure of the neat polymer material, and with more eCO added to the PHB, more and larger voids were present. This could be caused by the triglycerides of eCO (which have relatively large molecular sizes) forming clusters within the amorphous regions of the polymer (*i.e.* between PHB crystals), which led to the formation of these voids in the matrix (*i.e.* space without PHB). Similar observations have been found with the addition of epoxidized soybean oil to PHBV [28].

Cross-sectional SEM micrographs of the fracture surfaces of five different tensile tested samples can also be seen in Figure 4.4 and Figure 4.5. The images in Figure 4.4(a and b) show the hot-pressed NeatPHB sample at two different magnifications. In these images, the cross-section view of the sample shows a fairly brittle fracture surface; this type of fracture occurred without a noticeable amount of prior plastic deformation (as shown by the lack of dimple-like structure). The two images that follow (Figure 4.4(c and d)) show the PHB/PLA sample at the same two magnifications. In these images, the cross-section view shows a fracture surface that suggests that the failure was more brittle than that of the hot-pressed NeatPHB sample. This observation is supported by the mechanical data previously shown (Section 4.1) as the average ε_b for the NeatPHB samples was 1.3% greater than for the PHB/PLA samples – meaning the PHB/PLA samples have less flexibility as compared to the NeatPHB samples. The last two images (Figure 4.4(e and f)) show the PHB/PLA/Cat sample. The fracture surface of this sample is different than that of the PHB/PLA sample. First, the PHB/PLA/Cat sample appears to be more ductile when compared with the other samples in Figure 4.4. This observation is supported by an average ε_b that is 1.7% and 3% larger than the values for the NeatPHB and PHB/PLA samples, respectively. In addition, the fracture surface for the PHB/PLA/Cat sample resembles that of the hot-pressed NeatPHB sample as the matrix has fewer voids at its surface

and appears more homogeneous (see Figure 4.4(f)). Moreover, the hypothesis made in Section 4.1 – that the reduction in *E* between the PHB/PLA/Cat sample and the PHB/PLA sample is caused by zinc acetate crystals not completely dissolving and becoming stress concentrators in the sample – is not supported by the SEM analysis as no undissolved crystals were visible at the fracture surface of the PHB/PLA/Cat sample. Further investigation into the reduction in strength parameters is thus required (refer to Section 6.2).

Figure 4.5 shows the fracture surfaces of the PHB/10eCO and PHB/30eCO samples. With the addition of 10 wt% eCO to the PHB matrix (Figure 4.5(a and b)), the cross-section view shows a much more ductile fracture surface (compared to the hot-pressed NeatPHB sample, Figure 4.4(a and b)), which is consistent with its greater average ε_b. Voids, which were observed on the surface of the material (Figure 4.3(c)), were also seen at the fracture surface but were smaller and less numerous. With an increase in eCO content to 30 wt%, the larger and more numerous voids were consistent with those observed on the surface of the sample (Figure 4.3(d)), and were thus found to be present throughout the sample's thickness. This can at least partially explain the poorer mechanical properties of the sample (see Section 4.1). Moreover, the surface of this sample was much rougher and heavily pitted that that of the NeatPHB and PHB/10eCO samples, likely due to the larger amount of eCO molecules trying to blend into the polymer matrix. Similar observations were seen for the other samples with less eCO (*i.e.* 5 and 20 wt%), but with fewer and smaller pitting zones. This observed pitting with 10 wt% eCO could explain the increase in the polymer's average ε_b when compared to the NeatPHB samples (see Section 4.1).

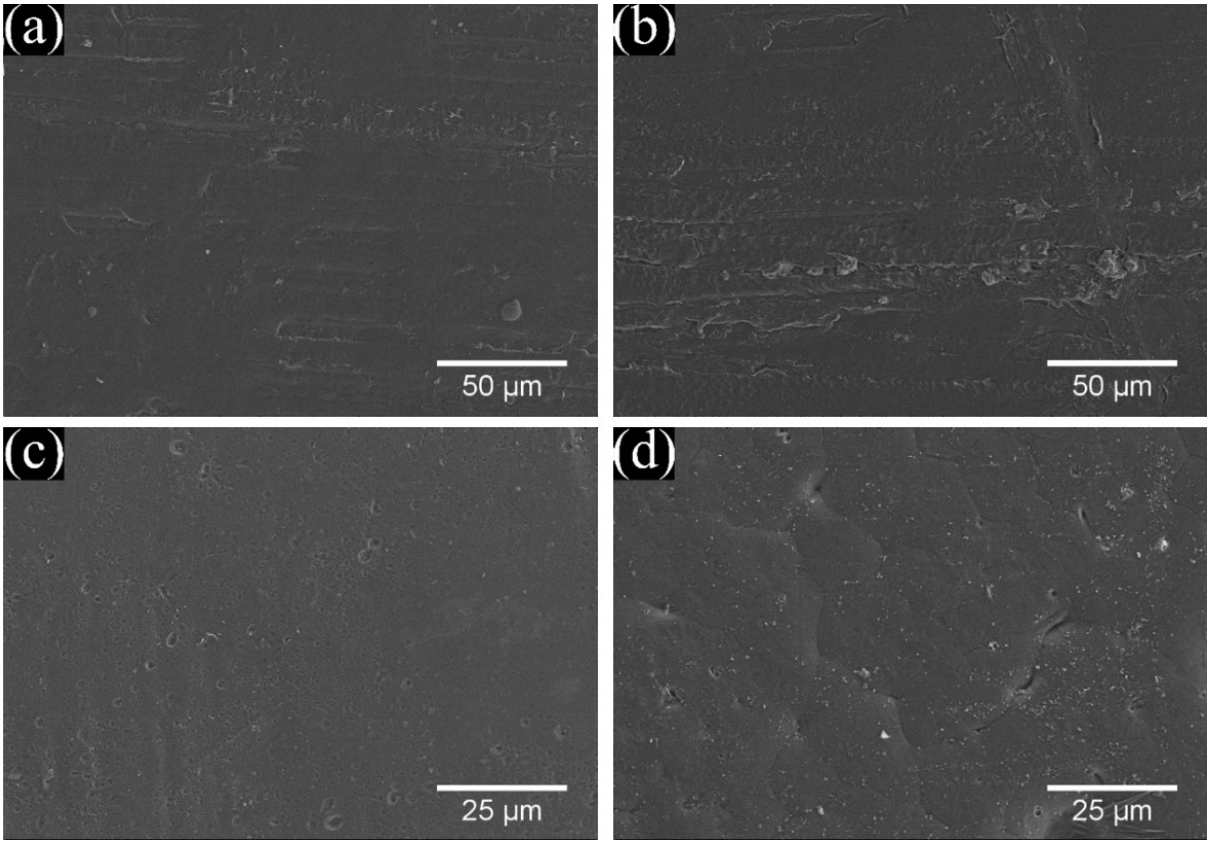

Figure 4.3: Top down SEM micrographs of NeatPHB (a), PHB/PLA (b), PHB/10eCO (c) and PHB/30eCO (d)

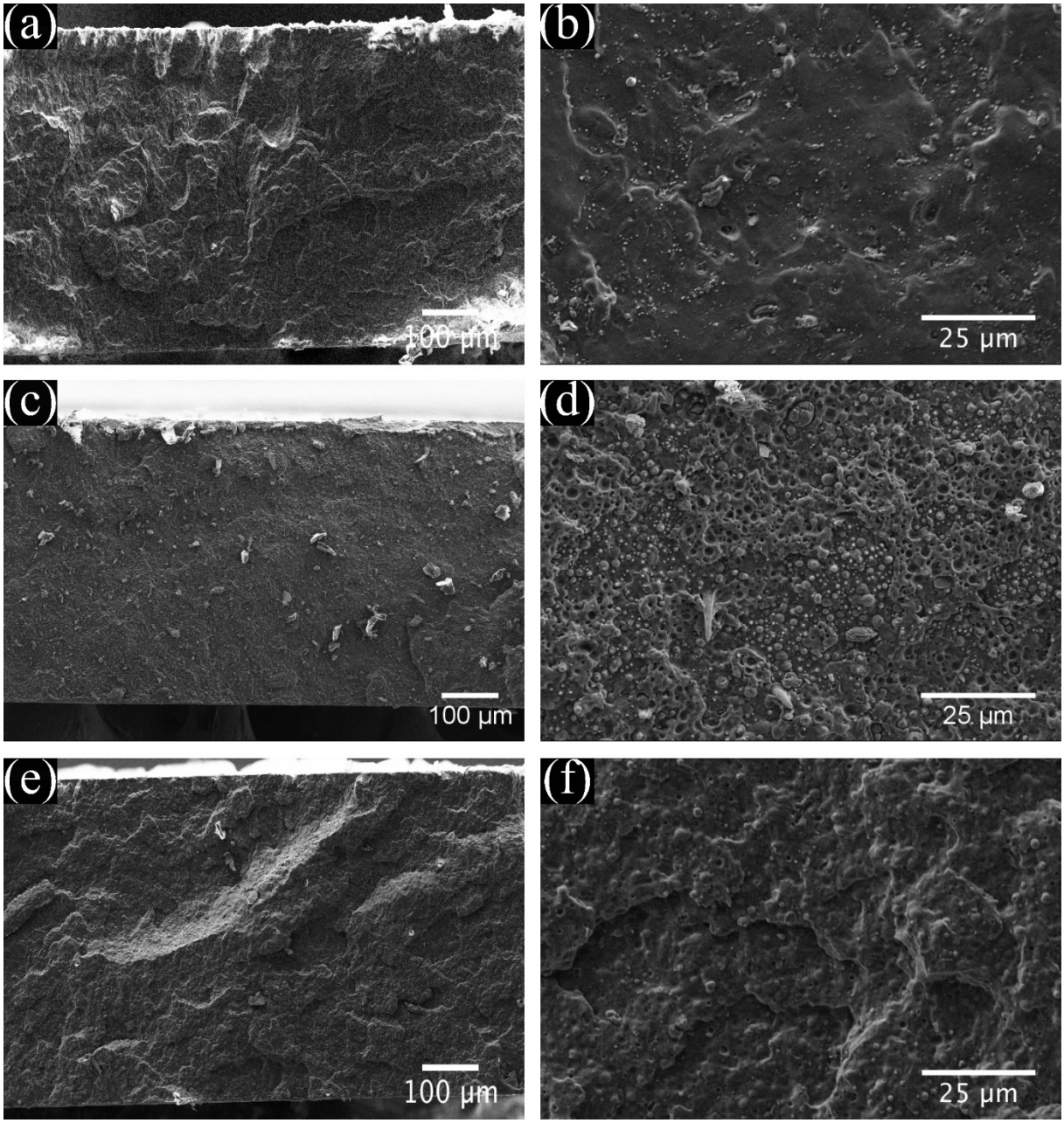

Figure 4.4: Cross section SEM micrographs of the fracture surface for three samples: NeatPHB at 125x (a) and 1000x (b); PHB/PLA at 125x (c) and 1000x (d); and PHB/PLA/Cat at 125x (e) and 1000x (f)

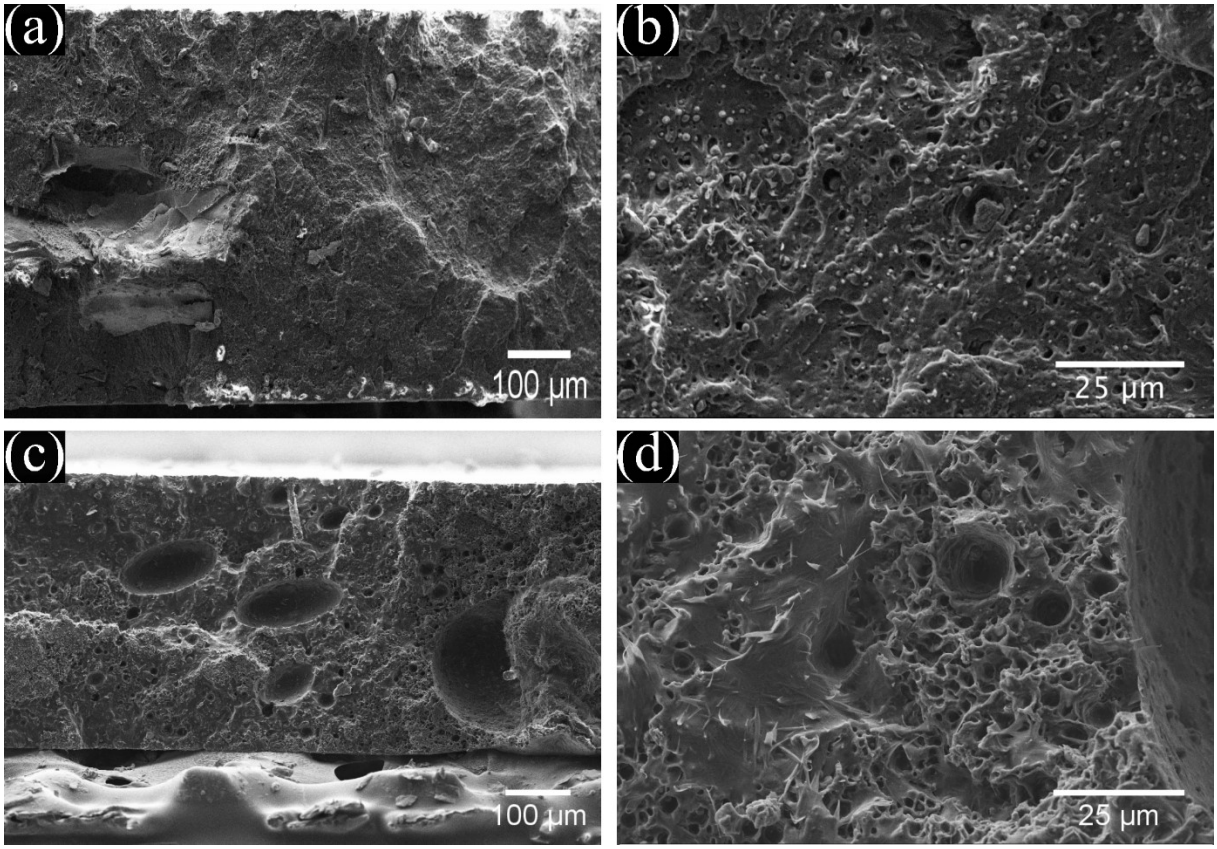

Figure 4.5: Cross section SEM micrographs of the fracture surface for two samples: PHB/10eCO at 125x (a) and 1000x (b); and PHB/30 eCO at 125x (c) and 1000x (d)

4.3 FTIR

FTIR spectra of hot-pressed NeatPHB, hot-pressed NeatPLA, and PHB/PLA blends with and without catalyst are shown in Figure 4.6, with the typical bands associated with PHB being highlighted. For the NeatPHB samples, the absorption bands located at 1275 and 1225 cm^{-1} are assigned to the stretching of the C-O-C bond of the crystalline parts of the material, while the band near 1178 cm^{-1} is formed from the amorphous state of the C-O-C stretching bond [40], [88], [111], [112]. The peak observed at 1718 cm^{-1} correlates to the stretching mode of the C=O bond in the crystalline region, while the two peaks at 1454 and 1379 cm^{-1} correspond to deformation vibration of the C-H bond [24], [40], [111]. In addition to the bands for PHB, typical bands for PLA are highlighted in Figure 4.6. The band at 1745 cm^{-1} relates to the C=O vibrational stretching of the amorphous region, while peaks at 1452 and 1383 cm^{-1} correspond to C-H deformation vibration (similar to the NeatPHB samples) [24], [25], [111]. C-O bond stretching is also observed with the peaks being located at 1181 and 1079 cm^{-1}, and the last of the amorphous bands are seen at 864 cm^{-1} (*i.e.* C-O-C bond) and 754 cm^{-1} (*i.e.* C-H bond) [25], [111]. PHB and PLA also have peaks that are very weak and cannot be clearly identified in the

spectrum. For PHB, the amorphous C=O bond vibration correlates to a peak at 1740 cm^{-1} while PLA has a weak peak at 1755 cm^{-1} that relate to the crystalline C=O bond vibration [24]. The literature on PHB and PLA FTIR spectra has also reported that any bands observed above 2993 cm^{-1} are usually associated with possible hydrogen bond formation (*i.e.* C-H···O) [88], [111].

The FTIR spectra for the PHB/PLA was very similar to that of the NeatPHB samples. For the vibration of the C=O bond (crystalline PHB at 1718 cm^{-1} and amorphous PLA at 1745 cm^{-1}), the peak itself couples into a single peak at 1718 cm^{-1} instead of two distinct peaks due to the large amount of PHB in the samples (*i.e.* 3:1 PHB to PLA). The slight decrease of intensity for the peak at 1225 cm^{-1} (as compared to the NeatPHB samples) is related to the decrease of crystalline parts of the C-O-C bond, as the addition of amorphous PLA likely reduces the PHB crystallinity; this effect will be explored further in Section 4.4 with the DSC results. Overall, these minor changes in spectra provide evidence that the PHB and PLA polymers blended well. A nearly identical curve (*i.e.* slight changes in peak intensities) to that of the PHB/PLA samples was seen for the samples that contain the transesterification reaction catalyst (*i.e.* PHB/PLA/Cat). This catalyst is supposed to improve the miscibility of the polymers by causing a blend between the two polymer chains through the exchange of an ester group of PLA and an alcohol group in PHB [97]. With the addition of zinc acetate (in amounts up to 0.4 wt%) to a polymer blend of PLA:PHBV (in a ratio of 2.33:1), Yang *et al.* observed slight shifts in the PLA/PHBV blend peak locations and decreases in intensity, along with the appearance of a new peak [97]. From the FTIR analysis completed in this work, and the fact that no new peak for the zinc acetate was visible in the curve (Figure 4.6), the conclusion that the zinc acetate (in an amount of 0.3 wt%) improves the blending between PHB and PLA (in the ratio tested) cannot be made without further study.

Epoxidized canola oil (eCO) has been studied on its own and a peak corresponding to the epoxy ring of the material was located at 826 cm^{-1}. When the eCO was added to the hot-pressed samples, a slight reduction of intensity in characteristic peaks of PHB was observed, similar to previous experiments with PHB and plasticizers [88]. However, besides this, no concrete evidence of change in the curves, compared to the ones observed in Figure 4.6, was observed (see Appendix A for figures containing more FTIR curves). From the SEM images, it was suggested that eCO was present in each sample (*i.e.* presence of voids and matrix structure changes) and the plasticizer blended well with PHB in low amounts; however, no clear phase separation or changes in density were observed and the peak associated with the

epoxy ring in the eCO itself is not intense enough to be visible in comparison to the other FTIR peaks.

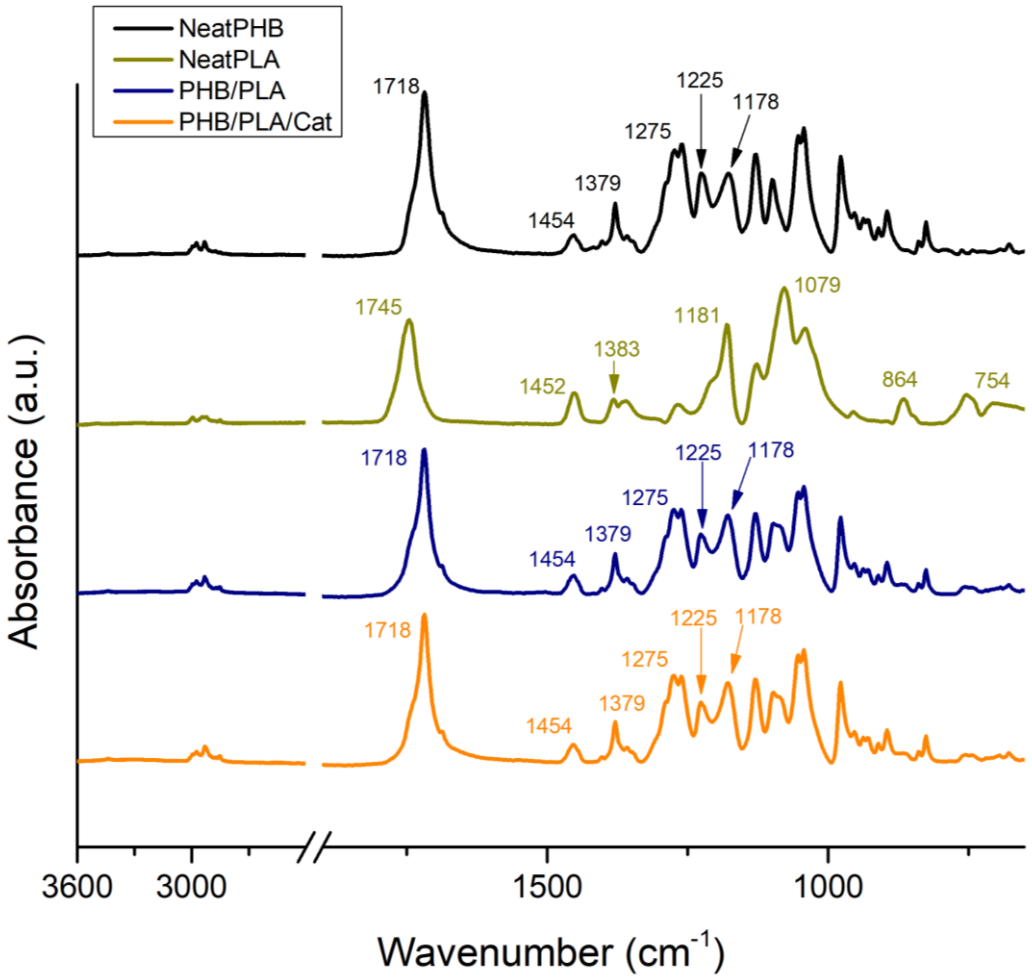

Figure 4.6: FTIR spectra of hot-pressed NeatPHB and NeatPLA along with two hot-pressed blended samples. Recall that the PHB/PLA composition is 3:1.

4.4 Thermal Properties

The thermal properties and crystallinity of PHB blends were evaluated using DSC and TGA. To make these hot-pressed plasticized samples, the PHB pellets and additives were extruded and the corresponding DSC melting curve (*i.e.* endothermic process) is shown in Figure 4.7. In addition, Table 4.1 summarizes the onset T_m, peak T_{m2} and crystallinity (X_{cDSC}) of the PHB and PHB/PLA blends collected, while melting curves of each sample are shown in Figure 4.8. The onset T_m is associated with the onset melting of the "as formed" unstable crystallites, while peak T_{m2} correlates to the maximum of the second melting peak or the melting of stable PHB crystals.

In this heating/melting stage of the cycle, PHB typically shows a double melting peak, with onset melting and second melting peaks occurring around 150 and 170 °C, respectively [13], [24]. A secondary peak was quite pronounced in each of the plasticized sample runs (Figure 4.8) and partially observed in the extruded PHB material run (Figure 4.7). For the as-received PHB pellets, a large melting peak was observed with a small shoulder located at a lower temperature (Figure 4.7). These initial peaks in pure PHB samples are common for PHB and are related to the melting of "as formed" and recrystallized PHB crystallites, as well as room temperature ageing. These small and imperfect crystals change successively into more stable crystals through each melting and recrystallization stage [13], [24], [28], [88], [113]. First, the PHB pellets are created by the supplier using a thermal pelletization technique. These pellets were then extruded and finally hot-pressed, leading to more PHB crystallites.

From the DSC data, it was determined that the onset T_m decreased after extrusion, as this process introduced more of the previously mentioned imperfect crystals. Hot-pressing, blending with PLA, and the addition of eCO did not have an effect on the onset or second melting point of the blended samples. In addition, during the cooling process for each of the samples, a crystallization peak was found around 109 ± 2 °C (n = 5), with no variation with the processing or blending of PLA or eCO. While these results indicate that the melting and recrystallization of PHB/PLA blends are led by those of neat PHB material, composites with PLA in the matrix showed a distinct PLA T_g at approximately 60 °C. The presence of a T_g at 55 °C in PLA and 4:1 ratio blends of PHB and PLA has been reported previously by Zhang *et al.* [24]

Enthalpy of melting (ΔH_m), the heat associated with the melting of the polymer, was estimated by the integration of the melting peaks from the DSC curves (Figure 4.7 and Figure 4.8). Using Equation 3.1, X_{cDSC} for each of the samples was calculated (and summarized in Table 4.1) by normalizing the measured ΔH_m to that of a 100% crystalline sample of PHB and the weight fraction of PHB in the tested sample [114] (*e.g.* 0.9 for the PHB/10eCO sample). Looking at the processes specifically, the X_{cDSC} of the PHB material after each stage increased from 28.9 ± 0.1% (n = 3) to 31.3 ± 0.5% (n = 3) and finally 34.5 ± 1.4% (n = 5) (*i.e.* PHB pellet, extruded PHB, and hot-pressed NeatPHB, respectively), with this increase being expected based on other works [40], [41], [50]. X_{cDSC}, which is affected by the addition of eCO and PLA, altering the ΔH_m while keeping the onset and peak T_{m2} relatively constant, was then calculated for the blended products. The crystallinity was 34.5 ± 1.4% (n = 5) for hot-pressed PHB, 31.1 ± 2.1% (n = 5) for PHB/PLA blends, and 30.6 ± 2.8% (n = 5) for the PHB/PLA/Cat

samples. These results suggest that the blending of PLA slightly decreased the crystallinity of PHB by decreasing its chain mobility and interfering with the formation of metastable and stable crystals during the cooling process followed by hot-pressing (Section 3.2.1). This decrease in crystallinity of PHB with the blending of PLA has been previously reported in other studies [24], [115], [116]. For instance, studying the effect of PLA in PHB blends, Gunaratne *et al.* [116] evaluated their crystallinity by individually dissolving the polymers in chloroform (2% w/v) and blending them in ranges from neat PHB to neat PLA. Following drying and heat pressing at 180 °C, they calculated the crystallinity of the blends by the same procedures as our work (DSC measurement and use of Equation 3.1) and reported a 12% decrease in crystallinity for a 4:1 ratio blend of PHB and PLA as compared to a neat PHB samples (samples are 3:1 PHB:PLA in the present study) [116].

In parallel to the effect of PLA, the changes in crystallinity of PHB with the addition of eCO were studied. Generally, with the addition of plasticizers such as eCO into a polymer matrix, no reduction in X_{cDSC} is seen, but there is a possibility of a slight increase in crystallinity, depending on interaction with the matrix [87], [88]. In this work, it was found that the addition of 5 and 10 wt% eCO did not affect the crystallinity of neat PHB (34.5 ± 1.4% (n = 5)), with 35.6 ± 2.1% (n = 5) and 34.8 ± 2.8% (n = 5) for PHB/5eCO and PHB/10eCO, respectively. Similarly, 5 wt% eCO did not affect the crystallinity of PHB/PLA blends, with 29.9 ± 0.9% (n = 5) for PHB/PLA/5eCO/Cat. However, introducing 20 and 30 wt% eCO to neat PHB did increase crystallinity to 37.1 ± 3.6% (n = 5) and 42.0 ± 3.4% (n = 5) for PHB/20eCO and PHB/30eCO, respectively, while 10 wt% gave a statistically significant increase in crystallinity of PHB/PLA blends, with 39.9 ± 1.4% (n = 5) for PHB/PLA/10eCO/Cat (*i.e.* $p < 0.05$). The invariability in the crystallinity sometimes observed is likely associated with the amount of eCO in the systems being studied (*i.e.* neat PHB and a PHB/PLA blend). Similar observations have been seen in previous research with PHB and other plasticizers. For example, Seoane *et al.* [88] reported that blending PHB with plasticizers such as glyceryl tributyrate did not increase the PHB crystallinity in concentrations of plasticizers lower than 30 wt%. For concentrations above 30 wt%, they attributed the increase in crystallinity to the increase in chain mobility that the incorporation of additives into an amorphous phase of semi-crystalline polymers provided [87], [88], [117], [118]. This increased chain mobility should also lead to a reduction in T_{m2} of the polymer, providing a larger window for thermal processing; however, as mentioned previously, very little change across all plasticized samples was observed.

Table 4.1: DSC data for as-received PHB pellets, extruded material and hot-pressed samples

DSC Results	Onset T_m (°C)	Peak T_{m2} (°C)	$X_{cDSC, PHB}$ (%)
PHB Pellet	158 ± 3	172 ± 1	28.9 ± 0.1
Extruded PHB	153 ± 2	172 ± 2	31.3 ± 0.5
NeatPHB	153	170	34.5
PHB/5eCO	153	170	35.6
PHB/10eCO	150	169	34.8
PHB/20eCO	150	168	37.1
PHB/30eCO	151	168	42.0
PHB/PLA	151	169	31.1
PHB/PLA/Cat	152	170	30.6
PHB/PLA/5eCO/Cat	154	168	29.9
PHB/PLA/10eCO/Cat	151	169	39.9

Note: n=3 for the PHB pellets and extruded PHB samples; n=5 for remaining samples. Max standard deviation for plasticized samples = ± 3 °C and ± 4.5% for T_m and X_{cDSC}, respectively

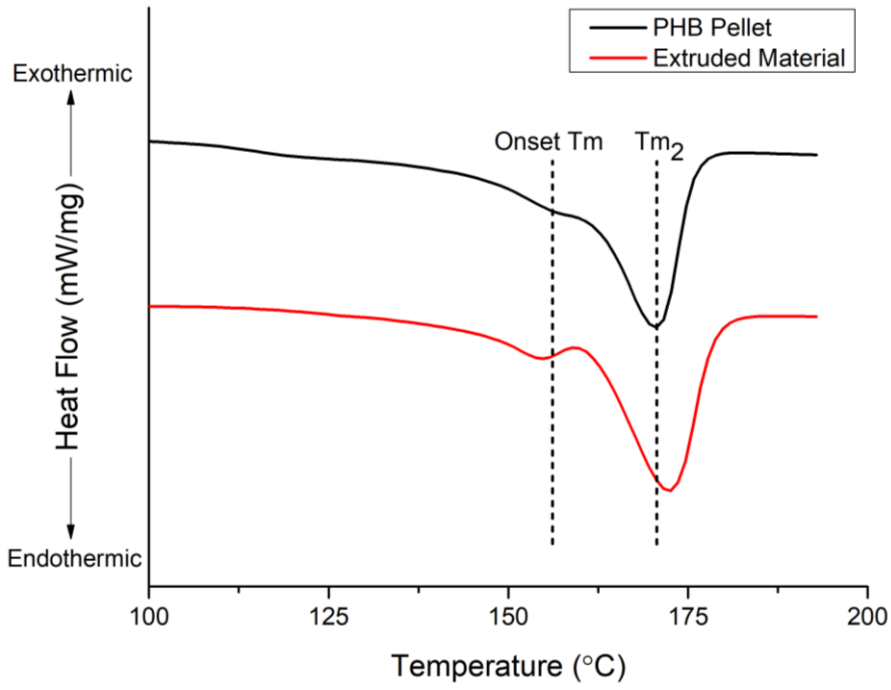

Figure 4.7: DSC melting curves for as-received PHB pellets and extruded PHB material

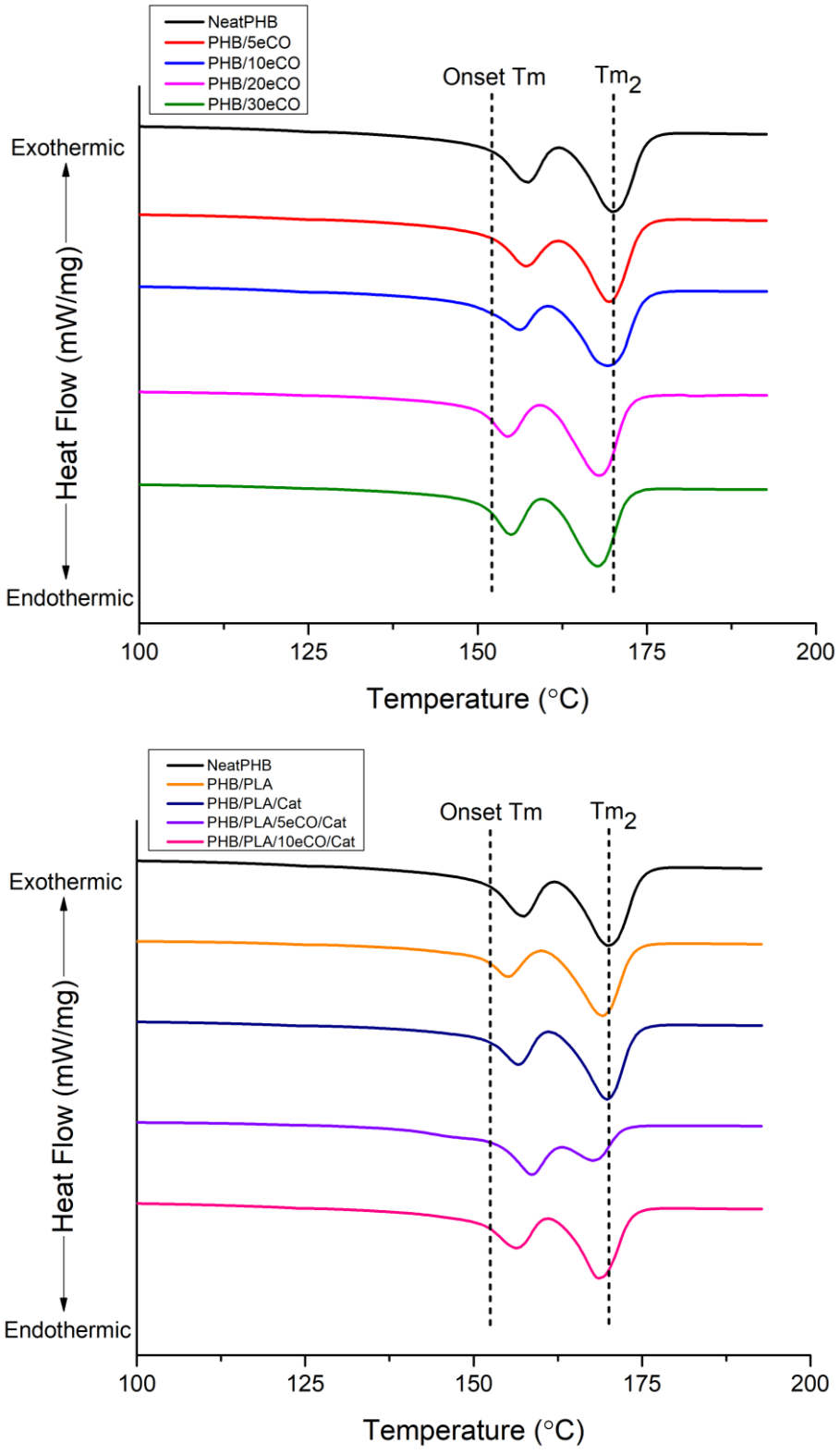

Figure 4.8: DSC melting curves for hot-pressed plasticized PHB samples

Thermal stability of PHB could be affected by the addition of eCO and/or PLA; this was studied using TGA. Onset degradation and peak degradation temperatures were collected from the characterization run with the onset degradation temperature being associated with

approximately 5% of mass loss of the sample due to thermal degradation. The peak degradation temperature value correlates to the point at which the degradation rate is highest during the TGA run. The values obtained are summarized in Table 4.2 for all plasticized samples, as well as the PHB pellets and extruded material. The results for six of the hot-pressed samples are represented in Figure 4.9 as weight loss (%) as a function of temperature (°C). In this figure, the curves follow roughly the same pattern with slight changes in degradation rate (*i.e.* slope of the curve) and the temperature at which the degradation begins. The main difference comes in the samples containing PLA (*i.e.* PHB/PLA, PHB/PLA/Cat and PHB/PLA/10eCO/Cat), which have another onset degradation temperature "peak" occurring around 340 °C, associated with the degradation of PLA. Additionally, due to the large amount of eCO present in the sample, the PHB/30eCO samples also has a second onset degradation temperature peak around 360 °C, associated with the degradation of eCO. Overall, each sample shown in Figure 4.9 (and the samples that are not shown) had some mass remaining (*i.e.* normalized mass did not reach 0%) after a temperature of 380 °C was reached. For example, the NeatPHB samples had as much as 2.9% of mass remaining after the TGA run; this mass is associated with material that was not completely degraded at the end of the run, although the TGA analysis could not give the composition of the left-over material. As outlined in Section 3.1, XPS results showed that the PHB pellets used in this work were found to have approximately 5 wt% of impurities on their surface (likely from the pelletization process) and a possible source of this difference in remaining mass is that XPS is a surface characterization technique while TGA is a bulk characterization technique. In addition, it was found that for multiple runs of the same TGA sample (n = 3), the amount of mass remaining after the analysis varied by as much as 3.0%, highlighting that this technique is qualitative in nature. Nonetheless, the curves in Figure 4.9 show only slight changes in degradation characteristics across each tested sample.

From the data, there was no visible change in the thermal stability of neat PHB after extrusion and hot-pressing processing, with each sample showing onset degradation at 292 °C and peak degradation around 305 °C. Therefore, there was no sign of thermal degradation occurring during the processing of the samples. If there was any degradation truly taking place from the process, it is not substantial since it is indistinguishable from the TGA (and DSC) characterization.

The TGA data also suggests that all of the blended samples were stable at onset temperatures as low as 281 °C. In agreement with other studies, this work found that the onset degradation temperature of neat PHB was approximately 290 °C [12], [40], [45], [88]. In

general, the addition of other materials to the PHB matrix (*i.e.* blending of PLA or eCO) did not result in the change in thermal stability of the material. The average onset degradation temperature was 290 ± 5 °C (n=9). This result suggests that while the degradation temperatures of neat PLA, 340 °C, and neat eCO, 360 °C, have been previously reported (and measured in this work) to be higher than that of neat PHB, the use of these additives did not affect its mechanisms of thermal degradation [119], [120]. Stronger evidence of this is presented in Figure 4.9, where the materials containing PLA presented an initial degradation at 290 ± 5 °C, arguably related to PHB, and a second stage, at around 25 wt% and 335 ± 15 °C, related to PLA and eCO. In conclusion, these TGA results show that while the addition of eCO in PHB and PHB/PLA blends lead to changes in mechanical properties (see Section 4.1), no significant change in thermal stability of the matrix was found.

Table 4.2: TGA data for as-received PHB pellets, extruded material, and hot-pressed PHB samples

TGA Results	Onset Degradation *T* (°C)	Peak Degradation *T* (°C)
PHB Pellet	292	306
Extruded Material	292	305
NeatPHB	292	303
PHB/5eCO	281	292
PHB/10eCO	288	297
PHB/20eCO	293	305
PHB/30eCO	293	303
PHB/PLA	297	307
PHB/PLA/Cat	293	306
PHB/PLA/5eCO/Cat	291	303
PHB/PLA/10eCO/Cat	286	298

Note: Max standard deviation = ± 5 °C (*n*=3)

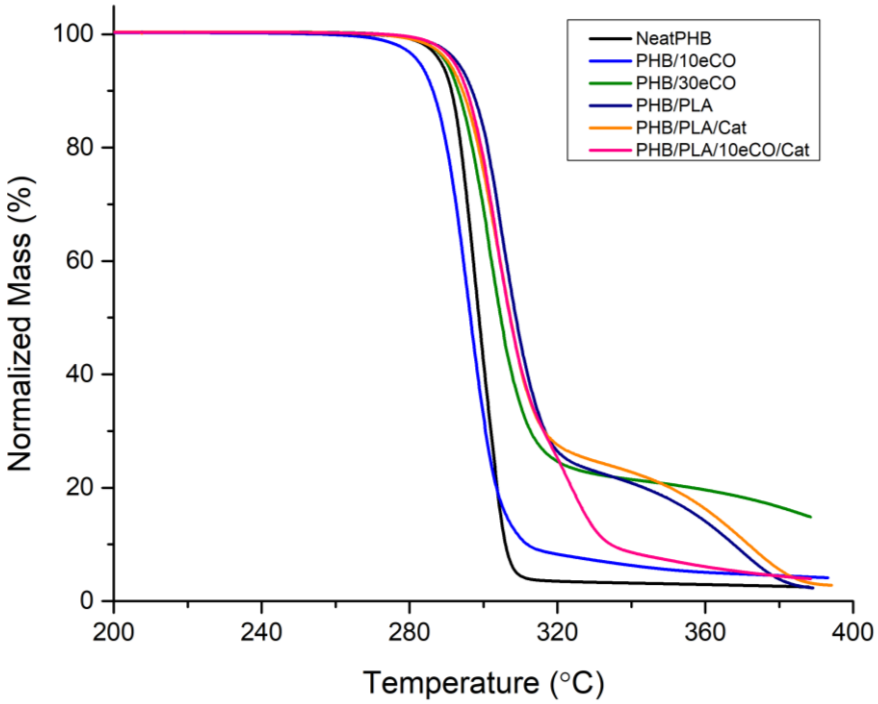

Figure 4.9: TGA plot for six hot-pressed PHB samples

4.5 Summary of Plasticizing Work

The plasticizer work highlighted in this section can be broken down into four separate areas: (1) processing techniques, (2) the addition of eCO, (3) the addition of PLA and zinc acetate, and (4) the addition of PLA, zinc acetate and eCO.

Firstly, the techniques of extrusion and hot-pressing were used to create these plasticized samples. TGA analysis helped conclude that the processing steps do not have a significant effect on the thermal stability of the PHB material, as very little change in thermal degradation was observable. For studying the thermal properties of the post-processing samples, DSC data was collected and it was found that secondary melting peaks became quite apparent in each of the hot-pressed plasticized samples. This same secondary melting peak trend was partially observed in the extruded PHB material and even less so in the as-received PHB pellets. It was determined that these peaks are associated with the formation of PHB crystallites (and room temperature ageing) following each thermal process that the material undergoes. These crystallites gave rise to increased PHB crystallinity for each post-processing sample (*i.e.* extruded material and hot-pressed NeatPHB).

With the addition of eCO alone (in different quantities), no significant change in thermal properties or stability was observed at the processing and analysis temperatures chosen. Small amounts of eCO (5 and 10 wt%) did not affect the crystallinity of neat PHB, however,

at larger quantities (20 and 30 wt%), the crystallinity was increased by approximately 3 and 8% over neat PHB, respectively. That being said, the addition of 10 wt% eCO had positive plasticizing effects on the PHB matrix. The larger amounts of eCO (20 and 30 wt%) gave poorer mechanical properties as compared to hot-pressed NeatPHB, due in part to the large voids observed in the SEM micrograph.

PLA (in a 3:1 ratio of PHB:PLA) and zinc acetate (0.3 wt%) were then examined as possible plasticizing additives for PHB. Similarly, to the sole addition of eCO, no significant change in thermal properties or stability was observed for the PHB/PLA blends (with and without catalyst). There was, however, a reduction in the crystallinity with the addition of PLA (and catalyst) to the PHB matrix, supported by previous studies [24], [115], [116]. That being said, a significant decrease in strength parameters (E and σ_{UTS}) and flexibility (ε_b) was observed for PHB/PLA samples as compared to NeatPHB samples. On the other hand, the introduction of the catalyst led to an increase in ε_b as compared to NeatPHB samples. This improvement in flexibility is very positive, however, the catalyst also reduced the strength of the sample as compared to both the PHB/PLA blend and NeatPHB samples. As this was not expected, and looking at the mechanical data alone, it cannot be concluded that the catalyst improved the blending of the PHB and PLA polymers; therefore, SEM and FTIR were explored. After examination of the samples using SEM, the fracture surface of the PHB/PLA/Cat sample did appear to be more homogeneous than the fracture surface of the PHB/PLA sample; however, there were no visible stress concentrators present that would lead to the reduction in E that was observed with the addition of zinc acetate. FTIR gave evidence that the PHB and PLA blended well as there was very little change in the observed peaks between the NeatPHB and PHB/PLA samples. Additionally, no significant change was seen for the samples containing the catalyst, and as such, further experiments are required to determine what kind of effect, if any, the zinc acetate catalyst (in an amount of 0.3 wt%) has on the PHB, PLA and the blending of the materials (refer to Section 6.2).

Lastly, PLA (in the same ratio) and the zinc acetate were blended with PHB along with 5 and 10 wt% of eCO. No change in crystallinity was observed when 5 wt% of eCO was added, as compared to the PHB/PLA and PHB/PLA/Cat samples. However, the addition of 10 wt% eCO did give a large increase (approximately 9%) in the crystallinity as compared to both PHB/PLA and PHB/PLA/Cat samples. Similar effects were observed for the mechanical properties with the addition of eCO in these quantities. At 5 wt%, strength (*i.e.* E and σ_{UTS}) and flexibility (*i.e.* ε_b) were maintained as compared to the PHB/PLA/Cat samples as the

differences were statistically negligible. For the sample containing 10 wt% however, a statistically significant decrease in both strength parameters and flexibility was observed as compared to the PHB/PLA/Cat samples. Additionally, this amount of eCO provided a reverse effect on the ε_b as compared to the samples without PLA in the matrix (*i.e.* PHB/10eCO). It was concluded (with support from literature) that an optimum point of eCO loading for the PHB/PLA blended product (specifically used in this work) had been surpassed, introducing a reduction in mechanical properties (*i.e.* a negative effect).

5. RESULTS AND DISCUSSION – FDM SAMPLES

In this chapter, the results obtained from the characterization techniques noted in Chapter 3 are highlighted for the FDM printed samples of PHB followed by a discussion of the findings. PHB pellets were initially extruded into 1.75 mm diameter filaments that were then used in a desktop FDM printer to create tensile specimens (with bracing) for characterization (see Figure 3.2). The goal of this work was to determine whether or not the commercially scalable process of FDM printing could be a viable option for processing PHB by exploring the impact of the processing steps (*i.e.* extrusion and printing) on the material properties, as well as possible thermal and mechanical degradation mechanisms of the polymer.

5.1 Mechanical Properties

A representative stress-strain curve for the tested FDM samples is shown in Figure 5.1 as compared to the curves for a hot-pressed NeatPHB sheet (see Chapter 4) and a solvent cast thin film of PHB (prepared in another work from this lab). The experimental results of the performed tensile tests for the three samples are summarized in Table 5.1.

In comparison to the hot-pressed NeatPHB samples, FDM printed PHB samples had statistically significant decreases in the strength parameters (*i.e.* E and σ_{UTS}). However, there was a statistically insignificant change in ε_b between the FDM samples and the hot-pressed NeatPHB samples ($p = 0.44$). Although the difference in strength parameters between the FDM printed PHB and hot-pressed NeatPHB samples were significant, decreases of approximately 24% and 27% were seen for the E and σ_{UTS} between the two samples, respectively. As mentioned in Section 2.2.2.2, FDM printed samples commonly show a reduction in mechanical properties as compared to their bulk counterparts (recall 45% decrease in E is observed while 30-60% decrease is often seen for σ_{UTS}) [73]. This expected decrease is associated with an anisotropic effect that is introduced by the layering of the deposited filaments and the direction in which they are printed [69], [72], [73]. Therefore, the printing process showed better than expected mechanical results as compared to hot-pressed NeatPHB samples. Additionally, the collected mechanical data for the FDM printed samples was also compared to that of solvent cast PHB thin films prepared in another work [13] and no statistical significance was found between all three of the tested parameters (p = 0.08, 0.08 and 0.16 for the E, σ_{UTS} and ε_b, respectively).

Table 5.1: Mechanical properties for FDM printed PHB compared to different processing techniques

Sample (n = 5)	Young's Modulus E (MPa)	Ultimate Tensile Strength σ_{UTS} (MPa)	Strain at Break ε_b (%)
FDM PHB Samples	910 ± 166	19 ± 2	4.6 ± 2.0
Hot-pressed NeatPHB	1,194 ± 102	26 ± 1	4.5 ± 0.4
Solvent Cast PHB Thin Films [13]	1,094 ± 163	17 ± 2	4.2 ± 1.0

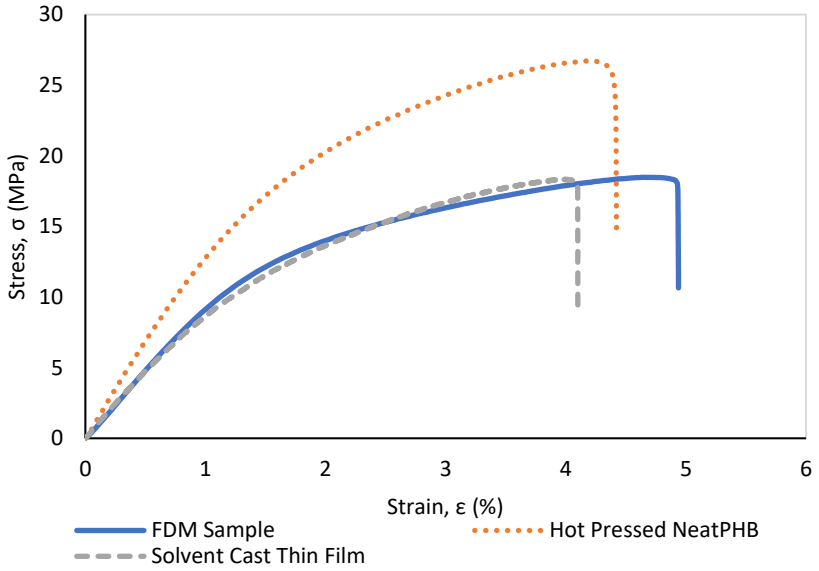

Figure 5.1: Stress-strain curves of three different processing techniques for PHB

5.2 Microscopy

Stereomicroscopy images of an FDM sample (Figure 5.2(a)) are presented in Figure 5.2(b and c). A wave pattern, commonly associated with the FDM printing process, was observed for both regions imaged [21]. The wave properties, such as printing wavelength, can be improved and controlled by the printing speed, temperature, and nozzle size. In Figure 5.2, the printed filaments appeared to have been well deposited with adhesion present between each printed line; no visible defects were observed that could lead to reduced mechanical properties. However, this microscopy technique does not clearly show the air gaps present in the samples. Consequently, confocal microscopy was used.

Figure 5.3 shows confocal microscopy images for the same FDM printed PHB sample as above. As mentioned in Section 3.3.2, this technique uses 3D imaging to create intensity map images that make it easier to compare the regions of PHB material versus volume of air

gaps in the FDM printed sample (highlighted in Figure 5.3). In Figure 5.3(a and b), a minimal amount of air gap was observed, relating to a well-deposited filament. In Figure 5.3(c) however, which corresponds to the edge of the tensile specimen neck, a large air gap was seen. This void space was present between filament 1, which was printed horizontally for the sample perimeter, and filament 2, which was printed at a 45-degree angle to the first, done in order to fill in the neck region of the sample. This air gap, commonly found in FDM printing, was visible along most of the neck edge in only some of the tested samples, and thus, may explain the decrease in mechanical properties (specifically for *E*), but also the large standard deviations reported (see Section 5.1) [69], [70], [72]. For example, the standard deviation for the strain at break of the FDM samples was likely associated with either the strong adhesion between densely packed printed filaments (*i.e.* upper limit) or the large amount of void space present in some samples (*i.e.* lower limit). Like the wave properties of the printed lines, the air gap can be reduced and print quality improved by optimizing the printing parameters and using extruded filaments with diameter's closer to 1.75 mm (rather than ranging between 1.60 and 1.75 mm) for better filament flow, deposition and adhesion (refer to Section 2.2.2.2) [69], [70], [72]. This, in turn, these improvements could enhance the mechanical properties of the PHB printed part.

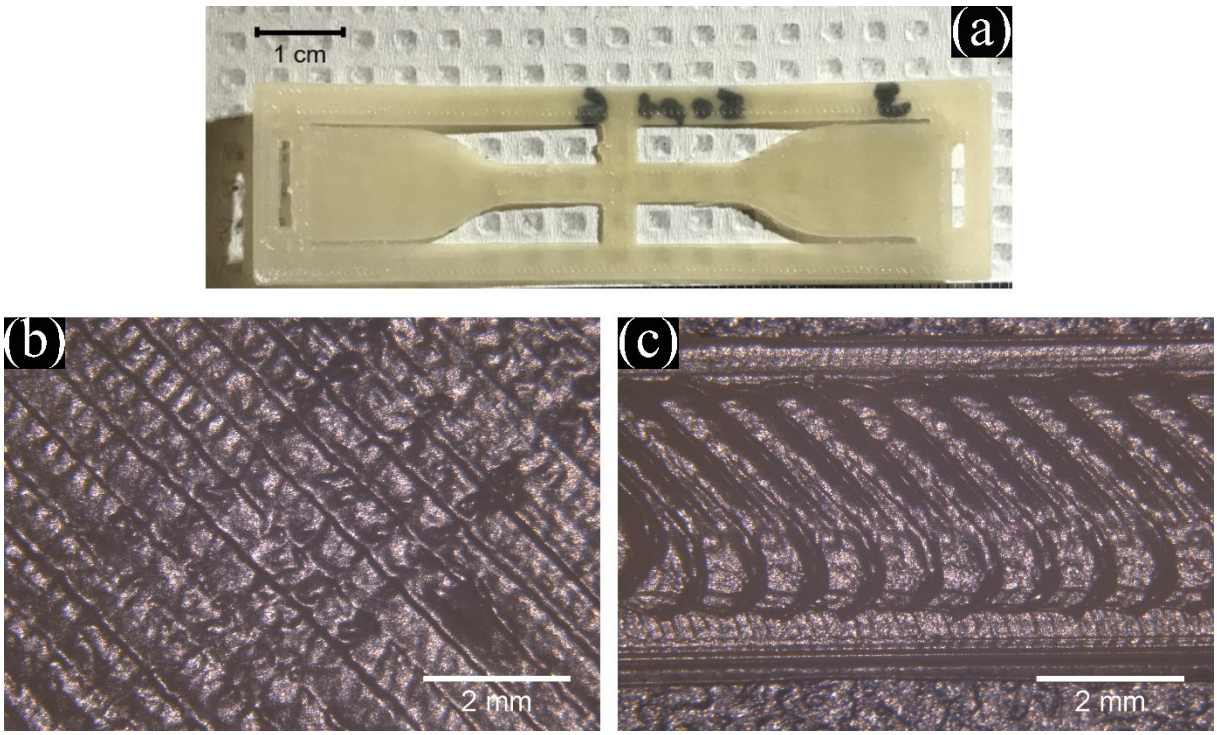

Figure 5.2: FDM printed PHB tensile specimen (a) and stereomicroscope images of the top surface of the sample; filament arrangement for grip portion (b) and neck portion (c) of the tensile specimen

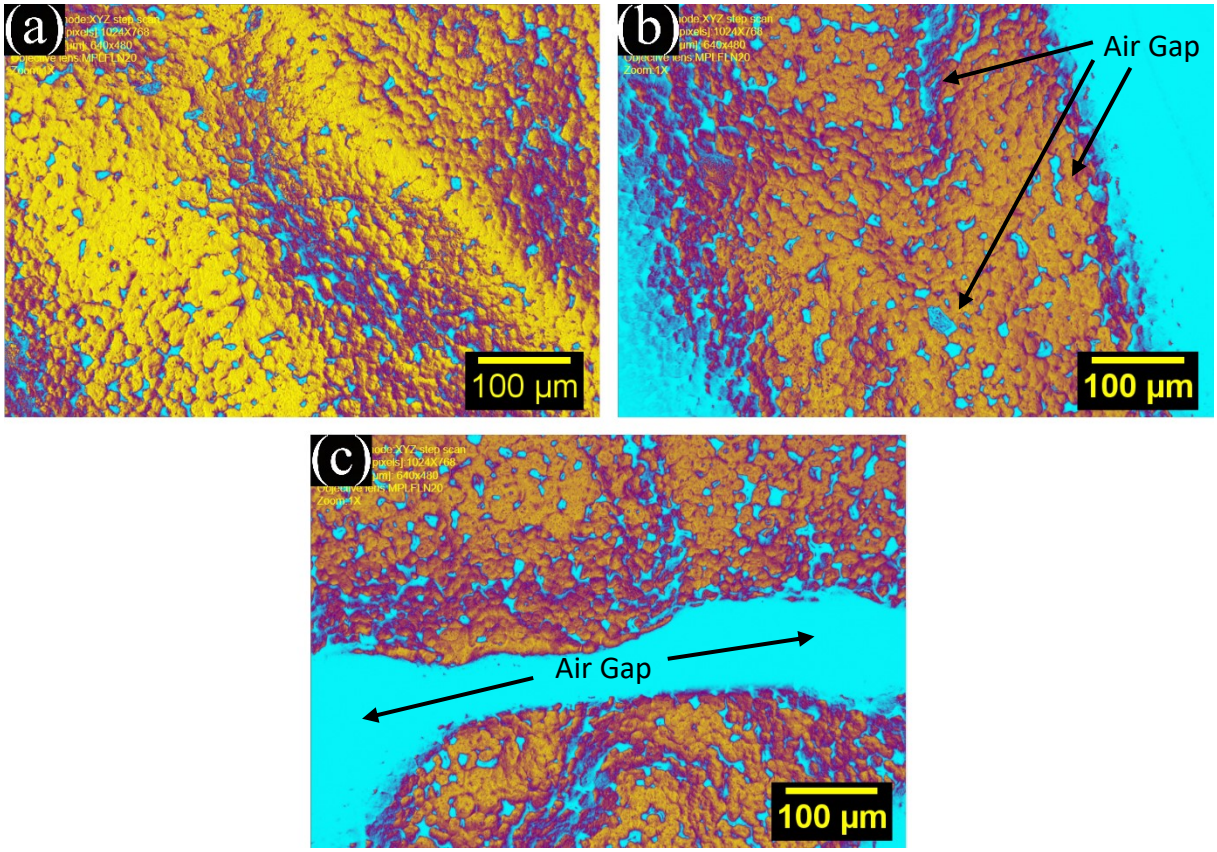

Figure 5.3: 3D images collected by confocal microscopy of the FDM tensile specimen; grip end (a), neck/bracing region (b) and the edge of the neck (c)

5.3 Thermal Properties

The DSC melting curves for the three stages of the FDM printing process (*i.e.* initial PHB pellets, extruded material and FDM samples) are shown in Figure 5.4 and the corresponding onset T_m, peak T_{m2} and X_{cDSC} for PHB are reported in Table 5.2. Note that the data for the hot-pressed NeatPHB sheet from Table 4.1 is shown for comparative purposes.

In this heating/melting stage of the cycle (Figure 5.4), a secondary peak was quite pronounced in the FDM sample run, partially observed in the filament run and even less so in the pellet run. As mentioned in Section 4.4, the peaks (and small shoulder in the PHB pellet run) are associated with "as formed" PHB crystallites. For both temperatures collected from the DSC run, the three stages of the printing process have identical values (within standard deviation). From this data alone, it can be concluded that there is little to no change in thermal properties after the processing steps, meaning FDM may be a viable option for processing PHB without changing its thermal properties.

X_{cDSC} for the samples after each stage of the FDM printing process was calculated using Equation 3.1 and ΔH_m, which was estimated by the integration of the melting peaks from the

DSC curves in Figure 5.4. These values are summarized in Table 5.2 and compared to the value previously shown for hot-pressed NeatPHB samples. These calculations show that the average X_{cDSC} of PHB increased following the extrusion step and the FDM printing step, from 28.9 ± 0.1% (n = 3) to 31.3 ± 0.5% (n = 3) and 36.3 ± 4.5% (n = 4), respectively. This relatively large increase in the average crystallinity of the material following the FDM printing can be associated with the rate of heating and/or cooling of the material during the processing, which has been observed with other printing materials such as ABS [72]. In this work, the FDM hotend was set at a temperature of 180 °C and the PHB filaments were deposited onto the print bed. In Figure 5.4, this hotend temperature is located near the end of the second melting peak associated with the melting of stable crystals. It is possible that some of these fully stable crystals did not completely melt during the rapid printing process, and thus, some of the residual crystals could act as nucleating sites for increased crystal formation during the cooling stage of the process. Additionally, the FDM printing process has a relatively slow cooling rate as compared to other thermal processes (extrusion for example) because of its temperature gradient between the printer hotend and the surface of the rising printed model, especially since the thickness of the samples in this work was so small [72]. Although the sample was extruded through the hotend at 180 °C into an ambient environment (similar to the extrusion process when making filaments), the print bed on which the material was deposited had a temperature of 110 °C, reducing the cooling time, and thus allowing increased crystallinity [50], [121]. In addition, each deposited and bonded layer of PHB was slightly reheated by the new filaments being extruded on top or nearby, which led to a slower cooling process overall [72].

Table 5.2: DSC data for the three stages of the FDM printing process compared to hot-pressed PHB

DSC Results	Onset T_m (°C)	Peak T_{m2} (°C)	$X_{cDSC, PHB}$ (%)
PHB Pellet*	158 ± 3	172 ± 1	28.9 ± 0.1
Extruded Filament*	153 ± 2	172 ± 2	31.3 ± 0.5
FDM Sample	156 ± 1	171 ± 1	36.3 ± 4.5
Hot-Pressed NeatPHB*	153 ± 2	170 ± 1	34.5 ± 1.4

Note: n=3 for the PHB pellets and extruded PHB samples; n=4 for FDM printed samples; n=5 for hot-pressed NeatPHB
*First shown in Table 4.1

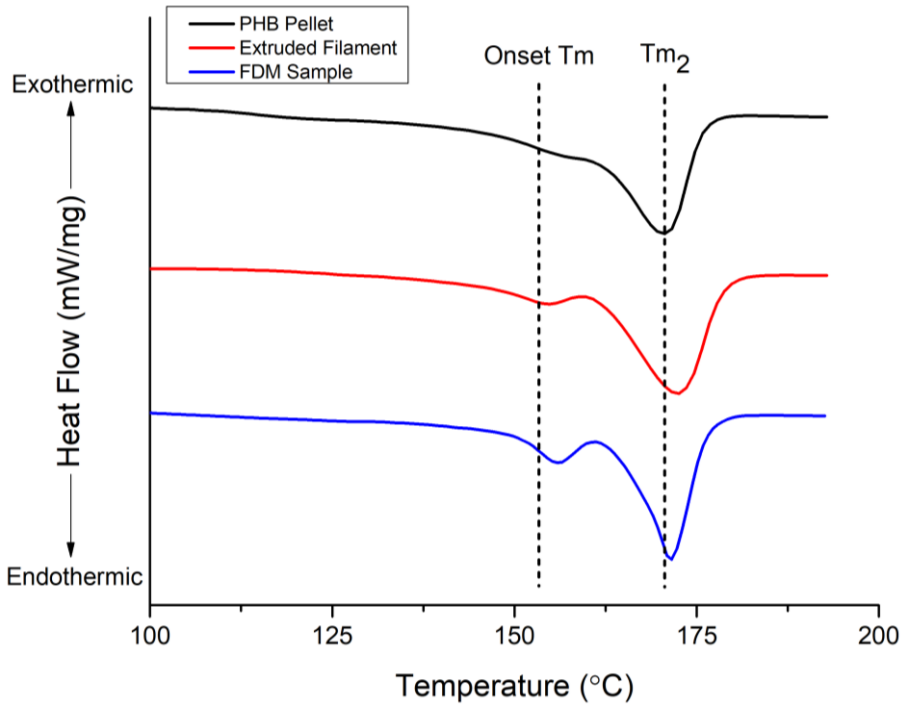

Figure 5.4: DSC melting curves for the three stages of the FDM printing process

To support the claim that the processing steps do not change the thermal stability properties of PHB, TGA characterization was also performed for the FDM samples with the onset degradation and peak degradation temperatures reported in Table 5.3 alongside the values for the PHB pellets and extruded filaments. The associated TGA curves are shown in Figure 5.5 along with the curves for the hot-pressed NeatPHB samples (from this research) and a solvent cast thin film of PHB (prepared in another work from this lab) for comparison [13]. From the results highlighted in the table, there was no sign of significant thermal degradation occurring during the extrusion and printing processes, and it is likely that the slight increase in crystallinity following these steps provided an increase in the thermal resistance of the material [72]. In addition, these results were quite similar to the hot-pressed and solvent cast samples. As noted in Section 4.4, any possible thermal degradation taking place during the printing process is not substantial as it is indistinguishable using these thermal characterization techniques.

Table 5.3: TGA data for FDM process as well as other processing techniques

TGA Results	Onset Degradation *T* (°C)	Peak Degradation *T* (°C)
PHB Pellet*	292	306
Extruded Filament*	292	305
FDM Sample	295	307
Hot-Pressed NeatPHB*	292	303
Solvent Cast Thin Film [13]	284	305

Note: Max standard deviation = ± 5 °C
*First shown in Table 4.2

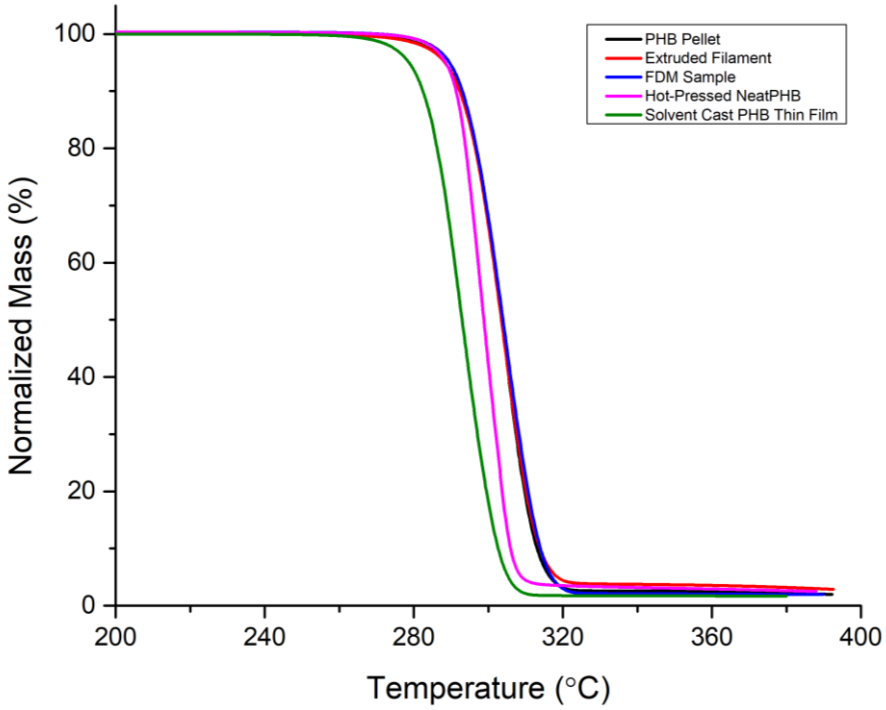

Figure 5.5: TGA plot for the three stages of the FDM printing process compared to two other techniques used to process PHB

5.4 Summary of FDM Printing Work

In this section, the FDM printing work was highlighted to show that the process of FDM could be used as a viable option for commercial processing of PHB. In this analysis, the extrusion and FDM printing steps had no significant effect on the thermal properties of PHB along with no measured thermal or mechanical degradation (at the processing and analysis temperatures chosen). However, the processing steps did have an effect on the crystallinity of PHB samples, as the value increased after each step (as compared to the as-received PHB pellets). In addition

to analysis of the thermal properties, mechanical testing was performed for the FDM printed samples and compared to hot-pressed NeatPHB samples (see Chapter 4) and solvent cast thin films of PHB (prepared in another work) [13]. In terms of strength (*i.e.* E and σ_{UTS}), the FDM samples had statistically significant decreases in the tested parameters as compared to the hot-pressed NeatPHB samples, while insignificant change was found between the FDM samples and solvent cast thin films for these same parameters. Moreover, when comparing the flexibility of the FDM printed samples to the other two processing techniques, the change in average ε_b between the three techniques was statistically insignificant. FDM printed samples commonly have reduced mechanical properties as compared to their bulk counterparts, but the FDM printed PHB samples created in this work showed very promising strength parameters and flexibility, with plenty of room for adjustment in the printing process still available.

6. CONCLUSIONS AND FUTURE WORK

6.1 Conclusions

In this study, eCO and PLA were introduced as possible plasticizers for PHB to potentially improve processability as well as thermal and mechanical properties. In addition, the processing of PHB products through the commercial scalable processes of extrusion, hot-pressing, and FDM/3D printing was investigated. Methods to fabricate hot-pressed plasticized PHB and FDM printed PHB specimens were presented. Given that the processing techniques use elevated temperatures, degradation of the polymer material could possibly occur. Therefore, this study not only explored the impact of the material properties as a function of the processing techniques but also the introduction of possible thermal and mechanical degradation mechanisms in the polymer system.

The green plasticizer, eCO, and polymeric plasticizer, PLA, were mixed with PHB and hot-pressed to create plasticized polymer sheets for testing. With the incorporation of these additives into the PHB matrix, no significant change in thermal properties or stability was observed (at the processing and analysis temperatures); however, these additives did affect the mechanical properties. It was shown that 10 wt% eCO provided a statistically significant improvement in flexibility over neat PHB samples. Additionally, combining PLA (at 25 wt%) with a transesterification-reaction-catalyst blended with PHB resulted in a decrease in strength parameters but increased flexibility. This result is critical, as the brittleness of PHB is one of the main reasons why it is not more commonly used in commercial applications; however, an unexpected decrease in strength parameters with the addition of the zinc acetate means that further exploration is required before making a conclusion on the benefit of using such a material. eCO (at 5 wt%) and PLA did blend well with PHB, maintaining improved flexibility over neat PHB material. On the other hand, the processing window, thermal properties and thermal stability were unaffected with the additives and processing parameters chosen.

PHB was successfully patterned using FDM. It was determined that the extrusion, hot-pressing, and FDM processing methods had no effect on the thermal properties of PHB and no thermal or mechanical degradation was observed. These techniques did have a slight effect on the crystallinity of the samples, as the value increased after each stage of processing (*i.e.* extrusion, then hot-pressing and extrusion, then FDM printing). In addition, the tested strength parameters of the FDM printed PHB specimens were significantly less than for the hot-pressed NeatPHB samples. However, an insignificant change in material flexibility as compared the two previous processing methods highlighted (*i.e.* hot-pressing and solvent casting) was seen

for the FDM printed PHB, along with insignificant changes in strength parameters as compared to the solvent cast thin films. For FDM specifically, improvements in mechanical properties are possible with slight adjustments in printing parameters. Therefore, PHB can be processed with extrusion, hot-pressing, and FDM printing without drastic changes to the properties of the material. Due to its ease of use, an assortment of adjustable parameters, cost efficiency, and commercial scalability, FDM especially could be used for the processing of usable PHB.

6.2 Future Work and Recommendations

6.2.1 Polymer Degradation from Processes and Plasticizers

The molecular weight distribution of the PHB pellets, extruded material, hot-pressed plasticized samples, and FDM printed samples can be collected and analyzed by GPC. Agilent Technologies Canada recommends using two Agilent PLgel 10 µm MIXED-B columns and suggests preparing each sample into a 0.2% w/v solution with chloroform and heating to 60 °C for 2 hours. Other run conditions to note are the injection volume, flow rate and temperature, which are recommended at 100 µL, 1.0 mL/min and ambient, respectively. These experiments will help determine the amount and rate of PHB degradation occurring after each of the processing steps as well as with the addition of the plasticizers studied in this work (*i.e.* eCO, PLA and zinc acetate). This can be done by collecting the polymer's molecular weight (both weight average, M_w, and number average, M_n) from the GPC analysis and comparing the initial value to that of the samples following each thermomechanical or thermal processing techniques and/or the addition of the plasticizing materials (see Section 2.2.4). For example, Yang *et al.* observed that melt blending zinc acetate (in amounts up to 0.4 wt%) into neat PHBV drastically reduced the M_w and M_n of the sample, indicating thermal degradation, whereas little change in M_w and M_n was seen when the same catalyst was added to neat PLA. However, the same analysis showed that the transesterification reaction between the PLA and PHBV (in a 2.33:1 ratio), catalyzed by the zinc acetate, suppressed the degradation of the PHBV. Therefore, GPC analysis on the samples prepared in this work could help determine (1) whether a reaction is being catalyzed between the PHB and PLA and (2) if the polymer samples are being degraded from either the processing techniques or plasticizers or both.

6.2.2 Other Work

The processing of PHB was investigated with two main focuses: (1) commercially scalable processes and (2) bio-based plasticizers for increased processability. However, some areas of

this work could be expanded upon to better understand how PHB can be affected and used in applications.

In the completed work, the FDM printing parameters were chosen as they helped limit the amount of air gap across the entire sample. However, some further fine-tuning could be performed to optimize the process. This can include printing temperatures (*i.e.* nozzle and bed), printing speeds, pattern, and fill density (*i.e.* can set it in the program above 100%) [69], [70], [72]. Additionally, placing the FDM printer within an enclosure designed to regulate the temperature of the entire sample can prevent uneven cooling of the sample that leads to internal stresses and sample warping [101]. This enclosure can also be used to control humidity that can help with filament deposition and adhesion, assisting in the reduction of air gaps [101]. In addition to the printing process itself, a technique of "recycling" (*i.e.* cut extruded filaments into small pellets and re-extrude them into new filaments) can be used to make filaments of higher bulk density, which can assist in the printing process by improving filament layer fusion and flow rates [122]. Ultimately, these recommendations may help reduce the air gap in the samples and improve the overall print quality, potentially leading to enhanced mechanical properties.

To improve the properties and processability, further exploration of the use of eCO, PLA and/or zinc acetate (in different quantities) or similar bio-plasticizers with PHB should be investigated. PHB can also be combined with another compatible polymer (or polymers) and/or a reinforcing or conductive filler. These polymers and fillers can be non-degradable and/or synthetic products, but this will take away the largest benefit of using PHB. Therefore, filler materials such as cellulose nanocrystals (CNCs) could also be examined, as they too are bio-based products that could lead to improvements in mechanical properties.

Further exploration of FDM printing of PHB can be completed with pure PHB material but also, the PHB blends highlighted in this work (*i.e.* addition of eCO and PLA) could be used with the FDM printing process. Additionally, if other polymers or fillers are used with PHB, these composite samples could also be tested using the FDM printing process. These blended materials would be extruded into filaments and then printed, where the properties could be compared to that of pure PHB samples that were already tested in this work. This additional research could give further insight into the use of PHB for commercial applications and whether or not FDM printing with pure PHB material is the best option, or if introducing additives could provide a superior product.

Lastly, the recyclability and degradability of the products created and tested in this work (and future works) should be explored and the results compared to PHB processed by techniques such as solvent casting. This would show what the effect of the processing stage has on the final properties of the material. Additionally, it can provide insight into how the tested additives (eCO and PLA) affect the biodegradation of the polymer, as some can have a negative impact, which would reduce the environmental benefits associated with PHB [7]. The recyclability of the material can be investigated by melting the final hot-pressed or FDM samples and then hot-pressing or printing again, with any number of cycles, testing the thermal and mechanical properties after each cycle to confirm consistency. Lab simulation of soil, compost, or landfills can be used for the study of the degradability of the PHB samples. These tests will have complex environments but controlled pH, temperature, and humidity. The samples can be buried and simple weight loss measurements can be completed following a burial timeline. Additionally, purified enzymes known to degrade PHB (*i.e.* PHB depolymerase) can be used with the samples and the results compared to solvent cast thin films of PHB that were previously completed by Martínez-Tobón *et al.* [44].

All of the future work noted above can expand the study of PHB as a possible alternative to fossil-fuel based polymers for commercial applications. This alternative use could potentially lead to a reduction in plastic waste around the world. This change in industry and larger use of biopolymers, such as PHB, will not occur rapidly; however, the work in this study is a stepping stone towards greater opportunity for these biodegradable polymers, which can help to ensure that our environment is not completely consumed by plastic waste.

REFERENCES

[1] N. G. McCrum, C. P. Buckley, C. B. Bucknall, and C. B. Bucknall, *Principles of Polymer Engineering*, 2nd ed. Oxford University Press, 1997.

[2] S. Li, "Investigation of Effect of Plasticizer and Compatibilizers on Soy Protein Ternary Blends," Washington State University, 2012.

[3] M. Šprajcar, P. Horvat, and A. Kržan, "Biopolymers and Bioplastics - Plastics Aligned with Nature," Ljubljana, Slovenia, May 2012.

[4] Markets and Markets, "Bioplastics & Biopolymers Market by Type (Bio-PE, Bio-PET, PLA, Starch Blends, Biodegradable Polyesters, Regenerated Cellulose and PHA), Application (Packaging, Bottles, Agriculture), and by Region - Trends & Forecast to 2021," Northbrook, Illinois, 2016.

[5] S. Mann, "Saltwater Creek Walkway," *Creative Commons*, 2009. [Online]. Available: https://www.flickr.com/photos/21218849@N03/3183610197. [Accessed: 30-Jul-2018].

[6] United States Fish and Wildlife Service, "Albatross at Midway Atoll Refuge," 2009. [Online]. Available: https://www.flickr.com/photos/usfwshq/8080507529. [Accessed: 30-Jul-2018].

[7] D. Roland-Holst, R. Triolo, S. Heft-Neal, and B. Bayrami, "Bioplastics in California: Economic Assessment of Market Conditions for PHA/PHB Bioplastics Produced from Waste Methane," Berkeley, California, 2013.

[8] M. Niaounakis, "Definitions of Terms and Types of Biopolymers," in *Biopolymers: Applications and Trends*, 1st ed., Rijswijk, Netherlands: William, Andrew, 2015, pp. 1–90.

[9] EPI Environmental Products Inc., "EPI - Oxo-Biodegradable Plastic Technology," 2018. [Online]. Available: http://www.epi-global.com/en. [Accessed: 06-Jul-2018].

[10] D. Jendrossek and R. Handrick, "Microbial Degradation of Polyhydroxyalkanoates," *Annu. Rev. - Microb.*, no. 56, pp. 403–432, 2002.

[11] V. Ryan, "BIOPOL - Biodegradable Plastic," 2014. [Online]. Available: http://www.technologystudent.com/prddes1/biopola.html. [Accessed: 05-Jul-2018].

[12] A. C. Mottin, E. Ayres, R. L. Oréfice, and J. J. D. Câmara, "What Changes in Poly(3-Hydroxybutyrate) (PHB) When Processed as Electrospun Nanofibers or Thermo-Compression Molded Film?," *Mater. Res.*, vol. 19, no. 1, pp. 57–66, Feb. 2016.

[13] P. Anbukarasu, D. Sauvageau, and A. Elias, "Tuning the properties of polyhydroxybutyrate films using acetic acid via solvent casting," *Sci. Rep.*, vol. 5, no.

17884, 2015.

[14] M. Niaounakis, “Packaging,” in *Biopolymers: Applications and Trends*, 1st ed., Rijswijk, Netherlands: William, Andrew, 2015, pp. 139–183.

[15] D. Z. Bucci, L. B. B. Tavares, and I. Sell, “PHB packaging for the storage of food products,” *Polym. Test.*, vol. 24, no. 5, pp. 564–571, 2005.

[16] T. Gredes, T. Gedrange, C. Hinüber, M. Gelinsky, and C. Kunert-Keil, “Histological and molecular-biological analyses of poly(3-hydroxybutyrate) (PHB) patches for enhancement of bone regeneration,” *Ann. Anat. - Anat. Anzeiger*, vol. 199, pp. 36–42, May 2015.

[17] G. Cleaver and Agilent Tehcnologies Inc., “GPC/SEC Analysis of Biodegradable Polyhydroxyalkanoate on Agilent PLgel 10 µm MIXED-B Columns,” USA, 2015.

[18] M. Niaounakis, “Properties,” in *Biopolymers: Applications and Trends*, 1st ed., Rijswijk, Netherlands: William, Andrew, 2015, pp. 91–138.

[19] International Association of Plastics Distribution, “Typical Properties of Polypropylene (PP).” IAPD, Overland Park, Kansas, 2018.

[20] International Association of Plastics Distribution, “Typical Properties of Polyethylene (PE).” IAPD, Overland Park, Kansas, 2018.

[21] Kholoudabdolqader, “Filament Driver Diagram,” *Wikipedia/Creative Commons*, 2017. [Online]. Available: https://commons.wikimedia.org/wiki/File:Filament_Driver_diagram.svg. [Accessed: 14-Aug-2018].

[22] T. F. Pereira *et al.*, “Effect of process parameters on the properties of selective laser sintered Poly(3-hydroxybutyrate) scaffolds for bone tissue engineering,” *Virtual Phys. Prototyp.*, vol. 7, no. 4, pp. 275–285, 2012.

[23] T. F. Pereira, M. F. Oliveira, I. A. Maia, J. V. L. Silva, M. F. Costa, and R. M. S. M. Thiré, “3D Printing of Poly(3-hydroxybutyrate) Porous Structures Using Selective Laser Sintering,” *Macromol. Symp.*, vol. 319, no. 1, pp. 64–73, 2012.

[24] M. Zhang and N. L. Thomas, “Blending polylactic acid with polyhydroxybutyrate: The effect on thermal, mechanical, and biodegradation properties,” *Adv. Polym. Technol.*, vol. 30, no. 2, pp. 67–79, 2011.

[25] B. W. Chieng, N. A. Ibrahim, Y. Y. Then, and Y. Y. Loo, “Epoxidized Vegetable Oils Plasticized Poly(lactic acid) Biocomposites: Mechanical, Thermal and Morphology Properties,” *Molecules*, vol. 19, no. 10, pp. 16024–16038, 2014.

[26] E. Bugnicourt, P. Cinelli, A. Lazzeri, and V. Alvarez, “Polyhydroxyalkanoate (PHA): Review of synthesis, characteristics, processing and potential applications in packaging,” *eXPRESS Polym. Lett.*, vol. 8, no. 11, pp. 791–808, 2014.

[27] Grand View Research Inc., “Bio Plasticizers Market Size Worth $2.68 Billion By 2025 | CAGR 10.7%,” San Francisco, California, 2017.

[28] M. Özgür Seydibeyoğlu, M. Misra, and A. Mohanty, “Synergistic improvements in the impact strength and % elongation of polyhydroxybutyrate-co-valerate copolymers with functionalized soybean oils and poss,” *Int. J. Plast. Technol.*, vol. 14, no. 1, pp. 1–16, 2010.

[29] P. Jia, M. Zhang, L. Hu, and Y. Zhou, “Green plasticizers derived from soybean oil for poly(vinyl chloride) as a renewable resource material,” *Korean J. Chem. Eng*, vol. 33, no. 3, pp. 1080–1087, 2016.

[30] H. Hosney, B. Nadiem, I. Ashour, I. Mustafa, and A. El-Shibiny, “Epoxidized vegetable oil and bio-based materials as PVC plasticizer,” *J. Appl. Polym. Sci*, vol. 135, no. 46270, 2018.

[31] Canadian Canola Growers Association (CCGA), “Canola: A Canadian Crop with Big Impact,” Ottawa, 2017.

[32] A. K. R. Somidi, P. K. Roayapalley, and A. K. Dalai, “Synthesis of O-propylated canola oil derivatives using Al-SBA-15 (10) catalyst and study on their application as fuel additive,” *Catal. Today*, vol. 291, pp. 204–212, 2017.

[33] Y. Tokiwa and B. Calabia, “Review Degradation of microbial polyesters,” *Biotechnol. Lett.*, vol. 26, no. 15, pp. 1181–1189, Aug. 2004.

[34] W. J. Orts, G. A. Nobes, J. Kawada, S. Nguyen, G. Yu, and F. Ravenelle, “Poly(hydroxyalkanoates): Biorefinery polymers with a whole range of applications. The work of Robert H. Marchessault,” *Can. J. Chem.*, vol. 86, no. 6, pp. 628–640, 2008.

[35] R. Lehrle, R. Williams, C. French, and T. Hammond, “Thermolysis and Methanolysis of Poly(P-hydroxybutyrate): Random Scission Assessed by Statistical Analysis of Molecular Weight Distributions,” *Macromolecules*, vol. 28, no. 13, pp. 4408–4414, 1995.

[36] J. Asrar, K. J. Gruys, Y. Doi, A. Steinbüchel, and Y. Doi, “Biodegradable Polymer (Biopol®),” in *Biopolymers Online*, 1 Edition., Y. Doi and A. Steinbüchel, Eds. Weinheim, Germany: Wiley-VCH Verlag GmbH & Co. KGaA, 2005, pp. 53–90.

[37] J. Rydz, W. Sikorska, M. Kyulavska, and D. Christova, “Polyester-based

(bio)degradable polymers as environmentally friendly materials for sustainable development," *Int. J. Mol. Sci.*, vol. 16, no. 1, pp. 564–596, 2015.

[38] Wikipedia Encyclopedia, "Polyhydroxyalkanoates (PHA)," 2017. [Online]. Available: https://en.wikipedia.org/wiki/Polyhydroxyalkanoates. [Accessed: 04-May-2017].

[39] C. R. Hankermeyer and R. S. Tjeerdema, "Polyhydroxybutyrate: plastic made and degraded by microorganisms," *Rev. Environ. Contam. Toxicol.*, vol. 159, pp. 1–24, 1999.

[40] W. Maurício Pachekoski, C. Dalmolin, and J. Augusto Marcondes Agnelli, "The Influence of the Industrial Processing on the Degradation of Poly(hidroxybutyrate) – PHB," *Mater. Res.*, vol. 16, no. 2, pp. 327–332, 2013.

[41] A. M. el-H. A. Ghaffar, "Development of a biodegradable material based on poly(3-hydroxybutyrate) PHB," Martin Luther University Halle-Wittenberg, 2002.

[42] A. Bonartsev *et al.*, "Biosynthesis, biodegradation, and application of poly(3-hydroxybutyrate) and its copolymers - Natural polyesters produced by diazotrophic bacteria," *Commun. Curr. Res. Educ. Top. Trends Appl. Microbiol.*, vol. 1, pp. 295–307, 2007.

[43] A. A. Shah, F. Hasan, A. Hameed, and S. Ahmed, "Biological degradation of plastics: A comprehensive review," *Biotechnol. Adv.*, vol. 26, no. 3, pp. 246–265, 2008.

[44] D. I. Martínez-Tobón, M. Gul, A. L. Elias, and D. Sauvageau, "Polyhydroxybutyrate (PHB) biodegradation using bacterial strains with demonstrated and predicted PHB depolymerase activity," *Appl. Microbiol. Biotechnol.*, Jul. 2018.

[45] N. Grassie and E. J. Murray, "The Thermal Degradation of Poly(-(D)-fl-Hydroxybutyric Acid): Part 2 Changes in Molecular Weight," *Polym. Degrad. Stab.*, vol. 6, pp. 95–103, 1984.

[46] C. Booth, "The Mechanical Degradation of Polymers," *Polymer (Guildf).*, vol. 4, pp. 471–478, 1963.

[47] E. Hablot, P. Bordes, E. Pollet, and L. Ave´rous, "Thermal and thermo-mechanical degradation of poly(3-hydroxybutyrate)-based multiphase systems," *Polym. Degrad. Stab.*, vol. 93, no. 2, pp. 413–421, 2008.

[48] Wikipedia Encyclopedia, "Polymer degradation," 2016. [Online]. Available: https://en.wikipedia.org/wiki/Polymer_degradation#Chemical_degradation. [Accessed: 04-May-2017].

[49] P. Anbukarasu, D. Martinez-Tobon, D. Sauvageau, and A. Elias, "A Diffraction-Based

Degradation Sensor for Polymer Thin Films," *Polym. Degrad. Stab.*, vol. 142, pp. 102–110, 2017.

[50] R. Narain, "Advanced Polymeric and Nanomaterials Lecture Notes." University of Alberta, Edmonton, AB, 2017.

[51] D. Lovera, L. Márquez, V. Balsamo, A. Taddei, C. Castelli, and A. J. Müller, "Crystallization, morphology, and enzymatic degradation of polyhydroxybutyrate/ polycaprolactone (PHB/PCL) blends," *Macromol. Chem. Phys.*, vol. 208, no. 9, pp. 924–937, 2007.

[52] Agilent Technologies Inc., "An Introduction to Gel Permeation Chromatography and Size Exclusion Chromatography." pp. 1–32, 2015.

[53] M. Itavaara and M. Vikman, "An Overview of Methods for Biodegradability Testing of Biopolymers and Packaging Materials," *J. Environ. Polym. Degrad. No. I*, vol. 4, no. 1, 1996.

[54] U. Pagga, "Testing Biodegradability with Standardized Methods," *Chemosphere*, vol. 35, no. 12, pp. 2953–2972, 1997.

[55] R.-J. Muller, "Biodegradability of Polymers: Regulations and Methods for Testing," in *Biopolymers Online*, 1 Edition., Y. Doi and A. Steinbüchel, Eds. Weinheim, Germany: Wiley-VCH Verlag GmbH & Co. KGaA, 2005, pp. 365–388.

[56] M. Niaounakis, "Medical, Dental, and Pharmaceutical Applications," in *Biopolymers: Applications and Trends*, 1st ed., Rijswijk, Netherlands: William, Andrew, 2015, pp. 291–405.

[57] A. Do, B. Khorsand, S. M. Geary, and A. K. Salem, "3D Printing of Scaffolds for Tissue Regeneration Applications," *Adv. Healthc. Mater.*, vol. 4, no. 12, pp. 1742–1762, Aug. 2015.

[58] M. Niaounakis, "Agriculture/Forestry/Fishery," in *Biopolymers: Applications and Trends*, 1st ed., Rijswijk, Netherlands: William, Andrew, 2015, pp. 185–232.

[59] M. Niaounakis, "Cosmetics," in *Biopolymers: Applications and Trends*, 1st ed., Rijswijk, Netherlands: William, Andrew, 2015, pp. 407–425.

[60] E. Ohashi *et al.*, "Biodegradable Poly(3-hydroxybutyrate) Nanocomposite," *Macromol. Symp.*, vol. 279, no. 1, pp. 138–144, May 2009.

[61] WACKER Chemie AG, "PHA/PHB Applications," 2017. [Online]. Available: https://www.wacker.com/cms/en/industries/plastics/co_binder/pha_phb/mcpphaphb_anwendungen.jsp?country=CA&language=en. [Accessed: 04-May-2017].

[62] Vacho, “Engine Oil Plastic Containers,” *Pixabay/Creative Commons*, 2017. [Online]. Available: https://pixabay.com/en/tara-oil-engine-oil-2338587/. [Accessed: 14-Aug-2017].

[63] J. Ramier *et al.*, “Biocomposite scaffolds based on electrospun poly(3-hydroxybutyrate) nanofibers and electrosprayed hydroxyapatite nanoparticles for bone tissue engineering applications,” *Mater. Sci. Eng. C. Mater. Biol. Appl.*, vol. 38, pp. 161–169, May 2014.

[64] X. Li *et al.*, “3D-printed biopolymers for tissue engineering application,” *Int. J. Polym. Sci.*, vol. 2014, no. 829145, pp. 1–13, 2014.

[65] A. Muraev *et al.*, “Development and Preclinical Studies of Orthotopic Bone Implants Based on a Hybrid Construction from Poly(3-Hydroxybutyrate) and Sodium Alginate,” *Adv. Res.*, vol. 8, no. 4, pp. 42–50, 2016.

[66] P. A. Holmes, “Applications of PHB - a microbially produced biodegradable thermoplastic,” *Phys. Technol.*, vol. 16, no. 1, pp. 32–36, Jan. 1985.

[67] S. Peters, *Material Revolution : Sustainable and Multi-Purpose Materials for Design and Architecture*, 2nd ed. Basel, Switzerland: Birkhäuser Architecture, 2010.

[68] M. R. Skorski, J. M. Esenther, Z. Ahmed, A. E. Miller, and M. R. Hartings, “The chemical, mechanical, and physical properties of 3D printed materials composed of TiO2-ABS nanocomposites,” *Sci. Technol. Adv. Mater.*, vol. 17, no. 1, pp. 89–97, 2017.

[69] M. Fernandez-Vicente, W. Calle, S. Ferrandiz, and A. Conejero, “Effect of Infill Parameters on Tensile Mechanical Behavior in Desktop 3D Printing,” *3d Print. Addit. Manuf.*, vol. 3, no. 3, pp. 183–192, 2016.

[70] J. F. Rodriguez, J. P. Thomas, and J. E. Renaud, “Characterization of the mesostructure of fused-deposition acrylonitrile-butadienestyrene materials,” *Rapid Prototyp. J.*, vol. 6, no. 3, pp. 175–185, 2000.

[71] S. Stratton, O. S. Manoukian, R. Patel, A. Wentworth, S. Rudraiah, and S. G. Kumbar, “Polymeric 3D printed structures for soft-tissue engineering,” *J. Appl. Polym. Sci.*, vol. 135, no. 24, pp. 1–13, 2018.

[72] C. Benwood, A. Anstey, J. Andrzejewski, M. Misra, and A. K. Mohanty, “Improving the Impact Strength and Heat Resistance of 3D Printed Models: Structure, Property, and Processing Correlationships during Fused Deposition Modeling (FDM) of Poly(Lactic Acid),” *ACS Omega*, vol. 3, no. 4, pp. 4400–4411, 2018.

[73] J. T. Belter and A. M. Dollar, “Strengthening of 3D Printed Fused Deposition Manufactured Parts Using the Fill Compositing Technique,” *PLoS One*, vol. 10, no. 4,

pp. 1–19, 2015.

[74] G. Hodgson, A. Ranellucci, and J. Moe, “Infill Patterns and Density,” *Slic3r Manual*, 2018. [Online]. Available: http://manual.slic3r.org/expert-mode/infill. [Accessed: 18-Apr-2018].

[75] X. Wang, M. Jiang, Z. Zhou, J. Gou, and D. Hui, “3D printing of polymer matrix composites: A review and prospective,” *Compos. Part B Eng.*, vol. 110, pp. 442–458, 2017.

[76] M. Meischel *et al.*, “Adhesive strength of bone-implant interfaces and in-vivo degradation of PHB composites for load-bearing applications,” *J. Mech. Behav. Biomed. Mater.*, vol. 53, pp. 104–118, 2016.

[77] 3D Printer and Printing News, “Russian researchers develop new method for 3D printing biodegradable bones,” 2016. [Online]. Available: http://www.3ders.org/articles/20160623-russian-researchers-develop-new-method-for-3d-printing-biodegradable-bones.html. [Accessed: 05-May-2017].

[78] X. Wentao, “CN 105462203 A - PHB based degradable 3D printing material,” 105462203A, 2016.

[79] M. A. Gunning, L. M. Geever, J. A. Killion, J. G. Lyons, B. Chen, and C. L. Higginbotham, “The effect of the mixing routes of biodegradable polylactic acid and polyhydroxybutyrate nanocomposites and compatibilised nanocomposites,” *J. Thermoplast. Compos. Mater.*, vol. 29, no. 4, pp. 538–557, 2016.

[80] M. Gurgel *et al.*, “Natural-based plasticizers and biopolymer films: A review,” *Eur. Polym. J.*, vol. 47, no. 3, pp. 254–263, 2011.

[81] Acute Market, “Global Plasticizers Market Size, Market Share, Application Analysis, Regional Outlook, Growth Trends, Key Players, Competitive Strategies and Forecasts, 2017 to 2025,” Global, 2017.

[82] I. Janigova, I. Lací, and I. Choda, “Thermal degradation of plasticized poly(3-hydroxybutyrate) investigated by DSC,” *Polym. Degrad. Stab.*, vol. 77, no. 1, pp. 35–41, 2002.

[83] M. Râpə *et al.*, “Effect of plasticizers on melt processability and properties of PHB,” *J. Optoelectron. Adv. Mater.*, vol. 17, no. 11–12, pp. 1778–1784, 2015.

[84] R. S. Kurusu, C. A. Siliki, É. David, N. R. Demarquette, C. Gauthier, and J.-M. Chenal, “Incorporation of plasticizers in sugarcane-based poly(3-hydroxybutyrate)(PHB): Changes in microstructure and properties through ageing and annealing,” *Ind. Crop.*

Prod., vol. 72, pp. 166–174, 2015.

[85] J. S. Choi and W. H. Park, "Effect of biodegradable plasticizers on thermal and mechanical properties of poly(3-hydroxybutyrate)," *Polym. Test.*, vol. 23, no. 4, pp. 455–460, 2004.

[86] R. C. Baltieri, L. H. I. Mei, and J. Bartoli, "Study of the influence of plasticizers on the thermal and mechanical properties of Poly(3-hydroxybutyrate) compounds," *Macromol. Symp. Recent Adv. Biodegrad. Polym. Plast.*, vol. 197, no. 1, pp. 33–44, 2003.

[87] N. C. Billingham, T. J. Henman, and P. A. Holmes, "Degradation and Stabilisation of Polyesters of Biological and Synthetic Origin," in *Developments in Polymer Degradation-7*, 7th ed., Glasgow, IK: Springer, Dordrecht, 1987, pp. 81–121.

[88] I. T. Seoane, L. B. Manfredi, and V. P. Cyras, "Effect of two different plasticizers on the properties of poly(3-hydroxybutyrate) binary and ternary blends," *J. Appl. Polym. Sci.*, vol. 135, no. 12, pp. 1–12, 2018.

[89] P. M. Lorz, F. K. Towae, W. Enke, R. Jackh, N. Bhargava, and W. Hillesheim, *Phthalic Acid and Derivatives*, 1st ed. New York: Wiley-VCH Verlag GmbH & Co. KGaA, 2000.

[90] D. F. Parra, J. Fusaro, F. Gaboardi, and D. S. Rosa, "Influence of poly (ethylene glycol) on the thermal, mechanical, morphological, physical-chemical and biodegradation properties of poly (3-hydroxybutyrate)," *Polym. Degrad. Stab.*, vol. 91, no. 9, pp. 1954–1959, 2006.

[91] Canola Oil Council of Canada, "Current Canola Oil, Meal, and Seed Prices - Canola Council of Canada," *Canadian International Merchandise Trade Database, Statistics Canada*, 2018. [Online]. Available: https://www.canolacouncil.org/markets-stats/statistics/current-canola-oil,-meal,-and-seed-prices. [Accessed: 30-Apr-2018].

[92] Intratec Solutions LLC, "Dioctyl Phthalate (DOP) Price History & Forecast," Houston, Texas, 2010.

[93] G. Strobl, *Physics of Polymers: Concepts for Understanding their Structures and Behavior*, 3rd ed. Freiburg, Germany: Springer-Verlag Berlin Heidelberg, 2007.

[94] A. Södergård and M. Stolt, "Industrial Production of High Molecular Weight Poly(Lactic Acid)," in *Poly(Lactic Acid): Synthesis, Structures, Properties, Processing, and Applications*, 1st ed., R. Auras, L. Lim, S. E. M. Selke, and H. Tsuji, Eds. USA: Wiley-Blackwell, 2010, pp. 27–41.

[95] J. Ren, *Biodegradable Poly (Lactic Acid): Synthesis, Modification, Processing and Applications.*, 1st ed. Shanghai, China: Springer, Berlin, Heidelberg, 2011.

[96] M. Xiuyu, W. Yufeng, W. Jianqing, and X. Yaning, “Effect of PBAT on Property of PLA/PHB Film Used for Fruits and Vegetables,” *MATEC Web Conf.*, vol. 88, pp. 1–6, 2017.

[97] J. Yang *et al.*, “Transesterification induced mechanical properties enhancement of PLLA/PHBV bio-alloy,” *Polymer (Guildf).*, vol. 83, pp. 230–238, 2016.

[98] C. Thellen, M. Coyne, D. Froio, M. Auerbach, C. Wirsen, and J. A. Ratto, “A Processing, Characterization and Marine Biodegradation Study of Melt-Extruded Polyhydroxyalkanoate (PHA) Films,” *J. Polym. Environ.*, vol. 16, no. 1, pp. 1–11, 2008.

[99] Clextral, “Benefits of twin screw extrusion,” 2017. [Online]. Available: http://www.clextral.com/technologies-and-lines/technologies-et-procedes/benefits-of-twin-screw-extrusion/. [Accessed: 04-May-2017].

[100] E. Fortunati, I. Armentano, A. Iannoni, and J. M. Kenny, “Development and thermal behaviour of ternary PLA matrix composites,” *Polym. Degrad. Stab.*, vol. 95, no. 11, pp. 2200–2206, 2010.

[101] Simplify3D, “Print Quality Troubleshooting Guide,” 2018. [Online]. Available: https://www.simplify3d.com/support/print-quality-troubleshooting/. [Accessed: 19-Sep-2018].

[102] “ISO 527-1: Plastics - Determination of tensile properties, Part 1: General principles.” International Organization for Standardization, 2012.

[103] “ISO 527-2: Plastics - Determination of tensile properties, Part 2: Test conditions for moulding and extrusion plastics.” International Organization for Standardization, 2012.

[104] B. L. Hurrell and R. E. Cameron, “A wide-angle X-ray scattering study of the ageing of poly(hydroxybutyrate),” *J. Mater. Sci.*, vol. 33, no. 7, pp. 1709–1713, 1998.

[105] W. Zhai, Y. Ko, W. Zhu, A. Wong, and C. B. Park, “A Study of the Crystallization, Melting, and Foaming Behaviors of Polylactic Acid in Compressed CO 2,” *Int. J. Mol. Sci.*, vol. 10, no. 12, pp. 5381–5397, 2009.

[106] D. Battegazzore, S. Bocchini, and A. Frache, “Crystallization kinetics of poly(lactic acid)-talc composites,” *Express Polym. Lett.*, vol. 5, no. 10, pp. 849–858, 2011.

[107] D. Ardal, E. Yilgör, and I. Yilgör, “Catalyst effect on the transesterification reactions between polycarbonate and polycaprolactone-B-polydimethylsiloxane triblock copolymers,” *Polym. Bull.*, vol. 43, no. 2–3, pp. 207–214, 1999.

[108] SD3D Printing, “PLA Technical Data Sheet,” Dallas, Texas, 2018.

[109] UL LLC, “Polylactic Acid (PLA) Typical Properties,” *UL Prospector©*, 2018. [Online].

Available: https://plastics.ulprospector.com/generics/34/c/t/polylactic-acid-pla-properties-processing. [Accessed: 07-Aug-2018].

[110] W. Groot, J. van Krieken, O. Sliekersl, and S. de Vos, "Production and Purification of Lactic Acid and Lactide," in *Poly(Lactic Acid): Synthesis, Structures, Properties, Processing, and Applications*, 1st ed., R. Auras, L. Lim, S. E. M. Selke, and H. Tsuji, Eds. USA: Wiley-Blackwell, 2010, pp. 1–18.

[111] I. Zembouai, M. Kaci, S. Bruzaud, A. Benhamida, Y. M. Corre, and Y. Grohens, "A study of morphological, thermal, rheological and barrier properties of Poly(3-hydroxybutyrate-Co-3-Hydroxyvalerate)/polylactide blends prepared by melt mixing," *Polym. Test.*, vol. 32, no. 5, pp. 842–851, 2013.

[112] R. T. H. Chan, C. J. Garvey, H. Marçal, R. A. Russell, P. J. Holden, and L. J. R. Foster, "Manipulation of polyhydroxybutyrate properties through blending with ethyl-cellulose for a composite biomaterial," *Int. J. Polym. Sci.*, no. 651549, pp. 1–8, 2011.

[113] B. Wittbrodt and J. M. Pearce, "The effects of PLA color on material properties of 3-D printed components," *Addit. Manuf.*, vol. 8, pp. 110–116, 2015.

[114] R. L. Blaine, "Determination of Polymer Crystallinity by DSC," New Castle, DE.

[115] M. P. Arrieta, J. López, A. Hernández, and E. Rayón, "Ternary PLA-PHB-Limonene blends intended for biodegradable food packaging applications," *Eur. Polym. J.*, vol. 50, pp. 255–270, 2014.

[116] L. M. W. K. W. K. Gunaratne and R. A. Shanks, "Miscibility, melting, and crystallization behavior of poly(hydroxybutyrate) and poly(D,L-lactic acid) blends," *Polym. Eng. Sci.*, vol. 48, no. 9, pp. 1683–1692, 2008.

[117] J. Zhang, K. Kasuya, T. Hikima, M. Takata, A. Takemura, and T. Iwata, "Effect of low molecular weight additives on enzymatic degradation of poly(3-hydroxybutyrate)," *Polymer (Guildf).*, vol. 41, no. 9, pp. 2130–2138, 2000.

[118] H. Li and M. A. Huneault, "Effect of nucleation and plasticization on the crystallization of poly(lactic acid)," *Polymer (Guildf).*, vol. 48, no. 23, pp. 6855–6866, Nov. 2007.

[119] H. Zhao, Z. Cui, X. Wang, L.-S. Turng, and X. Peng, "Processing and characterization of solid and microcellular poly(lactic acid)/polyhydroxybutyrate-valerate (PLA/PHBV) blends and PLA/PHBV/Clay nanocomposites," *Compos. Part B Eng.*, vol. 51, pp. 79–91, Aug. 2013.

[120] J. P. Mofokeng and A. S. Luyt, "Morphology and thermal degradation studies of melt-mixed poly(lactic acid) (PLA)/poly(ε-caprolactone) (PCL) biodegradable polymer blend

nanocomposites with TiO2 as filler," *Polym. Test.*, vol. 45, pp. 93–100, Aug. 2015.

[121] J. E. K. Schawe, "Cooling rate dependence of the crystallinity at nonisothermal crystallization of polymers: A phenomenological model," *J. Appl. Polym. Sci.*, vol. 133, no. 6, pp. 1–7, 2016.

[122] F. Ning, W. Cong, J. Qiu, J. Wei, and S. Wang, "Additive manufacturing of carbon fiber reinforced thermoplastic composites using fused deposition modeling," *Compos. Part B Eng.*, vol. 80, pp. 369–378, 2015.

APPENDICES

Appendix A: Additional Results

Table A-1: XPS surface analysis results for as received PHB pellets using a Kratos AXIS 165 Spectrometer

Peak	Atomic Mass (g/mol)	Atomic Concentration (%)	Mass Concentration (%)
O 1s	15.999	25.67	30.51
N 1s	14.007	1.22	1.26
Ca 2p	40.078	0.55	1.63
C 1s	12.011	71.01	63.36
Si 2p	28.086	1.55	3.24

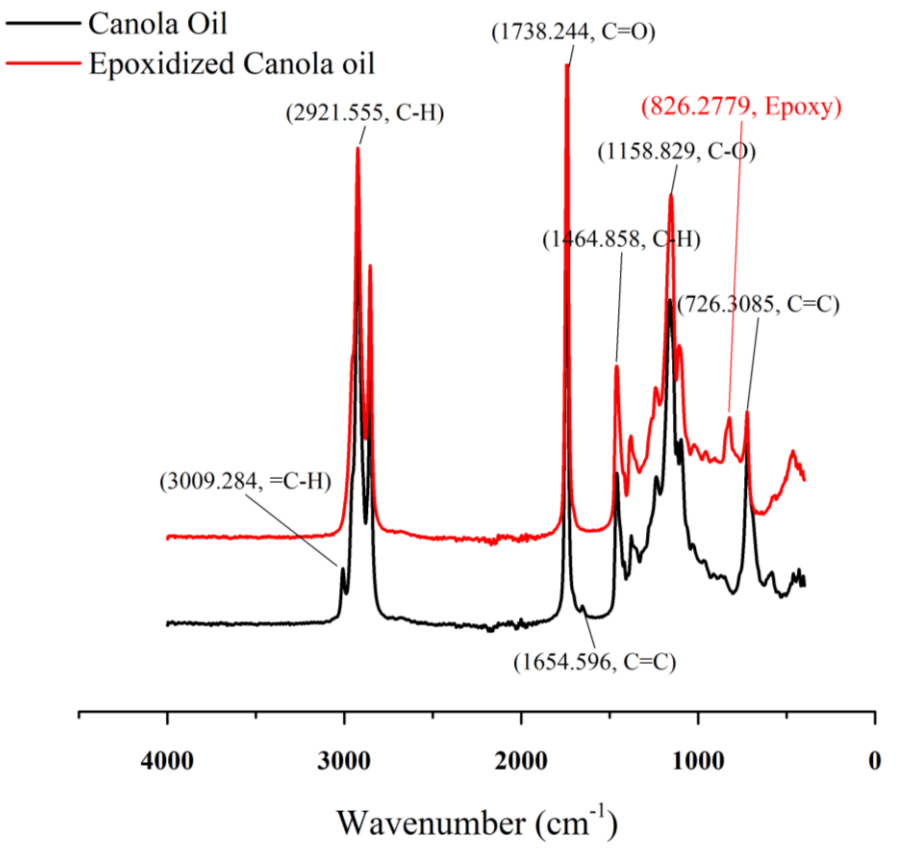

Figure A-1: FTIR results provided by Dr. Aman Ullah's lab for the epoxidized canola oil as compared to pure canola oil. Note the main difference between the two curves is the peak located at 826 cm^{-1} associated with the epoxy ring of the epoxidized canola oil

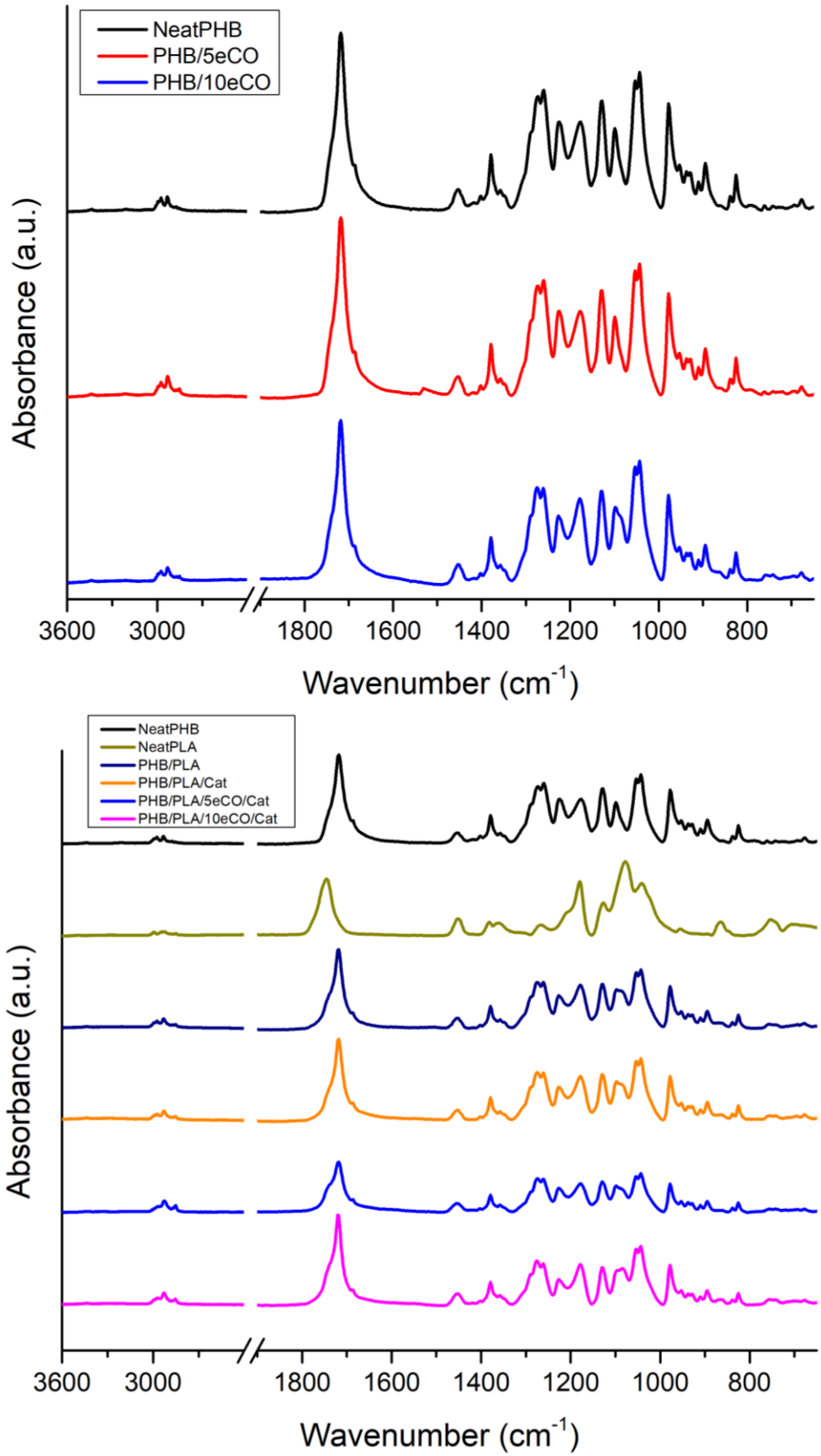

Figure A-2: FTIR spectra of plasticized samples containing eCO (top) and PLA, with and without eCO (bottom) as compared to NeatPHB and NeatPLA

Appendix B: Permission to Reproduce

- Thanks to Samuel Mann and U.S. Fish and Wildlife Services for their images of the Saltwater Creek Walkway and the Albatross at Midway Atoll Refuge, respectively (Figure 1.1). These images are licensed under a Creative Commons Attribution license (Attribution 2.0 Generic, https://creativecommons.org/licenses/by/2.0/ca/)
- Permission to reproduce the image in Figure 1.2, which was created and posted by Vincent Ryan on the website BIOPOL – Biodegradable Plastic (http://www.technologystudent.com/prddes1/biopola.html), has been granted by the author.
- Permission to reproduce Table 2.2, Figure 2.3 and Figure 2.4, which were published by Hankermeyer *et al.* in "Polyhydroxybutyrate: Plastic Made and Degraded by Microorganisms," has been granted by Springer Nature (License #4417200368713).
- Permission to reproduce Figure 2.5, which was published by Rolf-Joachim Müller in "Biodegradability of Polymers: Regulations and Methods for Testing," has been granted by John Wiley and Sons (License #4417200663570)
- Thanks to Kholoudabdolqader for their diagram of a Filament Driver of a 3D printer (FDM) (Figure 2.7). Changes were made to this image but the permission to modify it, and the image itself, is licensed under a Creative Commons Attribution license (Attribution-ShareAlike 4.0 International, https://creativecommons.org/licenses/by-sa/4.0/)
- Permission to reproduce Figure 2.8, which was published by Rodriguez *et al.* in "Characterization of the mesostructure of fused-deposition acrylonitrile-butadiene-styrene materials," has been granted by Emerald Publishing Limited (License #4366550750068)
- Thanks to Gary Hodgson for their diagrams of rectilinear printing pattern and infill pattern densities for FDM printing (Figure 2.9). These images are licensed under a Creative Commons Attribution license (Attribution-ShareAlike 3.0 Unported, https://creativecommons.org/licenses/by-sa/3.0/)
- Permission to reproduce Figure 2.10, which was published by Pereira *et al.* in "Effect of process parameters on the properties of selective laser sintered Poly(3-hydroxybutyrate) scaffolds for bone tissue engineering" has been granted by Taylor & Francis. Taylor & Francis is pleased to offer reuses of its content for a thesis free of charge contingent on resubmission of permission request if work is published.

- Permission to reproduce and modify Figure 2.12, which was published by Seydibeyoğlu *et al.* in "Synergistic improvements in the impact strength and % elongation of polyhydroxybutyrate-co-valerate copolymers with functionalized soybean oils and POSS," has been granted by Springer Nature (License #4417200922233).
- Permission to reproduce Figure 2.13, which was published by Yang *et al.* in "Transesterification induced mechanical properties enhancement of PLLA/PHBV bio-alloy," has been granted by Elsevier (License #4417200538532)